A NOVEL MICROCANTILEVER SENSOR SYSTEM FOR THE SELECTIVE DETERMINATION OF ANTIBIOTICS

ANTİBİYOTİKLERİN TAYİNİ İÇİN YENİLİKÇİ KANTİLEVER SENSÖR SİSTEMİ

MELTEM OKAN

Assoc. Prof. Dr. Memed DUMAN
Thesis Advisor

Submitted to Graduate School of Science and Engineering of Hacettepe University
as a Partial Fulfilment to the Requirements
for the Award of the Degree of Master of Science
in Nanotechnology and Nanomedicine

2016

The study on **"A Novel Microcantilever Sensor System for the Selective Determination of Antibiotics"** prepared by **MELTEM OKAN** is accepted as a **MASTER THESIS** in **NANOTECHNOLOGY and NANOMEDICINE DIVISION** by the jury below.

Assoc. Prof. Dr. İsmail Cengiz KOÇUM

Head

.....

Assoc. Prof. Dr. Memed DUMAN

Advisor

.....

Assoc. Prof. Dr. Ömür ÇELIKBIÇAK

Member

.....

This thesis is accepted as a **MASTER THESIS** by the Hacettepe University, Graduate School of Science and Engineering.

Prof. Dr. Salih Bülent ALTEN

Director of the Graduate School of Science and Engineering

This is presented as a work of science and dedicated to nobody.

ETHICS

I declare that in this thesis study, which was prepared according to the thesis writing guide of Hacettepe University Graduate School of Science and Engineering;

- all the information and documents were obtained within the framework of the academic rules,
- all audio-visual and written information and results were presented according to the rules of scientific ethics,
- in case of benefiting from others studies all information was addressed to related works in accordance with scientific standards,
- all cited studies were fully referenced,
- no falsification or alteration in the data provided was done,
- and any part of this thesis was not presented as another thesis study at this or at any other university.

16/12/2016

Meltem OKAN

ABSTRACT

A NOVEL MICROCANTILEVER SENSOR SYSTEM FOR THE SELECTIVE DETERMINATION OF ANTIBIOTICS

MELTEM OKAN

Master, Nanotechnology and Nanomedicine Division

Thesis Advisor: Assoc. Prof. Dr. Memed DUMAN

December 2016, 93 pages

This thesis focuses on the detection of ciprofloxacin and erythromycin antibiotics in water resources, which cause adverse effects on wildlife in aquatic environments and human life by polluting the drinking waters. Detection of these antibiotics down to picogram mass resolution is crucial, since even the presence in trace amounts refer to pollution of the water resources. The main objective of this thesis study was to detect ciprofloxacin and erythromycin antibiotics with a novel approach by merging the molecular imprinting technology and microcantilever mass sensors. The developed nanosensor relies on the detection via adsorption of these molecules to the template specific cavities of molecularly imprinted polymeric (MIP) nanoparticles. The ciprofloxacin and erythromycin imprinted polymers were synthesized with miniemulsion polymerization technique. Their size, shape and dispersity characterization was carried out with Scanning Electron Microscope (SEM) and their layer structure was characterized by Atomic Force Microscopy (AFM). SEM images yielded that ciprofloxacin and erythromycin imprinted polymeric nanoparticles were both spherical in shape had sizes of around 160 nm and 30 nm, respectively. Three different methods were tried during the immobilization of prepared polymeric nanoparticles on the surface of the cantilever. AFM images revealed the particle morphology that were absorbed on the cantilever. It was found that a monolayer surface coverage was accomplished with a covalent immobilization technique. The validation of prepared nanosensor was accomplished for both of the imprinted polymeric nanoparticles specific to chosen antibiotics by employing the dynamic sensing mode. During validation studies, binding kinetics both in liquid and in air were checked. As the polymeric nanoparticles were immobilized on the surface of the cantilever, any molecule adsorption resulted in a frequency shift to lower values. From the shifts recorded, masses of the total adsorbed molecules were calculated. The sensitivity of the sensor systems in air for the detection of ciprofloxacin and erythromycin were

determined as 2.2 Hz/pg and 1.6 Hz/pg, respectively. The limit of detection values were calculated as 2.2 μM for ciprofloxacin sensor and 1 μM for erythromycin sensor in air. The selectivity studies were performed by checking the affinities of physically and chemically similar antibiotics on ciprofloxacin and erythromycin imprinted polymers, which were found to show 7 and 8 fold lower affinities, respectively. Similarly, sensitivity of the nanosensor was checked by using non-imprinted polymeric nanoparticles, which were prepared with the same method except the template molecule inclusion. In that case, the binding affinities of ciprofloxacin and erythromycin towards non-imprinted polymers were found to be 5 and 3 folds lower compared to imprinted polymers. The obtained results were compared with data from the earlier studies done in this field and interpretations were made. Being one of the first studies in MIP based microcantilever sensor, the developed system has the potential to be pioneer in mass sensing applications.

Keywords: Microcantilever Sensor, Mass Sensor, Molecularly Imprinted Polymers, Pharmaceutical Emerging Contaminants

ÖZET

ANTİBİYOTİKLERİN TAYİNİ İÇİN YENİLİKÇİ KANTİLEVER SENSÖR SİSTEMİ

MELTEM OKAN

Yüksek Lisans, Nanoteknoloji ve Nanotıp ABD

Tez Danışmanı: Doç. Dr. Memed DUMAN

Aralık 2016, 93 sayfa

Bu tez çalışması kapsamında su kaynaklarındaki doğal yaşam üzerinde ve insanlar için yaşamsal önemi büyük olan içme suyu kaynaklarında olumsuz etkileri olan siprofloksazin ve eritromisin antibiyotiklerinin tespitine yoğunlaşılmıştır. Bu antibiyotiklerin su kaynaklarında iz miktarda bulunmaları bile kirlilik olarak nitelendirildiği için pikogram mertebesindeki miktarlarının tespit edilebilmesi önemlidir. Bu doğrultuda tez çalışmalarında yeni bir yaklaşım olan molekül baskılanmış polimer teknolojisi ile mikrokantilever kütle sensörler bir arada kullanılmıştır. Bu nanosensör sistemlerin temel çalışma prensibi, hedef moleküle özgü bağlanma bölgeleri olan baskılanmış polimerik nanopartiküller üzerine hedef moleküllerin adsorpsiyonudur. Tez çalışmasının hedef molekülleri olan siprofloksazin ve eritromisin molekülleri mini emülsiyon polimerizasyon tekniği ile baskılanmış polimer elde etmek için kullanılmıştır. Sentezlenen baskılanmış polimerik nanopartiküllerin şekilleri, boyutları ve yüzeye dağılımları Yüzey Elektron Mikroskopu (SEM) ile karakterize edilirken katman yapıları Atomik Kuvvet Mikroskopu (AFM) ile karakterize edilmiştir. Yüzey Elektron Mikroskopu ile elde edilen görüntülerde siprofloksazin ve eritromisin baskılanmış polimerik nanopartiküllerin boyutları sırasıyla 160 nm ve 30 nm olduğu görülmüştür. Baskılanmış polimerik nanopartiküller üç farklı yöntemle kantilever üzerine immobilize edilmişlerdir. İmmobilize edilen nanopartiküllerin kantilever üzerindeki morfolojileri AFM ile görüntülenmiştir. Baskılanmış polimerik nanopartiküllerin kantilever yüzeyine kovalent olarak bağlandığı nanosensörde nanopartiküllerin yüzeye dağılımı tek tabakalı şekilde olduğu AFM ile tespit edilmiştir. Hazırlanan nanosensörlerin dinamik modda seçici olarak çalışması her iki baskılanmış

polimerik nanopartikülün için başarılı olmuştur. Antibiyotiklerin polimerik nanopartiküllere bağlanma kinetikleri hem sıvı hem de hava deneylerinde kontrol edilmiştir. Kantilever yüzeyine immobilize edilmiş polimerik nanopartiküllerin yüksek seçicilikleri sayesinde kütlesel en ufak bir değişiklik bile frekans değişimine sebep olmuştur. Bu frekans değişimleri kaydedilmiş ve toplam adsorbe olan molekül kütlesi hesaplanmıştır. Bu nanosensör sistemleri kullanılarak hava deneylerinde siprofloksazin ve eritromisin tespit hassasiyeti sırasıyla 2.2 Hz/pg ve 1.6 Hz/pg olarak hesaplanmıştır. Hava deneylerinde siprofloksazin ve eritromisin nanosensörlerinin minimum tespit değerleri sırasıyla 2.2 μM ve 1 μM olarak hesaplanmışlardır. Her iki moleküle ait seçicilik çalışmaları için hem kimyasal hem de fiziksel açıdan benzer antibiyotikler kullanılmış ve baskılanmış polimerik nanopartiküllerin siprofloksazin için 7 kat, eritromisin için 8 kat daha az bağlanma ilgisi olduğu hesaplanmıştır. Aynı şekilde nanosensörlerin hassasiyetlerini kontrol etmek için moleküler baskılanmamış polimerik nanpartiküller kullanılmıştır. Bu partiküller, diğer baskılanmış olan partiküller ile aynı şekilde sentezlenmiş ancak yapılarına hedef molekül eklenmemiştir. Bu doğrultuda baskılanmamış nanopartiküller üzerine siprofloksazin ve eritromisin moleküllerinin bağlanma istekleri baskılanmış olan nanopartiküllere göre sırasıyla 5 ve 3 kat daha az olduğu görülmüştür. Elde edilen tüm bu sonuçlar daha önce bu alanda yapılan çalışmalar ile karşılaştırılmış ve yorumlanmışlardır. Alanında ilk olan baskılanmış polimerik nanopartiküller ile birlikte kullanılan kantilever sensör sistemlerleri ile yapılmış olan bu tez çalışması ilerideki kütlesel tespit uygulamalarına ışık tutacak niteliktedir.

Anahtar Kelimeler: Mikrokantilever Sensör, Ağırlık Sensörü, Moleküler Baskılanmış Polimerler, Farmasötik Kirleticiler

ACKNOWLEDGEMENT

I would like to thank my advisor Dr. Memed Duman, whose passion for finding novel ideas and desire to educate us as hardworking students set up new standard for anyone involved in his lab. He is the one who taught us to push the limits, no matter what, and to never give up on anything.

I spent three months in the Institute of Biophysics in Johannes Kepler University, Linz. I learned considerably valuable information regarding the Atomic Force Microscopy. I received a lot of support from Peter Hinterdorfer, Andreas Ebner, Rong Zhu, Michael Leitner, Lukas Traxler, Boris Buchroithner and Melanie Lindbichler. I want them to know that their helps are very much appreciated. I also want dearest Iuliana Moldoveanu to know that she gave meaning to my stay in Linz.

I am grateful to my friend Gülgün Aylaz for standing by my side when times get hard. I am forever in her debt.

Special thanks to my friend Esma Sari for providing me the molecularly imprinted polymeric nanoparticles that were used in this study and for her meritorious support, both scientifically and spiritually.

I thank Dr. Evren Çubukçu for helping me with the imaging process with Scanning Electron Microscopy. I thank my lab friends Pelin Tan, Selim Sülek, İpek Akyılmaz, Uğur Aydın and Soheil Malekghasemi;
my parents and my brother;
and the members of NS.

Lastly, Dear Benji, I wouldn't be able to get this far without you.

This thesis arose from a study supported by The Scientific and Technological Research Council of Turkey (TÜBİTAK), Project No: 113Z222. Also, the thesis itself was supported by the TÜBİTAK Foreground Areas Scholarship.

TABLE OF CONTENTS

TABLE OF FIGURES

SYMBOLS AND ABBREVIATIONS

Symbols

C: Concentration

F: Frequency

ΔF: Frequency shift

Δm: Mass change

Abbreviations

CPX: Ciprofloxacin

ERY: Erythromycin

CPX-IPN: Ciprofloxacin Imprinted Polymeric Nanoparticles

ERY-IPN: Erythromycin Imprinted Polymeric Nanoparticle

MIP: Molecularly Imprinted Polymer

NIP: Non Imprinted Polymer

Q: Quality Factor

LoD: Limit of Detection

LoQ: Limit of Quantification

AFM: Atomic Force Microscopy

QCM: Quartz Crystal Microbalance

SEM: Scanning Electron Microscopy

FTIR: Fourier Transform Infrared Spectroscopy

MeOH: Methanol

HAc: Acetic Acid

1. INTRODUCTION

Pharmaceutical Emerging Contaminants (PECs) in aquatic environments cause adverse effects on animals and plants living within and create serious threat on drinking water. Several antibiotics were recently added to the contaminant candidate lists of the United States Environmental Protection Agency (US-EPA). As a result of this growing threat against wildlife and human health resulting from PECs, new detection techniques are being developed in the field of biosensors. This thesis study was derived from the COST Action call that emerged from the demand to establish state-of-the-art sensing techniques to detect the PECs in water resources.

Among the concept of biosensors, during the last two decades micromechanical sensors have been of considerable interest. In this field, resonant mass sensors are quite commonly employed, for which Quartz Crystal Microbalance (QCM) and microcantilever sensors are the leading systems. Both these sensors are based on detection via frequency shift, which is triggered by the mass change on the surface. Allowing interactions to take place on the surface of these sensor systems, however, requires a recognition layer specific to an analyte. Using biological molecules as recognition elements has several drawbacks such as being high-priced and being very sensitive to temperature and humidity. An alternative to eliminate these deficiencies is to use mimetic structures instead of biological molecules directly. Molecularly imprinted polymer (MIP) technology had the potential to take their place as recognition elements and they are being used for over 20 years now. Their working principle relies on capturing the analyte by the cavities prepared physically and chemically specific to the molecule of interest. Their polymer structure allows them to stay steady and stable in tough conditions without breaking down. Moreover, they can be easily synthesized and are cost efficient. The usage of MIPs

has already been reported in mass-sensing applications with QCM. The combination of MIPs and microcantilever mass sensors, on the other hand, is still a novel approach. Even though a numbers of studies have been done so far, this system remains as an innovative model in mass sensing applications. These studies mainly focus on non-covalent immobilization of MIPs on the surface of cantilevers and fabricating cantilevers made of MIPs directly. This thesis, however, offers a different method regarding the combination of MIPs and microcantilevers by focusing on the immobilization of MIPs on the cantilever surface covalently.

For this thesis study, two antibiotics; ciprofloxacin and erythromycin, were chosen and their MIPs were synthesized. The prepared MIPs were immobilized on the surface of the cantilever by using different methods and comparison was made. Employing the dynamic sensing mode, frequency shifts triggered by the mass load which are caused by the molecule adsorption were determined. The prepared sensor has the potential to be a pioneer work in this very field of MIP and microcantilever mass sensor combinations.

The contents of this thesis cover the explanation of resonant mass sensor basics, their working principle, the areas in which they were and are being used, preparation and characterization of ciprofloxacin and erythromycin imprinted polymers, analysis of different immobilization techniques, development and validation of the microcantilever sensor system developed and the interpretation of results and possible further approaches on enhancing the sensor developed.

2. LITERATURE REVIEW

2.1. Antibiotics: Their Adverse Effects and Detection Techniques

There has been a growing interest in establishing novel techniques to identify Pharmaceutical Emerging Contaminants (PECs) in water resources since they threat drinking water and create adverse effects on both human health and wildlife. There exists a noteworthy increase in antibiotic resistance in bacteria which in return inhibits the treatment of infections. A great deal of hospital-acquired infections is caused by multidrug resistant bacteria [1] [2]. Several pharmaceuticals are now added to the latest contaminant candidate lists of the United State Environmental Protection Agency (US-EPA). Ciprofloxacin (CPX) (Figure 1a) and erythromycin (ERY) (Figure 1b) are suggested as two of the prior drinking water contaminants as antibiotics at the latest European Union Water Framework Directive (EU-WFD). Ciprofloxacin [1-cyclopropyl-6-fluoro-1,4-dihydro-4-oxo-7-(1-piperazinyl)-3-quinolone carboxylic acid] is a third generation fluoroquinolone. CPX shows a broad-spectrum of antibacterial activity. It is an easily affordable antibiotic with distinct curative effects, which makes it used prevalently and quite commonly [3] [4]. Nonetheless, CPX residues were found to imperil people's health by affecting mammalian cell replication as well as adverse drug reactions [4] [5] [6] [7]. Similar to many other antibiotics, CPX is not completely metabolized in the body as well. Therefore, the possibility of CPX to enter the environment through urine samples of patients and wastewater is quite high. ERY is produced by *Streptomyces erythraesus* in a fermentation step and is a macrolide antibiotic with broad-spectrum activity. It contains 14-membered lactone ring with two sugar molecules (L-cladinose and D-desoamine) and ten asymmetric centres. During the fermentation, number of

related substances are formed as well, named ERY A to F. The main component of commercially available ERY is included in ERY A, whereas the rest are chemically and physically analogues and are formed in small amounts [8] [9] [10] [11].

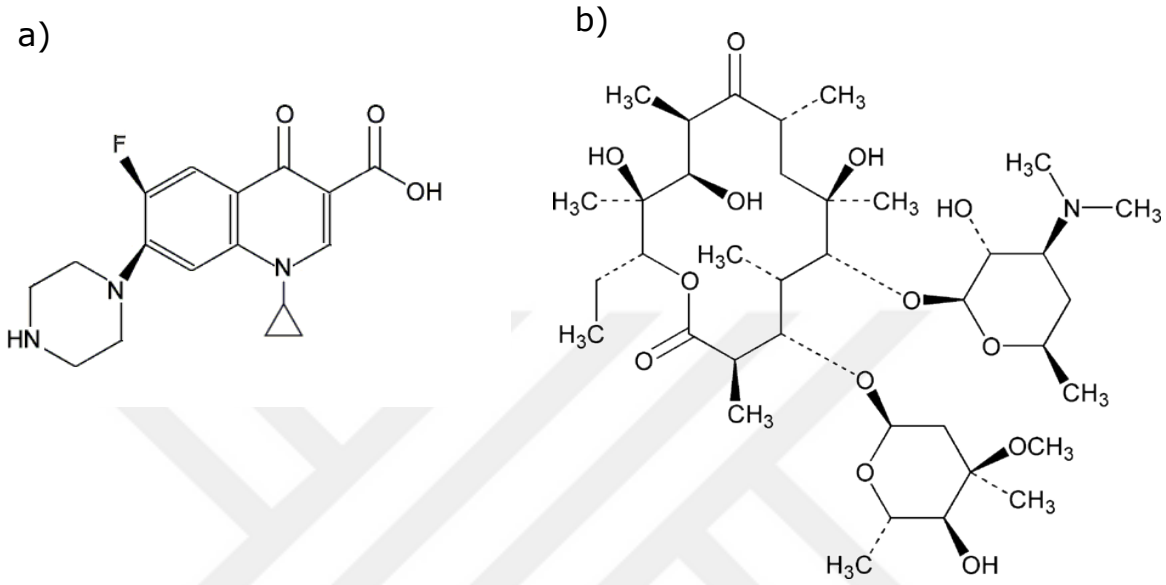

Figure 1: Chemical structures of a) ciprofloxacin, b) erythromycin.

It is crucial to detect the presence of broad spectrum antibiotics with high efficiency. There are several techniques employed for the determination of CPX and ERY so far. For CPX, these techniques were mass spectrophotometry [12], spectrophotometry [13], capillary electrophoresis [14] [15], liquid chromatography [16] [17], electrochemical techniques [18] [19] [20] and solid phase extraction (SPE) [21] [22]. Detection of ERY has been performed with ultraviolet (UV) [23], electrochemical detection [24] [25] [26], near infrared reflectance spectroscopy (NIR) [27], capillary electrophoresis chromatography (CEC) [28] [29], liquid chromatography–tandem mass spectroscopy (LC–MS/MS) [30] [31] [32] [33], high-performance liquid chromatography (HPLC) [34] [35] [36] and liquid chromatography–mass spectroscopy (LC–MS) [37] [38] [39]. Despite these techniques

are succesfully applicable, they all are overpriced, time-consuming, complicated and entail sophisticated automation and assist of experienced users. The need for cost efficient, highly selective and sensitive systems with fast response time still remains. During the last decade, novel detection techniques in the concept of biosensors advanced rapidly. These new sensors allow rather fast real-time measurements and enable achieving higher sensitivities.

2.2. Introduction to the Concept of Biosensors

The term "biosensor" was first introduced by L. C. Clark Jr. in 1956 and followed by studies of himself and C. Lyons in 1962 [40] [41]. Later on, it began to appear in scientific literature in late 70's and started to be reviewed in early 80's [42] [43]. In order to comprehend the basics of biosensors, first, one must understand what a chemical sensor is and how it works. In simplest form, chemical sensors are devices that produce signal from a chemical data. The obtained signal makes it possible to interpret the data analytically. They consist of three main parts; receptor, transducer and amplifier (Figure 2). The receptor part is where the recognition process takes place, and the transducer processes the chemical signal into an electronic or optical signal. Biosensors are also chemical sensors, only that the receptor part where the recognition system exists employs a biochemical mechanism [44]. As reported by Thévenot et al. in IUPAC Technical Report 1999, biosensors are self-sufficient integrated devices that are capable of providing quantitative or semi-quantitative analytical data specific to an analyte by employing a biochemical recognition section, that is maintained in contact with the transduction section [45]. According to Lowe, biosensors can have different definitions for different fields of science. But as an overall description, they are analytical devices that unites a physico-chemical transducer with a biological or non-biological recognition element to determine an analyte and convert the obtained

data into electrical signal [42] [46]. Biosensor's main role is to provide precise results rapidly, regarding the analyte to be tested without perturbing the sample [47].

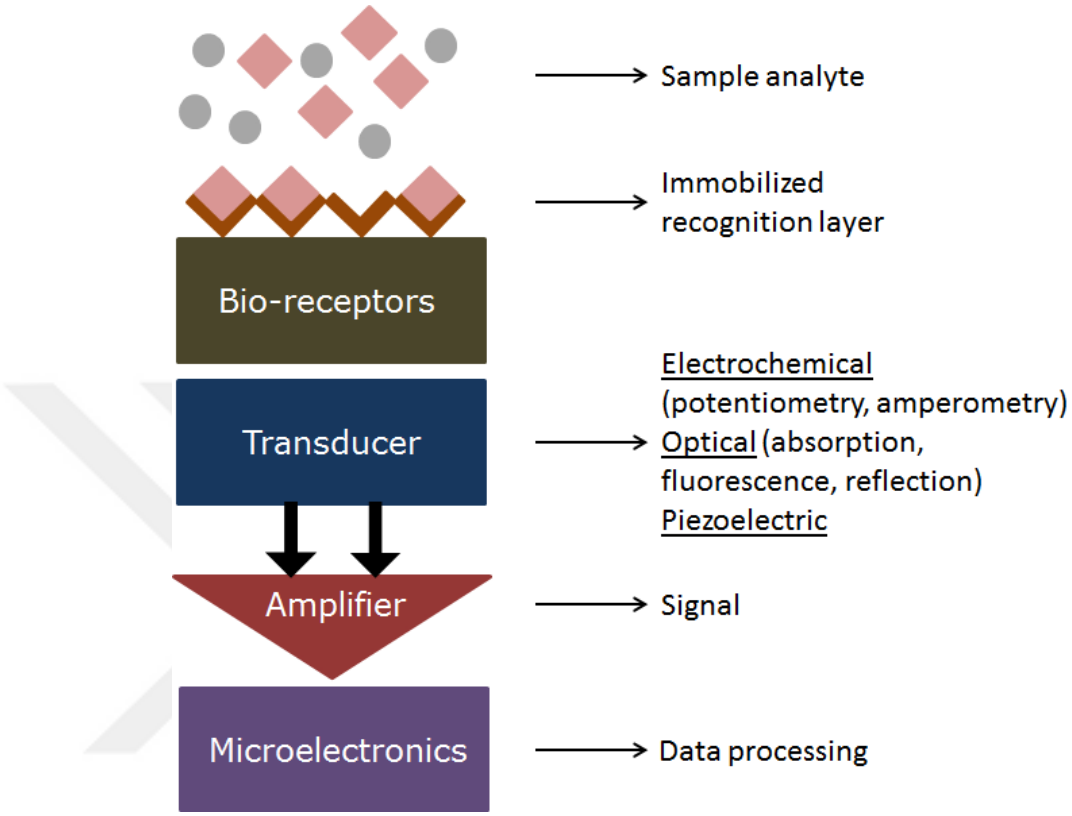

Figure 2: Schematic representation of the main parts of biosensors.

2.3. Quartz Crystal Microbalance, It's Working Principle and Applications

Recently, modern detection techniques under the name biosensors have been established, allowing for more sensitive measurements in much shorter time. In this field, one of the most frequently employed systems is resonant mass sensors. Resonant sensors are based on a unit that vibrates at its resonance and shifts this frequency as a function of a physical parameter [48]. Changes in resonator in terms of mass and/or stress allow the conversion of measure of vibrating element into resonance frequency. Resonant sensors work with high stability and

resolution and provide quasi digital output [48]. Its first discovery was in 1959 by Sauerbrey who focused on the shift in frequency for the determination of the mass of a film that was attached on a quartz resonator' surface, instead of focusing on the tipping angle of the beam balance [49]. Named as Quartz Crystal Microbalance (QCM) (Figure 3), the system was working in the following manner; the mass changes per unit area are measured via determining the quartz crystal resonator's frequency shifts (Figure 4). In QCM, the resonance is triggered with the adsorption or desorption of masses depending on the film deposition on the face of the acoustic resonator. This approach made it possible to detect masses down to 10^{-16} kg, whereas the commercial microbalances could identify masses only down to 10^{-10} kg [50]. Until early 80's QCM was being employed quite commonly. However, shortly after 1980, Kanazawa and Gordon measured the shift in frequency when single surface of a quartz resonator was inside of a liquid [51]. They came up with the conclusion that QCM's frequency response that is staying inside a liquid, rest not only on the liquid's density but also on its viscosity. It was found then that the Sauerbrey's equation was not credible for the viscoelastic layers when QCM is being used. According to Sauerbrey's equation, viscoelastic layer's mass is not taken into account and such situation results with a 'missing mass' [52]. Accordingly, it was no longer assumed to be a mass sensor, rather it began to be called a thickness shear mode (TSM) [53]. Even though there were a set of questions and unclarity about QCM being a mass sensor or not, it provided the information regarding the effect of acceleration on mass sensitivity on various spots over the surface of the quartz resonator [54].

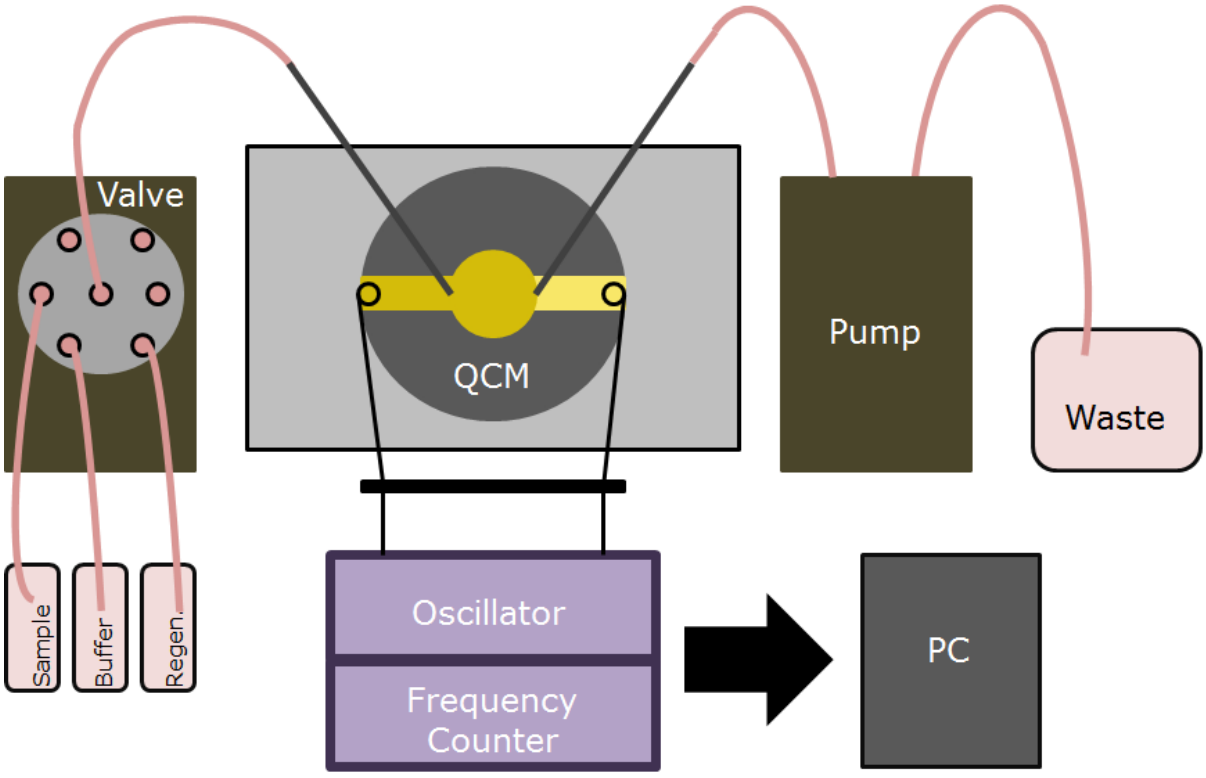

Figure 3: Schematic representation of QCM.

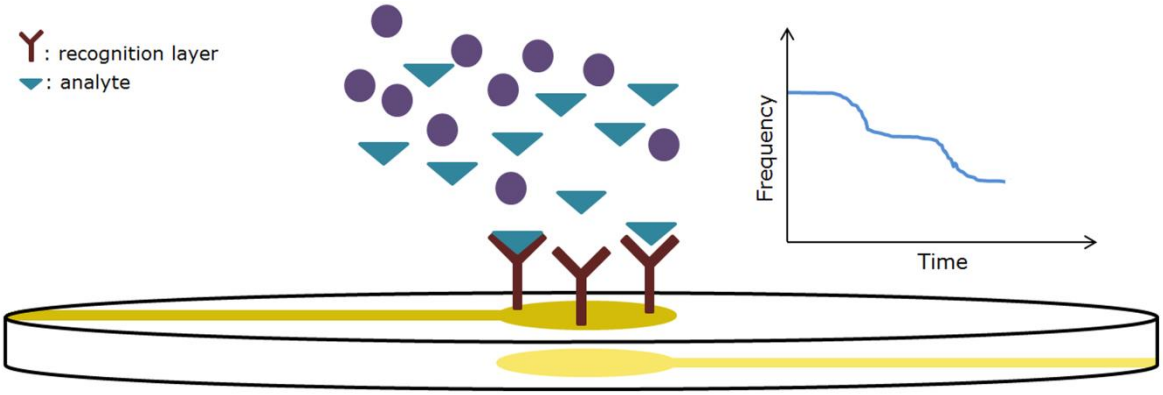

Figure 4: Schematic representation of the quartz crystal.

QCM has continued to be employed as a mass sensor, despite the dilemmas and contrary arguments. For instance, it was used to identify the organophosphorus pesticide DDVP (*o,o*-dimethyl-*o*-2,2-dichlorovinyl phosphate) adopting various conductive and nonconductive polymers immobilized on the QCM electrodes surface [55]. As nonconductive

polymers, poly(acrylic acid) (PAA) and poly(vinyl alcohol) (PVA) were employed due to their sensitivity towards DDVP and as conductive polymers, a copolymer of PEDOT with poly(styrene sulphonic acid) (PEDOT/PSS) and poly(3,4-ethylenedioxythiophene) (PEDOT) were chosen. The QCM chip was coated with the selected polymers, which had a resonance frequency range of 10-20 Hz. Results indicated that the range of frequency of the QCM chip was increased when conductive polymer coverage was used. Namely the increase in frequencies was from 20 Hz to 115 Hz and from 18 Hz to 60 Hz, respectively. A linear response was obtained with PEDOT coated QCM sensor, for a DDVP concentration range of 6.5-32.5 ppm. Another study, which also benefited from conductive polymers, focused on the application of QCM as a gas sensor to determine the volatile-organic-compounds. The QCM chip was covered in synthetic polypeptides and conducting polymers to detect ammonia, benzene, chlorobenzene, dimethyl amine, butyric acid, acetic acid and their mixtures [56]. The response of the developed QCM gas sensor was reported to be 0.9-440 Hz of frequency shift for a concentration range of 1.8-108 ppm. The prepared sensor showed high sensitivity and selectivity. Moreover, it also had the ability to distinguish the characterized odour profiles of all compounds used in the experiment. In another study, QCM sensor was combined with nucleic acid by employing a whole new immobilization approach for the following hybridization [57]. The surface of the QCM chip was treated with ethylene diamine (EDA) inside a glow-discharge tube to introduce amino groups on crystal's surface. These amino groups were, then, reacted with glutaraldehyde (GA) and converted into aldehyde groups. On the GA modified chips, extra 5'-end on the complementary strand containing double strand oligonucleotides were attached. The developed sensor was then used in the hybridization studies. The frequency shifts obtained were determined to be in good agreement with the concentration of the target strand. The QCM sensors were also used in a number of bacteria detection studies. In one of them, researchers

focused on the phenomenon known as the majority of microorganisms contain lectin and carbohydrate pockets on their surface [58]. A carbohydrate label-free mass sensor was developed for this aim. In this highly specific and selective sensor, lectin-bacterial O-antigen was used as recognition element and the aim was to detect high molecular weight bacteria. In the developed sensor system, QCM was used as the transducer. As recognition element a combination of functional mannose self-assembled monolayer (SAM) and Concanavalin A (Con A) was chosen to detect *Escherichia coli* (*E. coli*) W1485. The multivalent binding between Con A and *E. coli* surface allows a powerful adherence of *E. coli* toward SAM immobilized surface of QCM. As the contact area between the QCM chip's surface and the cell increases, it prompts a strong and rigid attachment by intensifying the binding among SAM and *E. coli*. Results showed that high specificity and sensitivity was achieved with the developed carbohydrate QCM sensor. A limit of detection of several hundred bacteria cells and a linear range between $7.5x10^2$-$7.5x10^7$ cells/mL were obtained in the study. A very recent study was to detect molecules with low molecular weight with an aptamer based QCM sensor containing dissipation monitoring (QCM-D) [59]. The study focuses on the aptamer conformational switches resulting from molecule adsorption. This in return induces the relocation of water that is coupled acoustically to the layer where sensing takes place. That way, the detection signal was empowered dramatically.

2.4. Theory behind Microcantilever Mass Sensors and Their Applications

After Sauerbrey showed that mass could be determined employing vibrations and that the change in mass was associated with the frequency change, number of vibration based systems were established to determine the mass [54]. It was an experimented technique back in 1968 to detect bending and frequency changes resulting from

adsorptions, employing large silicon beams as sensors [60]. The drive was understood by thermal expansion in piezo resistors, which were placed close to the cantilever support. These resistors produce a temperature gradient to trigger cantilevers at their resonance frequencies. They can, as well be used to monitor the defection. Microcantilever sensors became a trend as the micro fabricated cantilevers began to be commercially available. These cantilevers that are used in sensor systems do not contain a tip at their end point, unlike the traditional Atomic Force Microscopy (AFM) cantilevers and include a compound-specific layer. The surface of the cantilever is used as the sensor part, where molecules are adsorbed. If this adsorption happens only on single face of the cantilever, bending occurs and the stress on the surface can be monitored. To provide this single-side adsorption, only single face of the cantilever must be covered in the specific coating, mostly being the top one. The below one might be left bare, else, might be covered in passivation coating. In case of coating cantilever's both faces, frequency changes may be tracked rather than deflection. The surface can be coated with a polymer, a self-assembled-monolayer, hydrogels, antibodies, proteins, enzymes etc. depending on the study.

Employing the cantilevers for the detection of any interaction that takes place on the cantilever that is covered with a layer provides an optically label-free analysis down to picogram mass resolution. Detection studies using cantilevers is based on covering the cantilever's surface with a recognition element specific to the analyte of interest as stated. These measurements may take place both in liquid and in air [61]. Cantilever's high sensitivity and recognition element's selectivity on its surface enable the detection of molecules by following either of the detection modes or both at the same time [62]. The main issue that arises in resonant mass sensing with cantilevers is to understand whether the response obtained is due to the interactions or the

environmental effects. To express this issue more comprehensively, variations in environmental effects including viscosity, temperature and humidity, cause alterations in elastic modulus of cantilevers [63]. Variations in viscosity and humidity, for instance, affect the damping of the resonant and cause a drift in resonance frequency [64]. To resolve this issue, a separate resonator can be used as a reference [65]. For such a test series, both coated and uncoated cantilevers should be prepared and operated under the same ambient conditions. Frequency changes that result from molecular interactions can hereby be established by subtracting the final frequencies of the two cantilevers. This approach, however, might not be enough to solve the issue, as both cantilevers may not have exact mechanical properties. Any difference in their properties would lead to altered frequency responds and it is an inevitable fact that AFM chips in a same batch are never identical. Consequently, their nominal frequencies would never be identical as well. In this case, more reliable and certain solution is to examine various resonance modes or overtones [66] [67] [68].

Microcantilever sensors have been utilised in various fields of applications including DNA hybridization [69], protein detections with RNA aptamers [70], antigen-antibody reactions [71], toxin and pathogen detections [72] [73] and in cancer diagnostics [74]. Cantilevers are mainly operated either in static or in dynamic mode in sensors applications [75] [76]. In static mode, a signal is produced when specific adsorption occurs on single face of the cantilever which is covered in a sensing layer [77] [78]. The surface stress resulting from binding of molecules leads to bending. In dynamic mode, the cantilever oscillates at its resonance frequency. In this case, cantilever's both faces can be coated with compound specific surface coverage [79]. When molecules are adsorbed on the specific layer, cantilevers resonance frequency shifts to a lower value [80] [81] [82]. This process does not alter cantilever's mechanical properties. From the shift in

resonance frequency, the total adsorbed mass can be determined. Resonance characteristics of a cantilever rest on its mass and spring constant, as well as the environment in which the measurement is performed [83].

2.4.1. Static Deflection Mode

Static sensing is provided by the strain and bending characteristics of the cantilever. As molecules are adsorbed on the compound-specific layer, a signal is produced due to the mechanical response of the surface layer [79]. However, to operate the cantilever sensor in deflection mode and to get reasonable stress changes, only single surface of it must be covered in compound specific layer as shown in Figure 5. Blocking the unspecific interactions would help eliminating the complications regarding deflection not resulting from molecule-layer interaction. Moreover, when cantilever's single side is covered only, bending characteristics and the alteration in resonance frequency can be measured simultaneously [81]. The mechanical response, being stress, causes deflection of the cantilever. This stress (σ) can be denoted by the Stoney's law;

$$\sigma = \frac{Et^2}{6R(1-\nu)} \qquad (1)$$

where E is Young's modulus, t is the thickness, R is the radius of the curvature and ν is the Poisson ratio. One significant parameter here is the cantilever's thickness; as, it affects system's sensitivity directly. When thinner cantilevers are used, the amount of deflection is usually more, which is the key to achieve better sensitivity when this mode is employed.

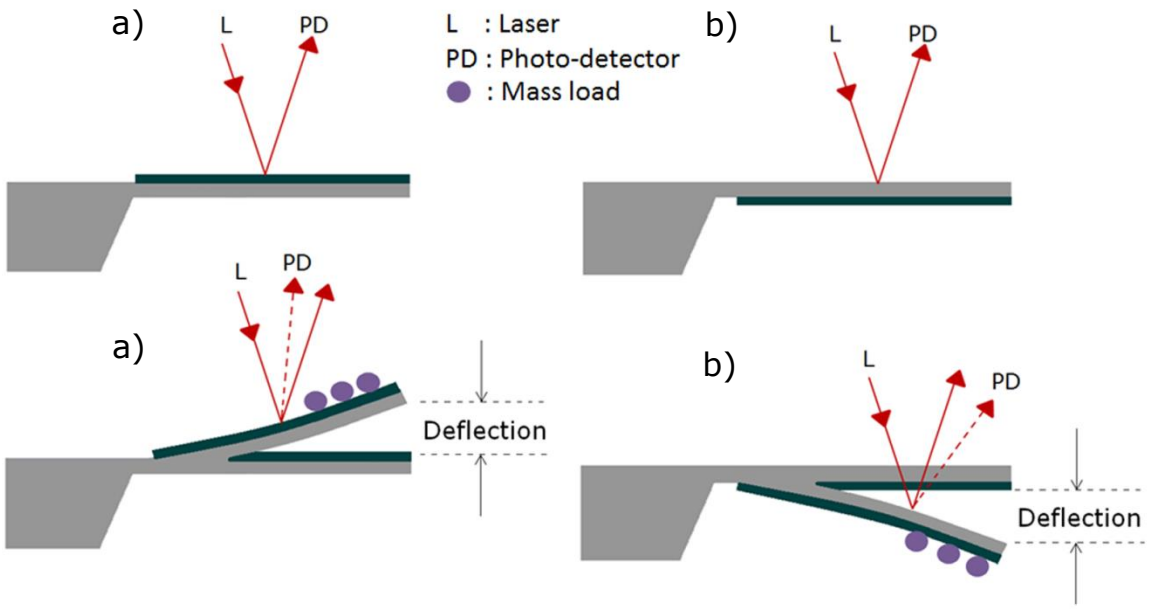

Figure 5: Schematic representation of static deflection mode a) upper surface coverage, b) lower surface coverage.

The deflection of the cantilever that is triggered either from added mass or surface stress result from molecule adsorption is directly proportional with the adsorbed material [84] [85] [86] [87] [88]. Yet, the surface stress does not depend entirely on the amount of molecules adsorbed. When the load, F, is applied to the free end of a rectangular shaped cantilever, the deflection, δ, would be;

$$\delta = \frac{FL^3}{3EI} \qquad (2)$$

where E is Young's modulus of the material, I is cantilever's second moment of the cross-sectional area and L is the length. When the load is uniform throughout the whole cantilever, the deflection would be;

$$\delta = \frac{w_0 L^4}{8EI} \qquad (3)$$

where w_0 is the load per unit length. When cantilevers are introduced with the molecules from one side, the stress originates only on that side. In that case, two sides of the cantilever experiences different stresses, which lead to a separate deflection of two sides. Stoney's equation can be used to relate this difference;

$$\frac{1}{r} = 6\frac{Pt}{Ed^2} \qquad (4)$$

where r is cantilever's radius of the bending, P is the surface stress, d is the thickness of the cantilever and t is the thickness of the surface coverage [89].

2.4.2. Dynamic Sensing Mode

The resonance characteristics of a cantilever (spring constant, mass, environment) affect the resonance features directly. Any interaction of molecules with upper and lower layers on the cantilever surfaces would lead to an alteration in resonance frequency and usually decrease it (Figure 6). The resonance frequency of an oscillated cantilever is;

$$F = \frac{1}{2\pi}\sqrt{\frac{k}{m^*}} \qquad (5)$$

where k is the spring constant and m* is the effective mass of the cantilever [90]. Assuming that k is unchanged during adsorption, the mass load can be calculated as;

$$\Delta m = \frac{k}{4n\pi}\left(\frac{1}{f_1^2} - \frac{1}{f_0^2}\right) \qquad (6)$$

where n is a parameter related with cantilever's geometry, f_1 is the frequency after the mass load and f_0 is the frequency before the mass load [81].

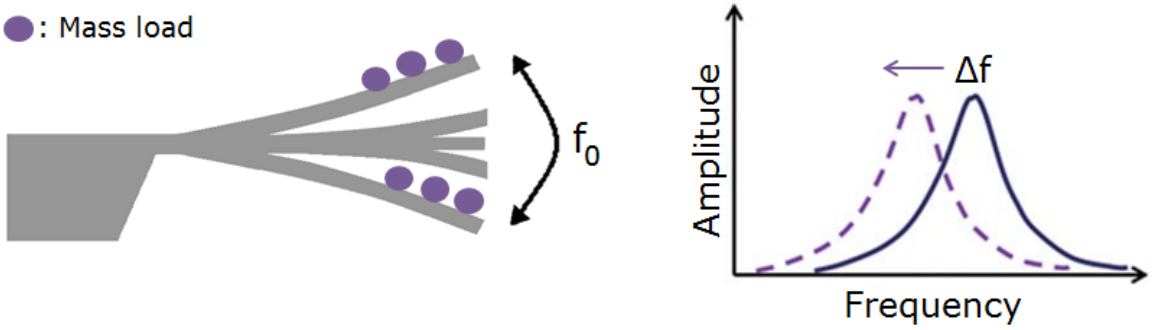

Figure 6: Schematic representation of the dynamic sensing mode.

A much detailed measurement can be carried out by employing different modes in dynamic sensing. The motion can be referred as in-plane and out-of-plane according to the plane based on cantilever's two largest dimensions. In-plane vibrations are longitudinal (extensional) and lateral motions whereas out-of-plane vibrations include transverse (flexural) and torsional motions. These motions display resonance when excited at their resonant frequencies. Assuming that cantilever's deflection is relatively small compared to its thickness, its geometry is rectangular cross-section with a single uniform layer, the material is isotropic and the aspect ratio is large enough; analytical expressions for different modes can be defined mathematically from the related equation of motion [91].

2.4.3. Parameters Affecting the Microcantilever Mass Sensing

One of the main factors the microcantilevers are used in mass sensing measurements is that they can be used in real-time measurements, as it is usually preferred to perform the binding experiments in liquid for biological detections. However, in liquid measurements, cantilever's quality factor (Q) decreases dramatically due to the damping of liquid. Thus, its ability to detect molecules in trace amounts is hindered [92].

Yet another crucial parameter would be to choose the proper resonance frequency for the given environment. Cantilever's physical properties and noise are other important parameters that affect the nature of the measurement.

2.4.3.1. Quality Factor

Q is an important parameter in such applications, since it provides a measurement for the energy loss like viscous damping [93] [94] [95]. Q is an influential parameter in high pressure environments like in air and in liquid during the determination of the resonance frequency. The resolution of the frequency shifts in experiments that take place in these high pressure environments may be more than one orders magnitude lower when compared with in vacuum conditions due to the low quality factor [96]. High Q values stand for low energy dissipations, as long as the energy stored does not change. In air measurements when a cantilever is resonating, its Q can be expressed either with extrinsic or with intrinsic energy loss. Extrinsic loss is related with the interactions with medium, whereas intrinsic loss is relevant to the interactions within the cantilever [97]. Q characterizes the frequency response curve's shape and defines peak's narrowness [98]. Accordingly, it alters in each resonance mode. High Q increases the resolution of the frequency by lowering the minimum detectable resonance shift. To make this statement clearer; for a Q of 10 the minimal measurable resonance frequency is 25 Hz whereas when the Q value increases up to 100 the minimum detectable resonance frequency goes down to 10 Hz [89]. Moreover, cantilevers with high Q have less thermal noise of resonance [99]. Thermal vibrations of the cantilever are of main cause for the noise in AFM [100]. Using thermal noise, effective spring constant of the cantilever can be determined. Amplitude and the width of the thermal noise peak conform to the integrated noise energy of the oscillator [101].The geometry of the cantilever and the

liquid in which it resonates also has an effect on Q as well [102] [103] [104] [105].

2.4.3.2. Physical Properties of the Cantilever

To focus more on the physical features of the cantilevers, its mass, dimensions and resonance frequency directly affect the nature of the measurement. Particularly while employing the static deflection mode, the thickness and the shape of the cantilever become rather significant. To give an example; in a study about the sensitivity of the cantilevers, deflection was found to increase from 2.8 nm to 44.5 nm with decrease in thickness from 0.5 μm to 0.2 μm. The results represent the integrity of the phenomenon, since the thinner cantilevers showed higher sensitivity [90]. In terms of shape, V-shaped cantilevers yield higher deflection, whereas for U-shaped and rectangular ones are found to give same amount of deflection and less than the V-shaped ones (Figure 7). An electromechanical resonator's resonance frequency is a sensitive function of its total mass [106]. The shift in frequency evolving out of the adsorption of a single molecule would be directly proportional with the ratio of mass of the resonator and the mass of the molecule. On this basis, a resonator with smaller mass is much sensitive compared to a one with larger mass. To be able to detect even the smallest mass variations, the resonator must have high Q and be light [106] [107]. As the size of the resonator decreases, number of binding sites on its surface increase. This increase is proportional with the total number of resonator atoms. That is; as the size of the cantilever decreases the ratio of surface to volume increases. Accordingly, the large-scale resonators are much less responsive to adsorption-desorption noise when compared to small-scale ones [108]. For cantilevers that have high spring constant, the deflection might not be readily measurable. In that case, the cantilever can be excited mechanically, magnetically or electrostatically [109] [110] [111]. It is important to choose a

cantilever with appropriate resonance frequency for the given environment. Ones with low resonance frequency are commonly employed in liquid environment measurements, while the ones with higher resonance frequency are usually used in air environment studies.

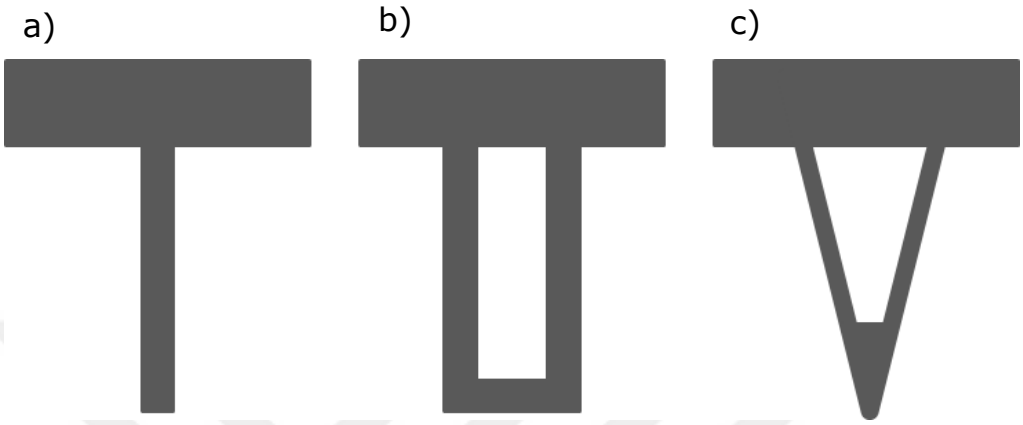

Figure 7: Schematic representation of a) rectangular, b) U-Shaped, c) V-shaped cantilevers.

2.4.3.3. Noise

Noise is another parameter that has an effect on the accuracy of the measurement. It is a crucial parameter in mass sensing applications in resonance mode to determine the final sensitivity. Noise causes fluctuations in resonance frequency in vacuum conditions with high Q, which result in ambiguities in the determination of the frequency [96]. These ambiguities might arise from temperature and thermomechanical fluctuations as well as adsorption and desorption [107]. The noise processes in the oscillator affects the capability to detect ultra-fine frequency shifts, which in return affects the determination of the mass sensitivity [96]. Temperature changes the frequency of every resonator. Since all structures display random fluctuations, all resonators present frequency noise induced by temperature. These fluctuations are due to the finite thermal conductance of the resonator [112]. The thermomechanical fluctuations are caused by the internal loss

mechanisms in the resonator [113]. This noise is originated from the nonzero dissipation and temperature of the resonator [99]. The surroundings of the resonator continuously exhibit a nonzero pressure of molecules that are adsorbed on the specific adsorption sites on cantilever's surface. This results in mass load and therefore a variation in the resonance frequency. While the molecules are adsorbed and desorbed on account of their finite binding energy and nonzero temperature, the resultant variations in frequency translate to a source of phase or fractional frequency noise [108]. The cycles of molecule binding and removal are not substantially dissipative. In other words, the approach and retreat times of the atoms are arbitrary, so the frequency shift of the resonator is discontinuous and the Q is not affected. This kind of noise, where the overall mass of the resonator is fluctuating, is not defined by the stress-strain relation [108].

2.4.4. Applications of Microcantilever Mass Sensors

Cantilever sensing has always been a promising technique because of their high sensitivity and small dimensions. The real breakthrough with microcantilever sensors, however, was the single particle detection. With a cantilever that had a length of 4-5 μm, determination of single virus particles in femtogram mass (9.5 fg, approximately) was accomplished [114]. With a longer cantilever that had a length of 15 μm and a resonance frequency of 1.08 MHz, identification of single *E. coli* cell with a mass of roughly 665 fg was successfully carried out [115]. In high vacuum environment, even a detection of mass change in attogram (ag) level was accomplished employing a nanoscale cantilever [116]. As expected, using cantilevers with high resonance frequencies allow for higher mass resolutions. For instance, a theoretical mass resolution of 17 ag/Hz was recorded with a cantilever that has a resonance frequency of 1.49 MHz [117].

Microcantilever sensors made it possible to detect ions inside a solution as well. Detection of calcium ions employing ion-selective self-assembled monolayer (SAM) modified microcantilevers was accomplished [118]. Prepared microcantilevers experienced bending once calcium ions were adsorbed selectively. Concentration down to 10^{-9} M was able to be detected using this system. A similar experiment was carried out using SAM modified microcantilevers for the detection of caesium ion *in situ* at concentration range of 10^{-11}-10^{-7} M [119]. The proposed system showed potential for the development of real-time *in situ* sensor for the determination of metal ions with high selectivity and sensitivity. In an advanced study mass of ragweed pollen was determined by locating it at various spots on a commercial rectangular microcantilever [120]. Studies were performed using first and second flexures and the first torsional modes in air. Frequency shift of the first and second flexural modes were recorded as 140 Hz and 700 Hz, respectively, whereas the shift for the first torsional mode was determined as 2.4 kHz. Results showed that the mass sensitivity of the first bending mode was lower than that of first torsional mode.

In a novel study, microfluidic channels were built in the microcantilever. Enclosing the fluid inside the cantilever enabled resonator to be driven on electrostatic forces. By ruling out the high damping and viscous drag, direct integration of microfluidic channels lead to an increase in sensitivity. Real-time detection of molecular interactions with this optimized system allowed the detection on the order of 10^{-19} g/μm^2 for the binding of avidin and biotinylated bovine serum albumin [121]. The optimization increased the Q of the resonator [122]. A liquid-cell-based cantilever sensor running in the dynamic mode was established for the detection of phospholipid vesicle [123]. The sensor was excited by a piezoelectric layer. The cantilever had resonance mode between 270-310 kHz with Q of 260 in air. In liquid environment, the resonance value decreased to 140 kHz and the Q went down to 60. Frequency

shifts were recorded upon the adsorption of vesicles on a cantilever oscillating in liquid. The decrease in frequency was observed within 1 minute and the system was stabilized in 8 minutes. A shift triggered by 450 pg adsorbed mass was recorded. In another similar advanced study, microfluidic systems were embedded on the cantilever, which helped decreasing the level of damping. Single nanoparticle detection with suspended microchannel resonators was demonstrated with sub-femtogram resolutions [124]. Obtaining showed that viscous loss resulting from the fluid was trivial compared to the intrinsic damping of silicon crystal resonator. The embedded microchannel translated the variations in mass into variations in frequency, where the fluid was flowing through channels consistently and was dispensing the molecules throughout. High resolution was obtained by decreasing the thickness of the wall and the fluid layer to micrometre scale and by keeping the cantilever under high vacuum. The system designed for a low resonator of 100 ng with high Q of 15000 led to advancement in mass resolution of six orders of magnitude over commercial QCMs.

Microcantilevers can as well be used in the chemical sensing of vapours and gases [125] [126]. Detection of gases and vapours based upon sequential position readout with beam-deflection method using microcantilever arrays was established in a study. Detection of H_2 was accomplished by adsorbing it on a Pt-coated sensor, where the surface stress change resulted in static bending [125]. Detection of hydrogen fluoride at low concentrations down to femtomolar level was carried out successfully employing the cantilever bending method that is led by the reaction between hydrogen fluoride and silicon dioxide [127]. In a similar study, comparison was made between cantilever's deflection and frequency shifts as a function of hydrogen fluoride concentration. The developed gas sensor could detect hydrogen fluoride at concentrations range of 0.26-13 ppm [128]. Determination of each component in gas

mixtures was another turning point with cantilever sensors. Binding kinetics of octane and toluene were determined using polydimethylsiloxane (PDMS) and polyetherurethane (PEUT) coated microcantilevers [129]. Obtained calibration curves represented high linearity for a concentration range of 0-6000 ppm. The reverse sorption behaviour of molecules resulted in sensitivities of 0.0055 Hz/ppm with PDMS coated and 0.0035 Hz/ppm with PEUT coated microcantilevers for octane, and 0.0033 Hz/ppm with PDMS coated and 0.0055 Hz/ppm with PEUT coated microcantilevers for toluene. Sensing gases with polymer coated cantilevers were subjected to many other studies. In another one, variations in resonance frequency resulting from adsorption of gas molecules on a polymer-coated cantilever were examined [130]. The study was carried out for volatile organic compounds such as n-octane, n-butanol and toluene, employing the first higher resonance mode of the cantilevers. The sensitivity of the prepared system was determined as 0.0988 Hz/ppm for low concentrations of n-octane. It was also stated that this sensitivity could be even lowered by changing the deposited polymer mass.

Microcantilever sensors were also used in the determination of the pH of the solution, employing silicon and silicon nitride cantilevers [131]. The study was based on tracing the cantilever bending as a consequence of different surface stress changes depending on solution's pH. Charge cumulated on modified cantilever's surface proportional with the solution's pH. Studies were performed for chemically (4-aminobutyltriethoxysilane, 11- mercaptoundecanoic acid) and physically (Au, Al) modified surfaces for a pH range of 2-12. SiO_2/Au cantilevers modified with aminosilane showed the best results for the pH range of 2-8, resulting with a cantilever deflection of 49 nm per pH unit, whereas Si_2N_4/Au cantilevers modified with aminosilane gave a cantilever deflection response of 30 nm per pH unit, for a range of 2-6 and 8-12.

Employing cantilevers as bioassays was established to detect the prostate cancer where prostate-specific antigen at a concentration of 100 ng/ml led to a frequency shift of 150 Hz [132]. Microcantilevers were also employed in the immunosensor applications for bacteria detection. Qualitative determination of *Salmonella enterica* bacteria via modified silicon nitride cantilevers and determination of *Bacillus anthracis* down to concentration of 300 spores/mL with piezoelectric-excited millimetre-sized cantilever were successfully carried out [133] [73]. Detection of myoglobin antibody with a concentration of 85 ng/mL was accomplished using deflection of the cantilever [134]. Employing the same method, detection of pesticide dichlorodiphenyltrichloroethane (DDT) was carried out [135]. Protein detections and highly sensitive glucose sensors using specificity of enzymes were established with microcantilever sensing technology [136] [137]. A surface stress study of microcantilevers during the generation of self-assembly 25-mer thiol-modified DNA-oligo layer was investigated [138]. In a similar study, nanomechanical bending of the cantilever was examined for DNA applications. The presented cantilever arrays allow multiple binding assays and are able to determine DNA down to femtomolar concentrations [69].

2.5. Molecularly Imprinted Polymers and Their Fields of Use

Molecularly imprinted polymers (MIPs) are synthetic materials that are formed to have specific recognition sites. The imprinted molecule's high affinity towards the binding sites results both from physical and chemical interactions. MIPs can be employed in a number of areas such as catalysis, extraction, purification and sensors. Their usage in sensors as artificial binding layers, allow users to no longer need real recognition elements. As illustrated in Figure 8, when the polymerization process is completed, the template molecule is removed

with desorption solutions and they leave physically and chemically specific binding cavities behind them.

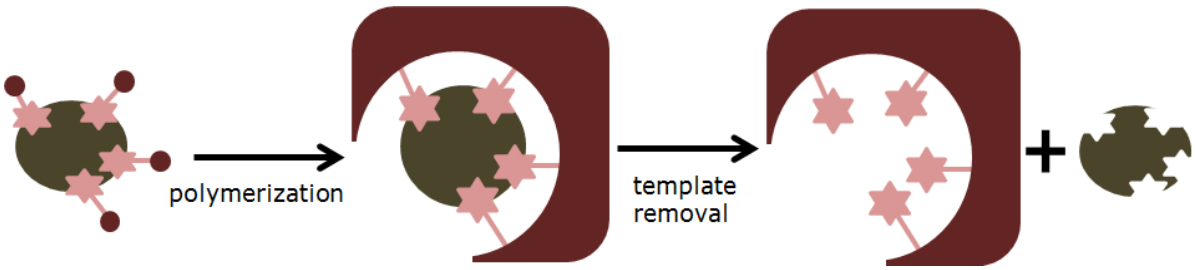

Figure 8: Schematic representation for the preparation of MIPs.

Monomers of the MIPs are chosen in accordance with their capability to interact with the functional groups of the template molecule to be imprinted. The interaction between template and monomer must be stable during the synthesis to be able to obtain homogenous population of binding sites and to eliminate the non-specific binding sites. An appropriate monomer-template complex must be arranged to make cleavage and formation of covalent bond reversible under mild conditions. Due to this requirement, the synthesis of MIPs is not an easy process. Still, even though the mechanism of MIPs is a bit challenging, their ability to mimic interactions that are originally established by natural receptors is quite useful without having any restriction regarding the stability. The MIPs synthesized show high stability and are resistant to pH, solvent and temperature changes [139].

The development of MIPs traces back to the studies of Polyakov and his laboratory partners. During an experiment they explored that silica gels showed high selectivity towards a solvent that was used in the preparation of the gel. This finding was later on associated with organic polymers by Wulff [140] and Haupt and Mocbach [141]. After their

discovery, MIPs were started to be used in chromatographic studies having the role as stationary phase. Along with this, they were begun to be employed in separation processes like chromatographic separations and purification elements for chiral separations to yield racemic resolution of drugs [142] [143].

Earliest experiments to benefit from recognition properties of MIPs for chemical sensing include the potentiometric measurements for the detection of enantiomeric separations using an HPLC column filled with MIPs [144], ellipsometric measurements employing Vitamin K1 imprinted polymers [145] and permeability studies of MIP membranes [146]. MIPs were also used quite commonly in solid phase extractions where they served as sorbents promoting cleaning, pre-concentration and extraction of target from the matrix. MIPs were even used as mimicked enzymes, for which they gained catalytic properties [147]. Not long after, they were introduced to the field of biosensors, where they served as alternatives to traditional recognition sections like antibodies, proteins and so on. The very first MIP based electrochemical sensor was established by Mosbach et al., which was a field effect capacitor phenylalanine anilide sensor. This sensor was based on the concept of detecting the decrease in capacitance when a target molecule was injected to the system [148]. The trend was then head towards the gold nanoparticle containing MIP based electrochemical sensors for the chemical analysis [149] [150] [151]. Detection limit down to $1.0x10^{-7}$ mol/L was reached employing this method. With a similar approach, Gam-Derouich et al. established an MIP based electrochemical sensor to detect dopamine where used gold nanoparticles on a gold electrode. With this sensor a detection limit of 0.35 nmol/L was calculated owing to highly selective dopamine cavities of the MIP [152]. Kan et al. also used MIPs for the recognition of dopamine, this time by applying it on a glassy carbon electrode. The developed sensor showed a linear response range of 5.0×10^{-7} to 2.0

$\times 10^{-4}$ M [153]. MIPs were also employed in the clinical analysis. A MIP based electrochemical sensor for the detection of streptomycin showed linear response for a wide range of 1.0×10^{-6} –1.0×10^{-3} mol L^{-1} and a detection limit of 1.5×10^{-9} mol L^{-1} was reached [154].

Polar porogens, hydrophilic co-monomers and crosslinkers or monomers that are designed to stoichiometrically interact with template molecule allow the recognition of molecule of interest by MIP cavities in aqueous media [155] [156] [157] [158] [159] [160]. As hydrophilic co-monomers, 2-hydroxyethyl methacrylate or acrylamide etc. and as cross-linkers pentaerythritoltriacrylate and methylene bis acrylamide etc. can be used. Methacrylic acid (MAA) and ethylene glycol dimethacrylate (EGDMA) are the most commonly used functional monomer and cross-linker, respectively. Apart from them 4-vinylpyridine (4-VP), 2-(trifluoromethyl)-acrylic acid (TFMAA) and trimethylolpropane trimethacrylate (TRIM) can be used as monomer and divinyl benzene (DVB), 2-hydroxyethyl methacrylate (HEMA) can be used as crosslinker.

The most commonly used method to synthesize MIPs is the two phase miniemulsion polymerization technique (Figure 9). In this method, two different aqueous phases and an oil phase are used. The oil phase is the one where the template molecule is added and is blended with the functional monomer, crosslinking monomer and the co-monomer in a certain ratio. This phase is then mixed with the first aqueous phase and allowed for homogenization. Once this process is completed, the second aqueous phase is combined with the mixture of first and oil phases and blended with a magnetic stirrer. Then, the polymerization mixture is heated to a certain temperature to allow polymerization to take place. In the last step, the initiator pair is added to the resulting blend and the polymerization progress is let for the next 24 hours (the duration may vary depending on the reaction) [161]. Characterization of the prepared

MIPs can be carried out with a number of devices. For instance; Fourier Transform Infrared Spectroscopy (FTIR) can be employed for the detection of unstable substances and more importantly to enlighten the mechanism of chemical reactions. The size and dispersity of the MIPs can be checked with Zetasizer, which measures the average size and polydispersity index of the synthesized MIP particles. Scanning Electron Microscopy (SEM) can be employed to characterize the size, morphology and the degree of aggregation of the MIP particles immobilized on a surface.

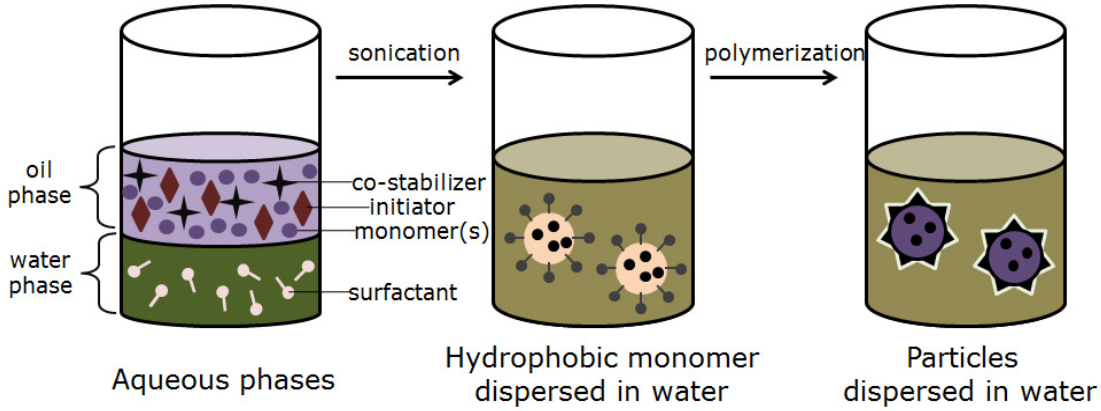

Figure 9: Diagram for the miniemulsion polymerization.

The phenomenal stability of MIPs, their tailor-made feature and low price make them notably suitable for sensor applications.

2.6. Towards the Combination of Micromechanical Systems and MIPs

The very first MIP combined sensor reported had capacitance features [148]. The system was composed of a thin phenylalanine anilide imprinted polymer membrane with a field effect capacitor. The analyte adsorption led to variations in capacitance, which enabled qualitative detection of the molecule of interest. The capacitive detection approach

was employed by other researchers as well. For instance, phenol was electropolymerized and used as receptor layer at gold electrodes with the existence of phenylalanine and insulating properties of the polymer layers were studied [162].

During the period between 1997-2000, mass-sensitive acoustic transducers like Love-wave oscillator [163], Surface-Acoustic Wave (SAW) oscillator [164] [165] and QCM [164] [165] [166] [167] [168] [169] [170] became quite popular for their usage in MIP based sensors. One of the first examples where MIPs met mass-sensitive transducers was by Dickert et al [164]. In the study, MIP technology was applied to QCM and SAW oscillator, both consisting of quartz substrate which undergoes deformation when electrodes are exposed to an altering voltage. The resonance frequency of both devices change with their masses, therefore, adsorption and desorption could be easily tracked. In the study, the sensitivity of 10 MHz QCMs and 433 MHz SAWs in organic solvent vapour detection were compared in respect of the dependency on sensitivity of the device's oscillation frequency. This approach was followed by Haupt et al., where an enantioselective chemical sensor was developed [167]. The sensor was based on MIPs and QCM, which were the recognition element and the transducer, respectively. The increase in the polymer's mass resulting from adsorption of analyte was detected with piezoelectric microgravimetry employing QCM. The sensor could distinguish R- and S-propanol enantiomers in acidified acetonitrile solutions due to the enantioselectivity of the imprinted cavities of MIPs. The detection limit of the sensor was determined as 50 mmol/L.

Even though MIP based multisensors were foreseen quite a while ago [171], merely a single study was reported which may be specified as MIP multisensor [172]. Up to that point, optofluidic systems were not yet used in on-chip sample preparations. In that study, microfluidics

were combined with MIPs for the detection of cholesterol, progesterone and testosterone simultaneously, employing Surface Plasmon Resonance (SPR) [172].

A crucial factor during the establishment of MIP sensors is the proper combination of polymer with the transducer. Mostly, MIP should touch to transducer's surface. Integrating this stage in an automated design process would make the work easier. The polymer may be allowed to forn *in situ* at the transducer's surface or the surface itself may be coated with the polymer [173]. *In situ* formation of polymer may be performed with electropolymerization over a conducting surface such as gold [162] [168]. This technique, however, requires specialized polymer prescription. Rather applicable techniques are standard surface coatings including spin and spray coating [163] [164]. Using these methods, polymer coatings can be thin and homogeneous. Another method to produce a polymer layer over a flat surface is called the sandwich method. The polymer solution is poured between the flat surface (like a glass or a quartz disk) and the transducer and the process is initiated [167] [174].

Being a new research area, combination of microcantilevers and MIPs has only been subjected to a few studies. Usage of MIP arrays as sensors in an applicable form has always been a challenge. Nonetheless, the first study was revealed in 2006 by Johansson et al., where a polymeric cantilever-based biosensor was prepared [175]. Surface stress changes due to binding of biomolecules to the cantilever' surface was detected using a SU-8 cantilever with integrated piezoresistors. Surface stress changes of around 0.1 N/m were recorded for the detection of mercaptohexanol. It should be noted that SU-8 is a photoplastic polymer and provides a wide range of application areas in microtechnology [176]. SU-8 cantilevers were also used in another study where they were fabricated and processed and investigated over

a certain period of time in terms of initial bending, release and time stability [177]. SU-8 cantilevers were fabricated employing dry release method and two step photolithography. The processing was optimized in order to obtain low initial bending resulting from residual stress gradients. Finally, SU-8 cantilevers were used to develop ultrasensitive nanomechanical cantilever sensor system. An organic field effect transistor sensitive to strain was integrated in a polymer nanomechanical cantilever [178]. The sensor developed had a surface stress sensitivity of 401 $[mN/m]^{-1}$ with low-noise floor and became a potential biochemical sensor with a minimal measurable surface stress in the range of 0.18 mN/m.

After the breakthrough in the combination of polymers with variety of sensor systems, Ayela et al. combined the resonant piezoelectric micromembranes with MIPs [179]. They showed the first experimental proof-of-concept for MIP combined resonant MEMS. The micromembrane arrays were fabricated and covered in MIPs employing a cantilever array based deposition tool. The MIP dribbles were then polymerized with the exposure of UV light. To record the dynamic characteristics of MIPs throughout the polymerization process, an electronic setup was used which provided the multiplexed online tracing of micromembranes' resonance frequency. During polymerization, resonance frequency was said to be increased dramatically. It was estimated that a stiffness increase induced the rise in frequency. Layer enhancement via cross-linking polymerization seemed to be responsible for the increase in resonance frequency. The online tracing of the polymerization progress provided background information regarding the minimum amount of time for polymerization to take place. Results showed that the frequency values recorded afterwards the dribble addition and polymerization was linearly dependent on the added amount of the precursor solution. The verification of the results was carried out by the negligible frequency variation for the non-functionalized micromembranes. Dip-and-dry technique was employed

during the binding experiments. The changes in frequency were recorded as the template molecule was adsorbed and desorbed. After the first washing step where the template molecule was desorbed from the MIP cavities, a large increase in frequency was observed whereas smaller change was observed for the non-imprinted polymer (NIP) membrane. Because the resonance frequency did not produce the post-polymerization value after the incubation, the statement was made that the effectivity of binding sites in the course of the imprinting was below 100%. The standard deviation was calculated as 1.7 kHz after four adsorption and desorption cycles, which was less than 0.3% of the post-polymerization value. The group concluded that the low power consumption and stability of the MIP based MEMS as acoustic transducers showed great potential in biomimetic sensor systems.

In a further study by Ayela et al., cantilevers were fabricated directly with MIPs using an all-organic approach [180]. In the study, high cost equipment problem in the patterning of MIPs was solved by employing the shadow masking printing method. First flexible microstencil was fabricated by photolithography using highly cross linked negative epoxy based photoresist SU-8. Once the photopolymerization was complete, resultant MIP patterns were transformed onto cantilevers by superimposing thick SU-8 supports. The working mechanism of the prepared sensor system relies on the dynamic sensing mode; that is, the binding of template into cavities of imprinted polymer leads to a direct mass change which then changes the resonance frequency of the MIP cantilever. However, there exists a possibility to observe changes in viscoelasticity of the material as well. For the validation of the sensor system, a low molecular weight analyte was chosen. NIP cantilevers and opposite enantiomer of the analyte were also used for the control studies to check the specificity and selectivity, respectively. Results showed that the relative shift in frequency was much larger in MIP cantilever than that of the NIP cantilever. In liquid experiments, no

specificity was obtained; as the analyte was adsorbed equally by both MIP and NIP cantilevers. This situation was guessed to be due to the non-specific hydrophobic interactions. The limit of detection (LoD) of the prepared sensor was determined as 100 nM.

3. MATERIALS AND METHODS

3.1. Materials

The functional monomer, co-monomer, and crosslinker used for the synthesis of MIPs, namely methylacrylic acid (MAA), 2-hydroxyethyl methacrylate (HEMA) and ethylene glycol dimethacrylate (EGDMA) were purchased from Sigma (St. Louis, MO, USA).Template molecules CPX and ERY were purchased from Sigma-Aldrich (St. Louis, MO, USA). CPX stock solution was prepared by dissolving CPX (0.005 g) in 50 mL acetate buffer at pH 4.7 to make the final concentration 300 μM (100 ppm) and two different stock solutions of ERY were prepared by dissolving ERY (0.005 g) in 50 mL ethanol (EtOH) and hydrochloric acid (HCl) to make the final concentration 136 μM (100 ppm). Acetic Acid (HAc) was obtained from Fluka (St. Gallen, Switzerland) and EtOH and HCl were purchased from Sigma-Aldrich (St. Louis, MO, USA). All solutions were prepared with ultra-pure water obtained from Milli-Q water purification system (Millipore Corp., Bedford, MA) with resistivity of 18.2 MΩ cm. Methanol (MeOH) used in the preparation of desorption solution was purchased from Sigma-Aldrich (St. Louis, MO, USA). A mixture of MeOH:HAc (9:1, v/v) was prepared as the desorption solution [181] [182]. (3-Aminopropyl)triethoxysilane (APTES) and trimethylamine (TEA) used in amination process and the chemicals used in activation step; *N*-Hydroxysuccinimide (NHS), *N*-(3-dimethyl aminopropyl)-*N'*-ethylcarbodiimide hydrochloride (EDC) and phosphate buffered saline (PBS) were all obtained from Sigma-Aldrich (St. Louis, MO, USA). It should be noted that APTES, TEA and EDC must be handled in fume hood only. EDC box should be filled with Argon after use, and must be sealed properly. All-In-One-Al-Tipless Budget Sensors AFM chips were purchased from NanoAndMore (Wetzlar, Germany).

3.2. Preparation and Characterization of CPX and ERY Imprinted Polymeric Nanoparticles

3.2.1. Preparation of CPX and ERY Imprinted Polymeric Nanoparticles

Both MIPs were synthesized with two phase miniemulsion polymerization technique. In the preparation of CPX imprinted polymeric nanoparticles (CPX-IPN) (Figure 10), first aqueous phase was obtained by dissolving polyvinyl alcohol (PVA) (93.75 mg), sodium dodecyl sulphate (SDS) (14.425 mg) and sodium bicarbonate (11.725 mg) in 5mL ultra-pure water. Dissolving PVA (50 mg) and SDS (50 mg) in ultra-pure water (100 mL) gave the second phase. 100 µmol CPX and 254.1 µL of MAA were mixed with a molar ratio of 1:16 for the oil phase. 1.05 mL EGDMA and 225 µL HEMA were then added to this mixture. The oil phase then mixed with the first aqueous phase and in order to initiate the miniemulsion, a homogenizer was used at 2500 rpm (T10, 1ka, Labortechnik, Germany). As soon as the homogenization was complete, the resulting mixture was combined with the second aqueous phase in a magnetic stirrer (Radleys Carousel 6, UK). The final mixture was stirred at 600 rpm while heated to 40 °C slowly, at which the polymerization process begins. Lastly, the initiator pair of 125 mg sodium bisulfide and 125 mg ammonium persulfate was added and the polymerization was allowed to continue for the next 24 hours. To remove the un-polymerized particles, prepared polymeric nanoparticles were centrifuged at 26500 rpm (Allegra- 64 R Beckman Coulter, USA) for an hour. After the first centrifuge, particles were rinsed in order to remove the unreacted monomers, surfactants and initiators by using water: EtOH (1:1, v/v) mixture. The template removal was performed washing the particles with desorption solution and centrifuging after each step until a clear solution was obtained. The washed particles were dispersed in ultra-pure water and stored at 4 °C.

The non-imprinted polymeric nanoparticles were synthesized with the same procedure in the absence of the template molecule [183].

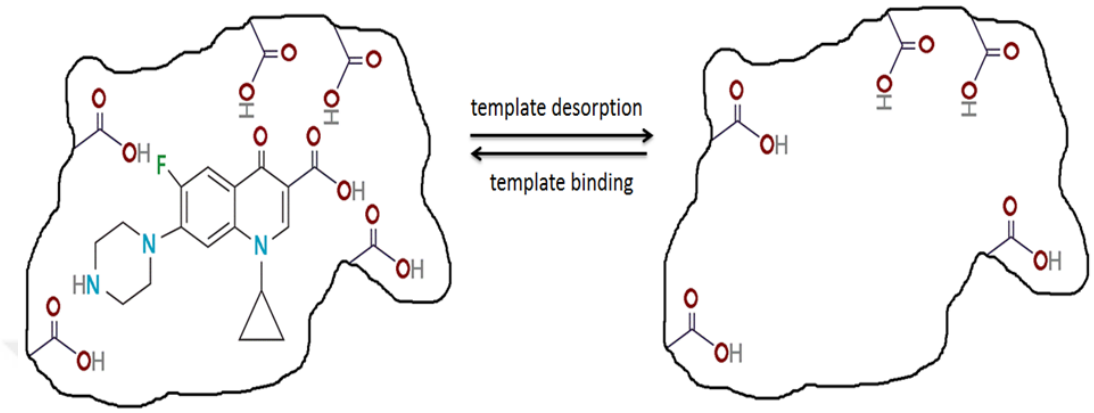

Figure 10: Schematic representation of CPX-IPN.

The ERY imprinted polymeric nanoparticles (ERY-IPN) (Figure 11) were prepared likewise. First aqueous phase was obtained by dissolving PVA (93.75 mg), SDS (14.425 mg) and sodium bicarbonate (11.725 mg) in 5 mL ultra-pure water. Second aqueous phase was then obtained by dissolving PVA and SDS (50 mg each) in 100 mL ultra-pure water. For the organic phase, 190 µL MAA, 225 µL HEMA and 1.05 mL EGDMA were mixed. The molar ratio between monomer and template was again set to 1:16, for this purpose 100 mg ERY (135 µmol) was added to the organic phase. The organic phase was then combined with the first aqueous phase. In order to initiate the miniemulsion, the mixture was placed into a homogenizer (T10, 1ka, Labortechnik, Germany) and homogenized at 2500 rpm. The resulting mixture was merged with the second aqueous phase after the homogenization and stirred at 600 rpm in a magnetic stirrer (Radleys Carousel 6, UK) and heated to 40 °C. Lastly, initiators sodium bisulfide (125 mg) and ammonium persulfate (125 mg) were added and left untouched for the next 24 hours. Once the polymerization was complete, the large particles were removed by

centrifuging at 5000 rpm. The left nanoparticles were then centrifuged for 90 min at 26500 rpm (Allegra-64R Beckman, Coulter, USA). In order to remove the unreacted monomers, surfactants and initiator, the particles were washed with water:EtOH (1:1, v/v). Finally, the particles were washed with ultra-pure water until a clear solution was obtained. The washed nanoparticles were dispersed in ultra-pure water and stored at 4 °C. The non-imprinted polymeric nanoparticles were synthesized with the same procedure in the absence of the template molecule [161].

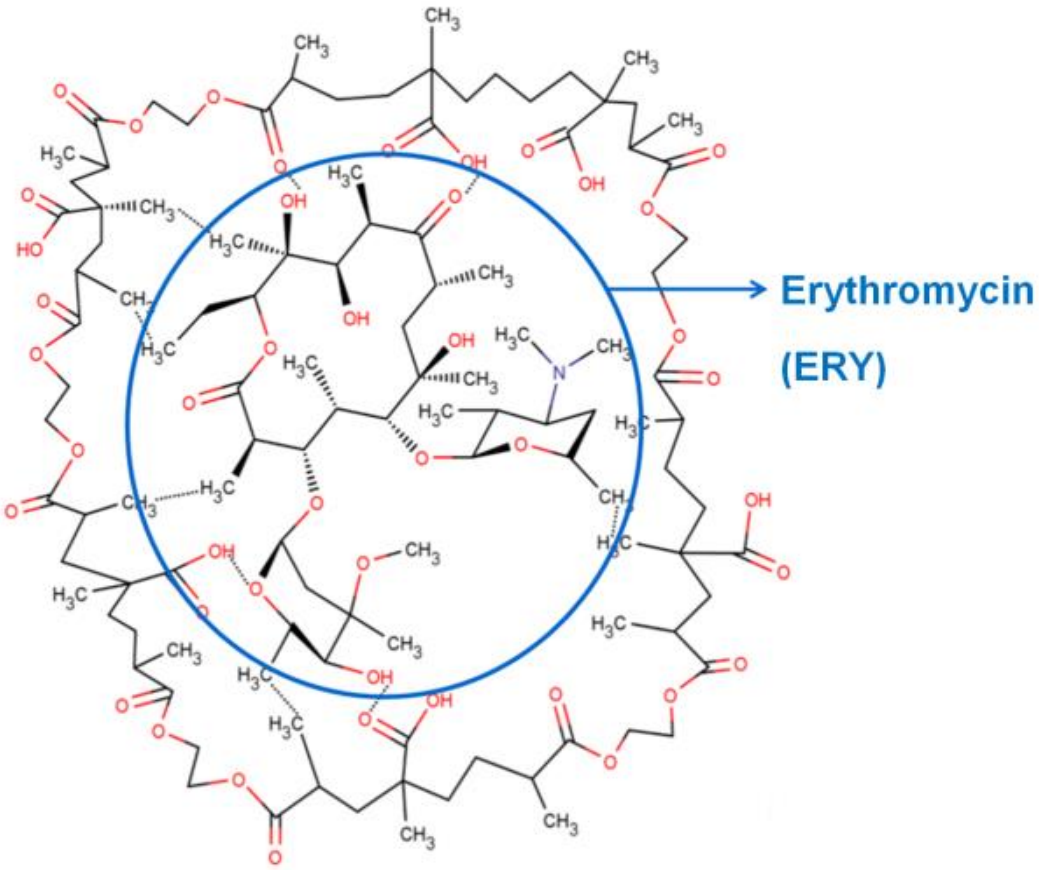

Figure 11: Schematic representation of ERY-IPN.

3.2.2. Characterization of CPX and ERY Imprinted Polymeric Nanoparticles

Characterization was performed by using several instruments. Size distribution was done by Nano Zetasizer (NanoS, Malvern Instruments, London, UK). Light scattering from the nanoparticle solution measured at an incident angle of 90° at 25°C. Each result was obtained by calculating the average value of three measurements. In order to analyse the functional groups present, Fourier Transform Infrared Spectrometer (FTIR, Thermo Fisher Scientific, MA, USA) was used. For this investigation, a homogeneous MIP/KBr was mixture was prepared. The samples to be tested were processed by blending 2 mg MIP with 98 mg KBr, from which disks were formed. Spectra from surface were collected at 2 cm^{-1} resolution within the range of 650-4000 cm^{-1} [161].

3.3. Instruments and Setup

All-In-One-Al-Tipless chips have four cantilevers with 15, 80, 150 and 350 kHz frequencies (Figure 12). These cantilevers have different lengths and spring constants. The cantilever D and C, which have the highest frequency values were chosen for dynamic mode experiments in air, as they give the highest quality factor, which directly affects the sensitivity of the sensor system. The binding experiments were carried out employing the dynamic mode, which were performed using Atomic Force Microscopy (Nanomagnetics Instruments, Ankara, Turkey) (Figure 12). The excitation amplitude was set to 100% during all experiments.

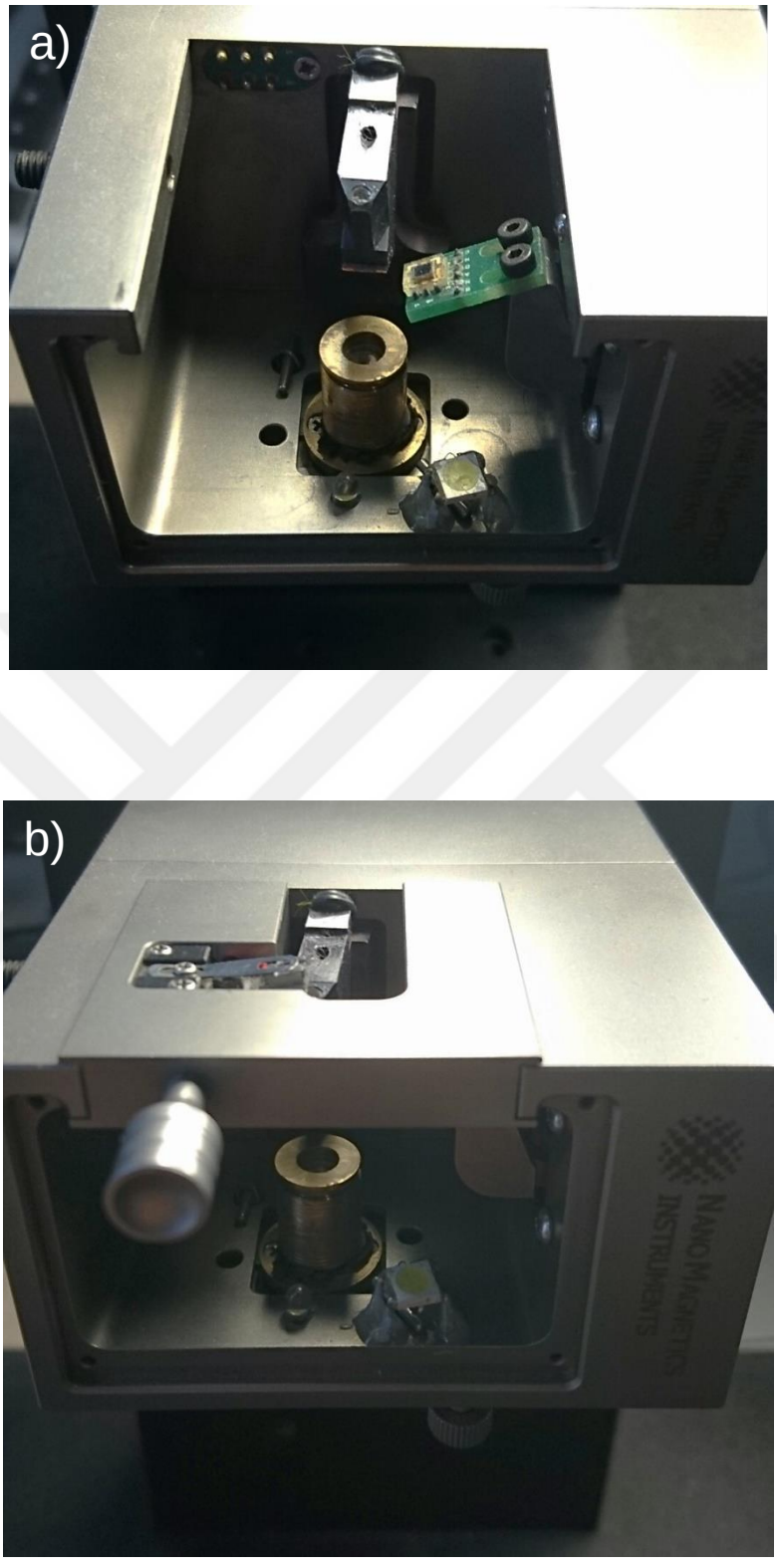

Figure 12: Real images of AFM used during validation studies; a) without and b) with the cantilever holder apparatus.

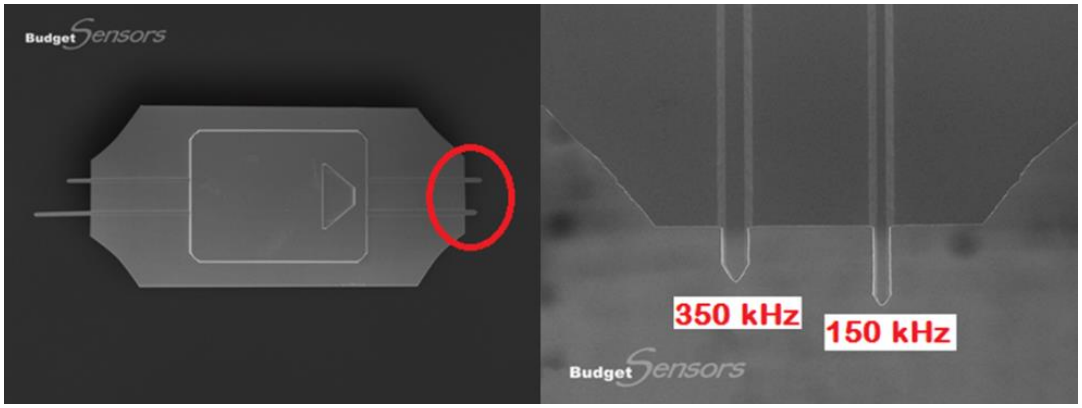

Figure 13: SEM image of the AFM chip (left) and cantilevers used (right). (http://www.nanoandmore.com/AFM-Probe-All-In-One-Al-Tipless.html)

3.3.1. Preparation of and Characterization over Microcantilever Sensor System

Immobilization of the MIPs on the surface of the cantilevers was performed in three different approaches.

- ✓ In the first method, 50 µL of MIP nanoparticles were dropped on the cantilevers. After 30 min, the cantilevers were washed with ultra-pure water.
- ✓ In second method, 50 µL of MIP nanoparticles were similarly dropped on the cantilevers, however this time the cantilevers were then exposed to UV light and the nanoparticles were allowed to dry on them.
- ✓ In the third method, covalent immobilization of MIP nanoparticles onto surface of cantilever via EDC/NHS activation. Cantilevers must be cleaned before being subjected to any functionalization. Therefore, all chips were first left in chloroform for 5 min for 3 times to remove any unwanted residues. They were dried with nitrogen immediately after. In order to attach the MIPs on cantilevers covelently, the chip surface must be introduced with

the amine groups. For the amination process, 30 µL APTES and 10 µL TEA was dropped separately in a Teflon® petri dish and placed in an Argon-filled desiccator together with the chips (Figure 13). Argon is an inert gas that allows for a better environment for the reaction to take place. After 2 hours, Teflon® petri dish was taken from the desiccator and the chips were left for the following 2 days to undergo the curing process [184]. The APTES modification provides a better control over the chemistry of the surface, as it acts like a self-assembled monolayer.

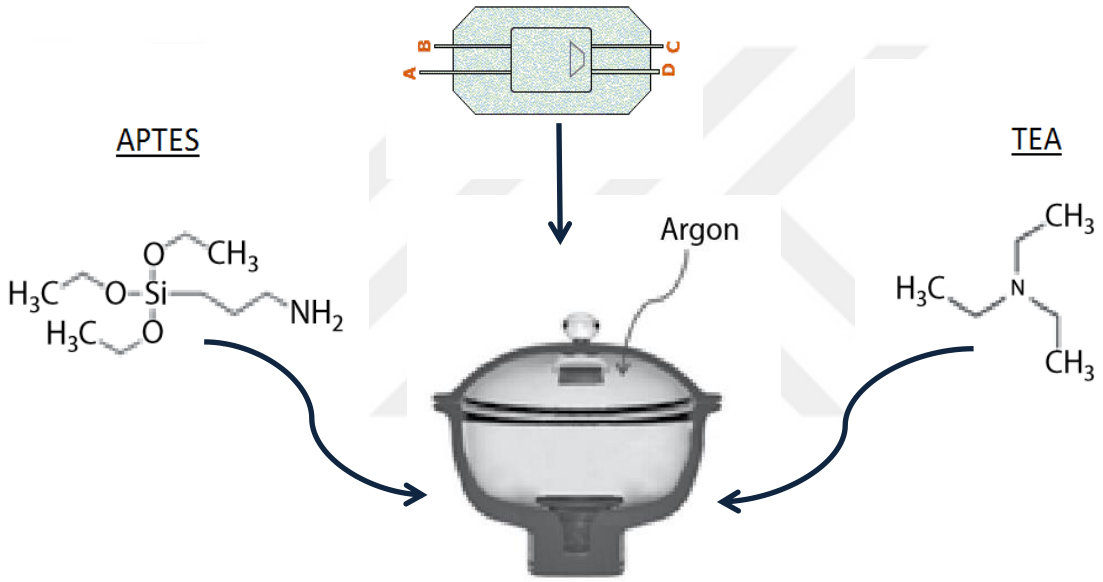

Figure 14: Schematic representation of the amination process.

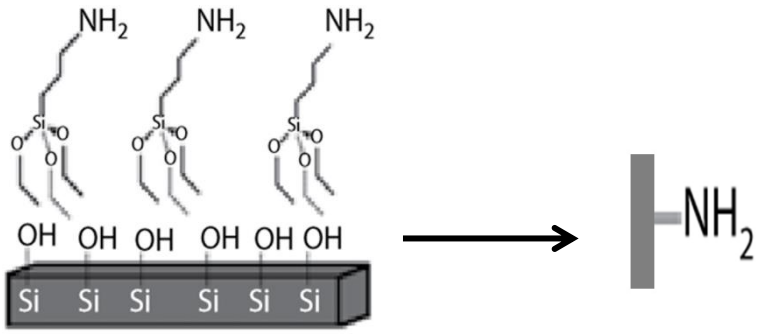

Figure 15: Schematic representation of the aminated cantilever surface.

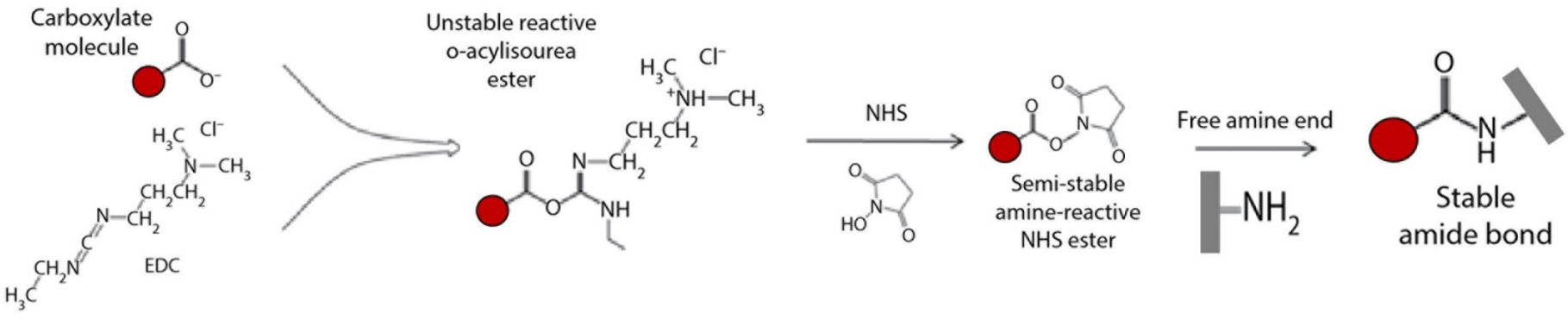

Figure 16: Schematic reaction chain of EDC/NHS activation.

Normally, a template-monomer ratio of 1:8 is sufficient for imprinted polymers to form. Yet, covalent attachment of the polymeric nanoparticles requires the usage of carboxyl groups of the nanoparticles. These groups are also responsible for capturing the template molecules. Therefore, in order to create additional carboxyl groups this ratio was increased to 1:16. Thus, further carboxyl groups were formed to adsorb the template molecules, while the rest of these groups were being used to their covalent attachment on the surface of the cantilever.

Conjugation of carboxyl groups within the MIPs to primary amines formed on the surface of the cantilever was provided by carbodiimide crosslinking agent EDC, which activates the carboxyl groups for spontaneous reaction. NHS converts the carboxyl groups into amine-reactive NHS esters to predispose MIPs for immobilization (Figure 14). For this reaction chain, 31.25 mM EDC and 6.25 mM NHS were mixed with MIPs in 10 mM PBS buffer and allowed to stay together for 2 hours. The excess EDC and NHS were then removed from the mixture by centrifuging and the pellet was re-suspended in PBS buffer at pH 6.0. The APTES coated chips were left in this solution overnight for immobilization of MIPs to take place on the surface (Figure 15). It should be noted that pH is a significant parameter during this process. The ligand must uncharged for reaction with activated ester to occur.

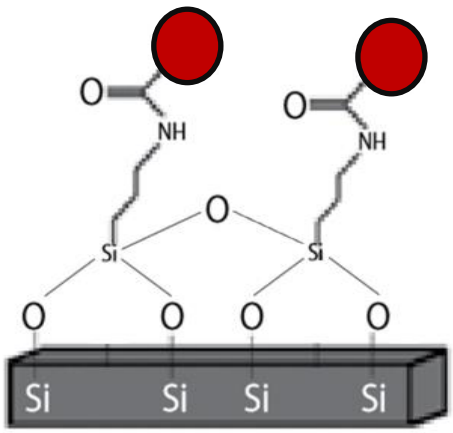

Figure 17: Schematic representation of the immobilization of MIP nanoparticles on the aminated surface of a cantilever.

To investigate the shape and localization of the MIPs and their level of aggregation Scanning Electron Microscope (SEM) was used. Imaging with SEM (JEOL JSM 5600, Tokyo, Japan) was performed for the cantilevers with MIPs immobilized on. The morphology and distribution of the MIPs immobilized on the cantilever was characterized by AFM (Agilent, 5500, USA).

3.3.2. Validation of Microcantilever Sensor System

Validation of microcantilever sensor system was performed both in liquid and in air. Also, an online immobilization of MIP nanoparticles on the cantilever surface was recorded. For the real-time MIP immobilization, first the cantilever was oscillated in 1 mL of 0.01 M PBS buffer until the system reached equilibrium. Once a stable signal was obtained, 350 µL of the activation solution (EDC and NHS in 0.01 M PBS buffer) together with 350 µl of MIP solution was delivered to the system and left for 30 min for reactions to set in.

In air measurements, cantilevers were excited at their resonance frequencies. By doing a narrow scanning, exact frequencies of the cantilevers were determined. For the binding experiments in air, dip-

and-dry method was used. In a detailed manner, first the cantilevers were dipped into 500 µL of template molecule solution and left in it for 10 min to allow for adsorption to take place. Then, they were washed with buffer solutions (acetate buffer for CPX molecule and HCl or EtOH for ERY molecule) and ultra-pure water to eliminate the nonspecific interactions and dried with nitrogen immediately afterwards. This procedure was repeated for all concentrations (0.5, 1, 5, 10, 20, 50 ppm). For the desorption process of the template molecules, the same method was followed; cantilevers were immersed in the desorption solution for 30 min and dried with nitrogen subsequently. Before and after each step, the cantilever resonance frequencies were recorded.

For the real-time detection of template molecules in aqueous media, MIP modified AFM chips were placed into the liquid cell of the device, which has a liquid capacity of 2 mL. The system was first introduced with the buffer solution specially chosen for the analyte of interest; that is 100 mM acetate buffer for CPX molecule. For ERY molecule, either HCl or EtOH could be used; however both these chemicals harm the epoxy of the cantilever holder. Therefore, the liquid measurements were only performed for CPX molecule. Once a stable signal was obtained, different concentrations of CPX molecule in 100 mM acetate buffer was delivered into the system at a constant rate of 5 µL/min. When the adsorption took place and a shift in frequency was observed, 100 mM acetate buffer was send to the system once more to wash the nonspecific interactions away by using ultra-pure water. The final frequency was recorded when the signal was stable again.

Throughout the study temperature was set to 25.0 ± 0.1 °C. Calibration curve was drawn by calculating the frequency shifts. The adsorbed mass (Δm) and the limit of detection (LoD) were calculated via this curve.

4. RESULTS, DISCUSSIONS AND CONCLUSION

4.1. Results and Discussions

4.1.1. Characterizations

4.1.1.1. Characterization of Ciprofloxacin Imprinted Polymeric Nanoparticles

The polymerization process of CPX-IPN resulted in a narrow size distribution with a polydispersity index of 0.210 and average diameter of around 110.20 nm as determined by the Nano Zetasizer (Figure 16). Same analysis was also performed for the NIPs in which their polydispersity index and average diameter was found to be 0.256 and 100.53 nm, respectively. FTIR spectroscopy was used to obtain the chemical characterization of MIPs and NIPs (Figure 17). Because both polymers were synthesized using same functional monomer and crosslinker, namely MAA and EGDMA, their FTIR spectra were similar. The most prominent bands in both spectra were observed to be the O-H stretching bands at around 3200-3300 cm^{-1}, which correspond to the MAA hydroxyl group. The aliphatic C-H stretching (around 2900-3000 cm^{-1}) and bending (around 1150-1250 cm^{-1}) bands observed correspond to the methyl groups of MAA and EGDMA. The C=O stretching bands (1700-1750 cm^{-1}) and the C-O stretching bands (1150-1250 cm^{-1}) correspond to the carbonyl and carboxyl groups of MAA and EGDMA. Overall, both spectra proved that functional monomer MAA was found in both MIP and NIP nanoparticles.

a)

MIP	Size (d.n...	% Intensity:	St Dev (d.n...
Peak 1:	43,43	100,0	18,81
Peak 2:	0,000	0,0	0,000
Peak 3:	0,000	0,0	0,000

Z-Average (d.nm): 36,70
PdI: 0,144
Intercept: 0,948
Result quality Good

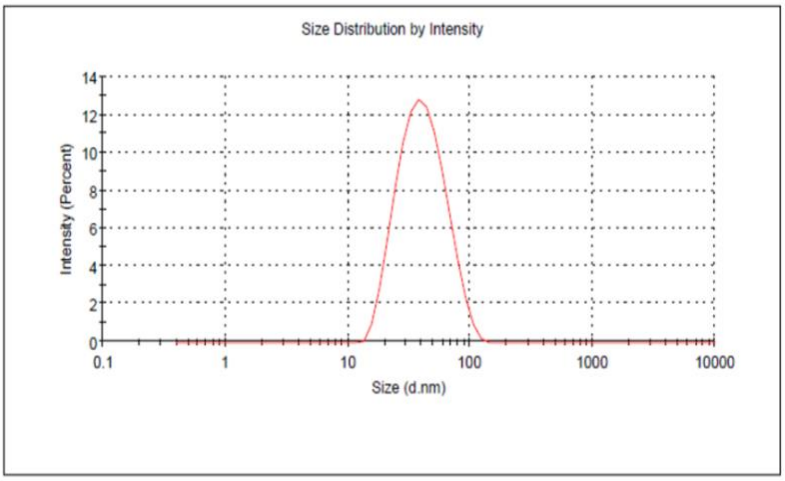

b)

NIP	Size (d.n...	% Intensity:	St Dev (d.n...
Peak 1:	42,60	100,0	17,28
Peak 2:	0,000	0,0	0,000
Peak 3:	0,000	0,0	0,000

Z-Average (d.nm): 36,55
PdI: 0,134
Intercept: 0,948
Result quality Good

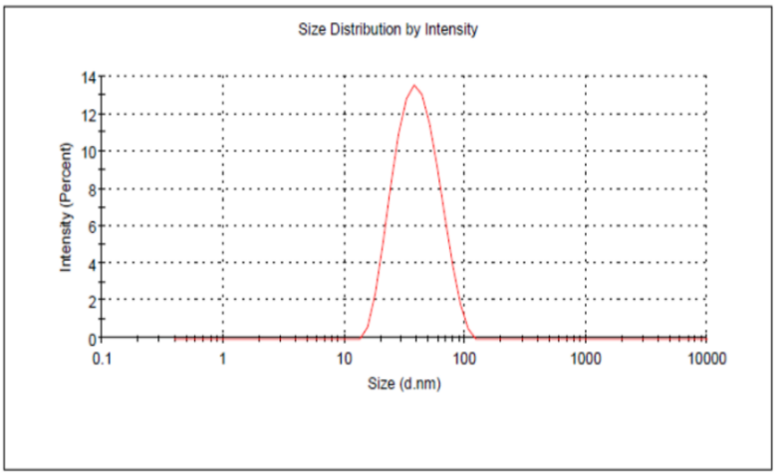

Figure 18: Zetasizer results of a)CPX-IPN, b) NIPs.

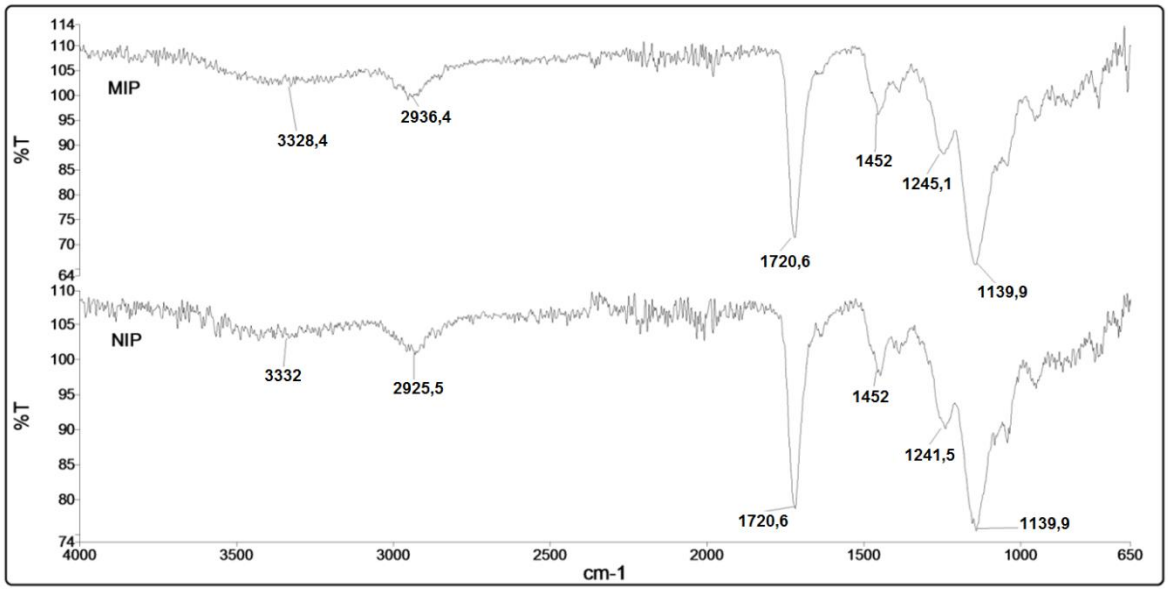

Figure 19: FTIR spectrum of CPX-IPN (upper) and NIP (lower).

4.1.1.2. Characterization of Erythromycin Imprinted Polymeric Nanoparticles

The configuration of the synthesized polymeric nanoparticles was carried out with Zetasizer by Sari et al. [161] (Figure 18). The polydispersity index of ERY-IPN and NIP were determined as 0.134 and 0.132, respectively. The average size of MIP and NIP nanoparticles were found as 42.60 nm and 41.25 nm, respectively. The chemical structures of the ERY-IPN and NIP were revealed using FTIR spectroscopy by Sari et al. [161] (Figure 19). Due to almost-the-same synthesis procedure, both spectra were again quite similar. The common bands in these spectra can be listed as following; aliphatic C-H stretching bands at 2950 cm^{-1} due to methyl group and C=O stretching bands at 1720 cm^{-1} due to MAA and EGDMA carbonyl group, O-H stretching bands at 3440 cm^{-1} due to hydroxyl group and C-O stretching bands at 1250 cm^{-1} due to MAA carboxyl group, C-O stretching bands at 1130 cm^{-1} due to

EGDMA ester group. The listed bands in indicate that functional monomer MAA was found in MIP and NIP nanoparticles [161].

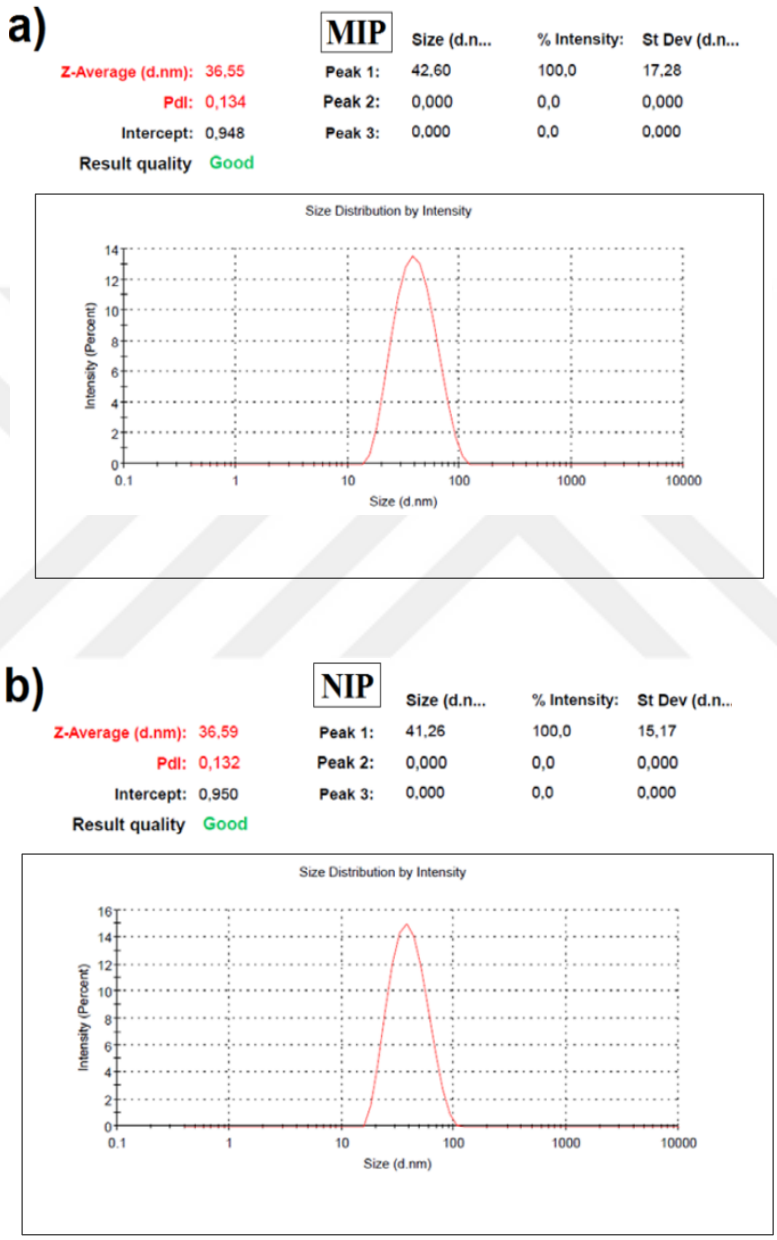

Figure 20: Zetasizer results of a) ERY-IPN, b) NIPs [161].

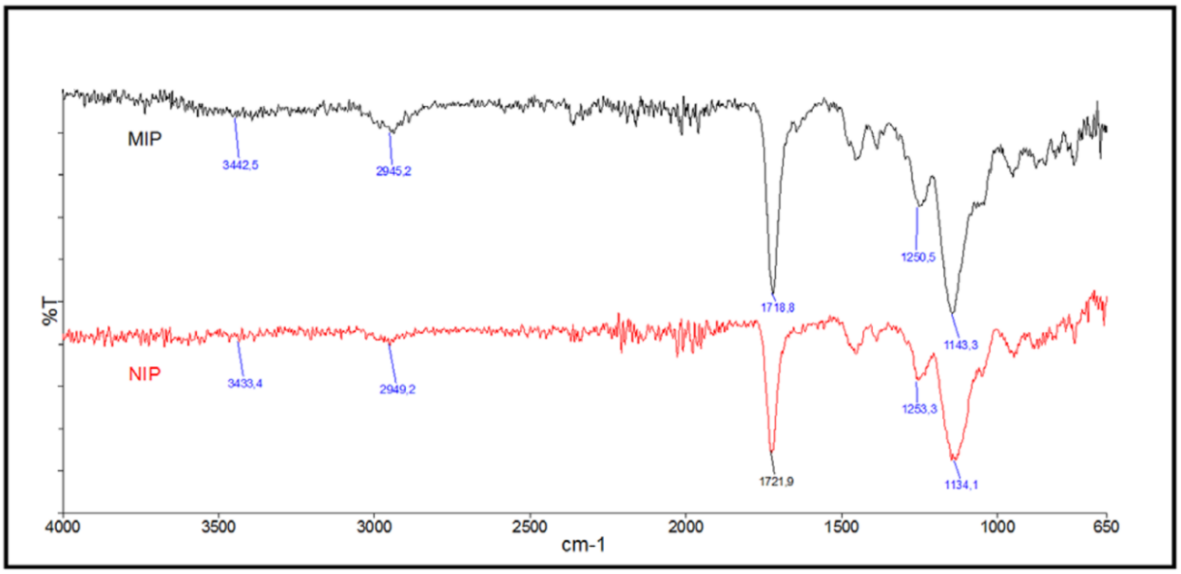

Figure 21: FTIR spectrum of ERY-IPN (upper) and NIPs (lower) [161].

4.1.1.3. Characterization of MIP Modified Microcantilevers

Size and distribution characterization of the immobilized MIPs was carried out with SEM. To begin with, surface of a bare cantilever was imaged with SEM (Figure 20). Three different immobilization approaches explained in detail in Materials and Methods section were performed for the CPX-IPN to see how each approach result in and to make a decision on which method to continue with, as they were larger in size.

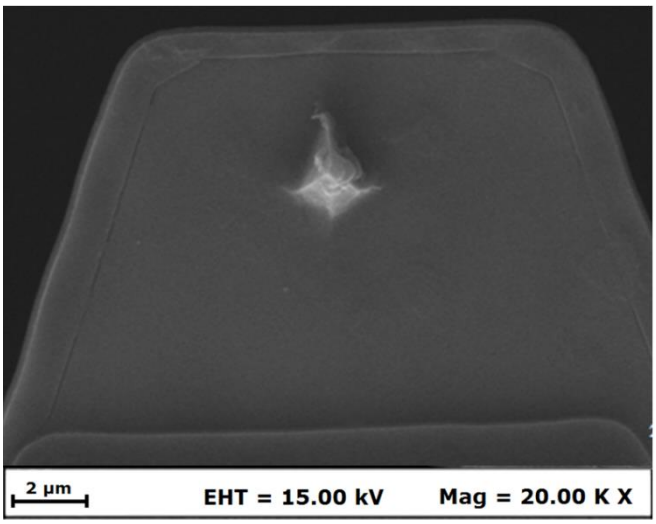

Figure 22: SEM image of the bare cantilever without any MIP nanoparticles immobilized.

The SEM images of the cantilever that was prepared using the first approach showed that direct incubation of nanoparticles does not work, as significant amount of the particles was removed from the surface after the washing step. Moreover, no difference was observed in the resonance frequency, which meant that there wasn't any load resulting from the immobilization of the MIP nanoparticles since they were washed away. The SEM images of the cantilever that was prepared using the second approach showed that drying the MIP nanoparticles on the surface by exposing it to UV light resulted in over-accumulation and multilayer coverage. Also, the cantilever's resonance frequency shift after the immobilization was too large, and the reading changed in each measurement. These obtaining showed that the physical immobilization techniques listed above do not work properly; therefore these methods can and should not be used as immobilization methods for the further experiments in the validation of the sensor system.

The SEM images of the cantilever that was prepared using the third approach were agreed to be promising (Figure 21). Characterization of the cantilever prepared with the third method was carried out with both

SEM and AFM, where shape, size, dispersity and layer properties were investigated. The CPX-IPN were found to be spherical in shape and to have size of around 160 nm by SEM images. Same characterization results displayed that the particles showed high monodispersity.

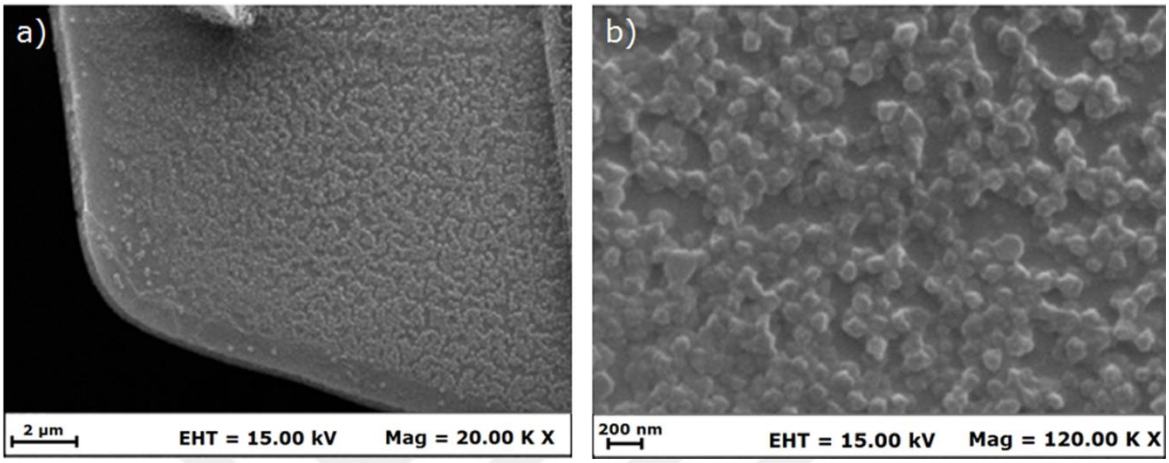

Figure 23: a) SEM image of the cantilever with CPX-IPN immobilized on via EDC/NHS activation, b) zoomed in version of the particles.

The MIPs-modified cantilever surface was scanned with AFM (Figure 22). According to the line profile obtained from the AFM image, a monolayer surface coverage was accomplished. Roughness of the surface has a significant role in the determination of functional performance of the device. It shows the shagginess of the immobilized nanoparticles on the surface. The roughness value of the bare cantilever in terms of Root Mean Square (RMS) was determined to be approximately 2.3±0.1 nm, whereas this value was increased to 7.4±0.5 nm after the immobilization of MIP nanoparticles using the third method, namely the EDS/NHS activation.

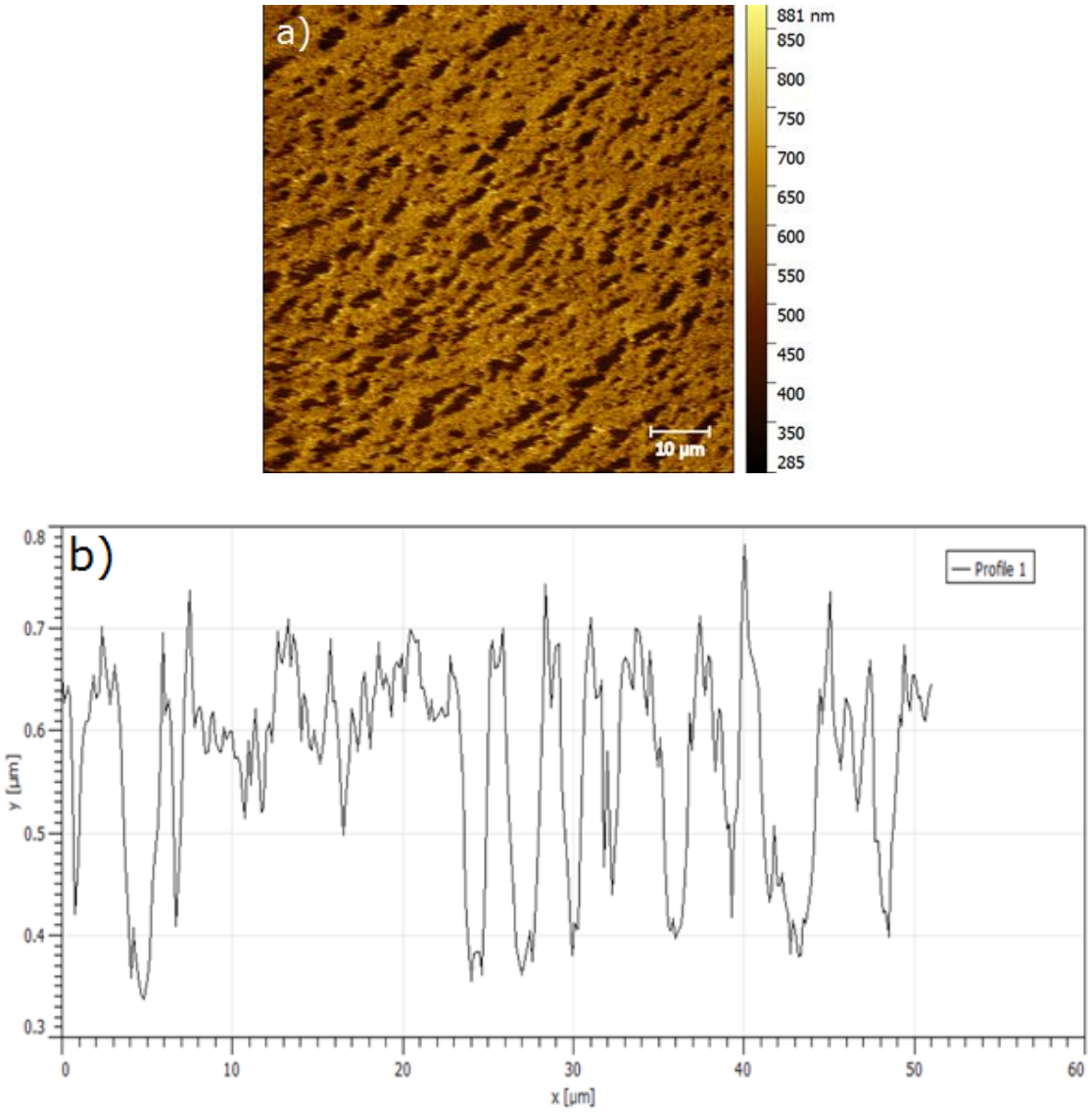

Figure 24: a) AFM image of CPX-IPN immobilized on the cantilever via EDC/NHS activation, b) line profile of the AFM image.

Having determined the proper immobilization technique for the MIPs, preparation of ERY-IPN modified cantilever was directly carried out using EDC/NHS activation. Size and distribution of the particles were once more characterized with SEM (Figure 23). This time however, the SEM imaging process was rather difficult because the ERY-IPN were too small. SEM investigation of the cantilever showed that the particles were spherical and around 30 nm.

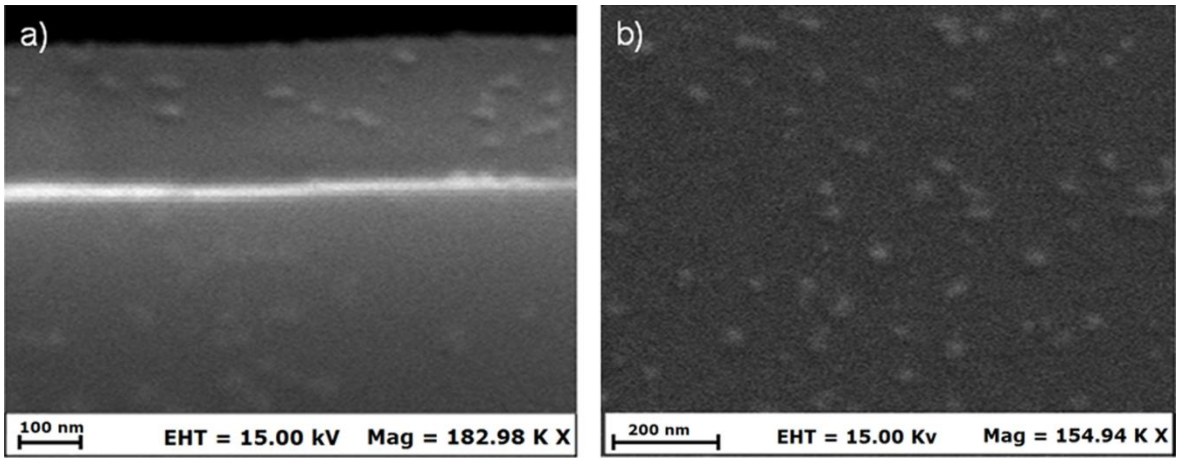

Figure 25: a) SEM image of the cantilever with ERY-IPN immobilized on via EDC/NHS activation, b) zoomed in version of the particles.

Further characterization of the particles on the cantilever surface was performed with AFM (Figure 24). The AFM images showed that a monolayer surface coverage was accomplished. The RMS roughness of the bare cantilever surface was previously determined as approximately 2.3±0.1 nm, while this value went up to 4.3±0.3 nm after the immobilization of MIP nanoparticles.

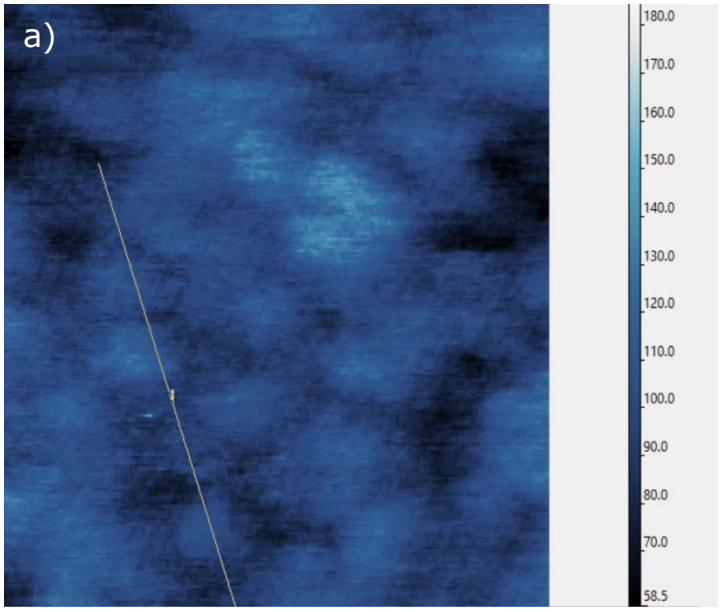

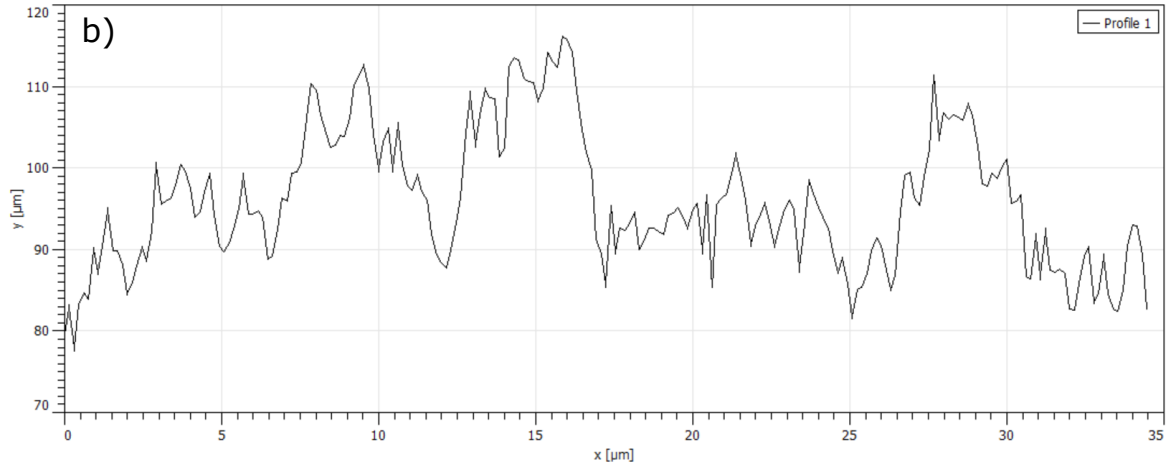

Figure 26: a) AFM image of ERY-IPN immobilized on the cantilever via EDC/NHS activation, b) line profile of the AFM image.

4.1.2. Validation of the Microcantilever Sensor System

4.1.2.1. Validation of CPX Specific Microcantilever Sensor

In all binding studies, whether it was performed in air or in liquid, cantilever with highest nominal frequency (D), 350 kHz, was used. This was mainly because it yielded the highest Q of 603.43, which is one of the most important parameters in these type of studies. The exact resonance frequency of the cantilever was determined as 410.5±0.01 kHz in air (Figure 25a). In validation studies in air, frequency shift resulted from the particles was determined by checking the cantilever's frequency before and after the immobilization process.

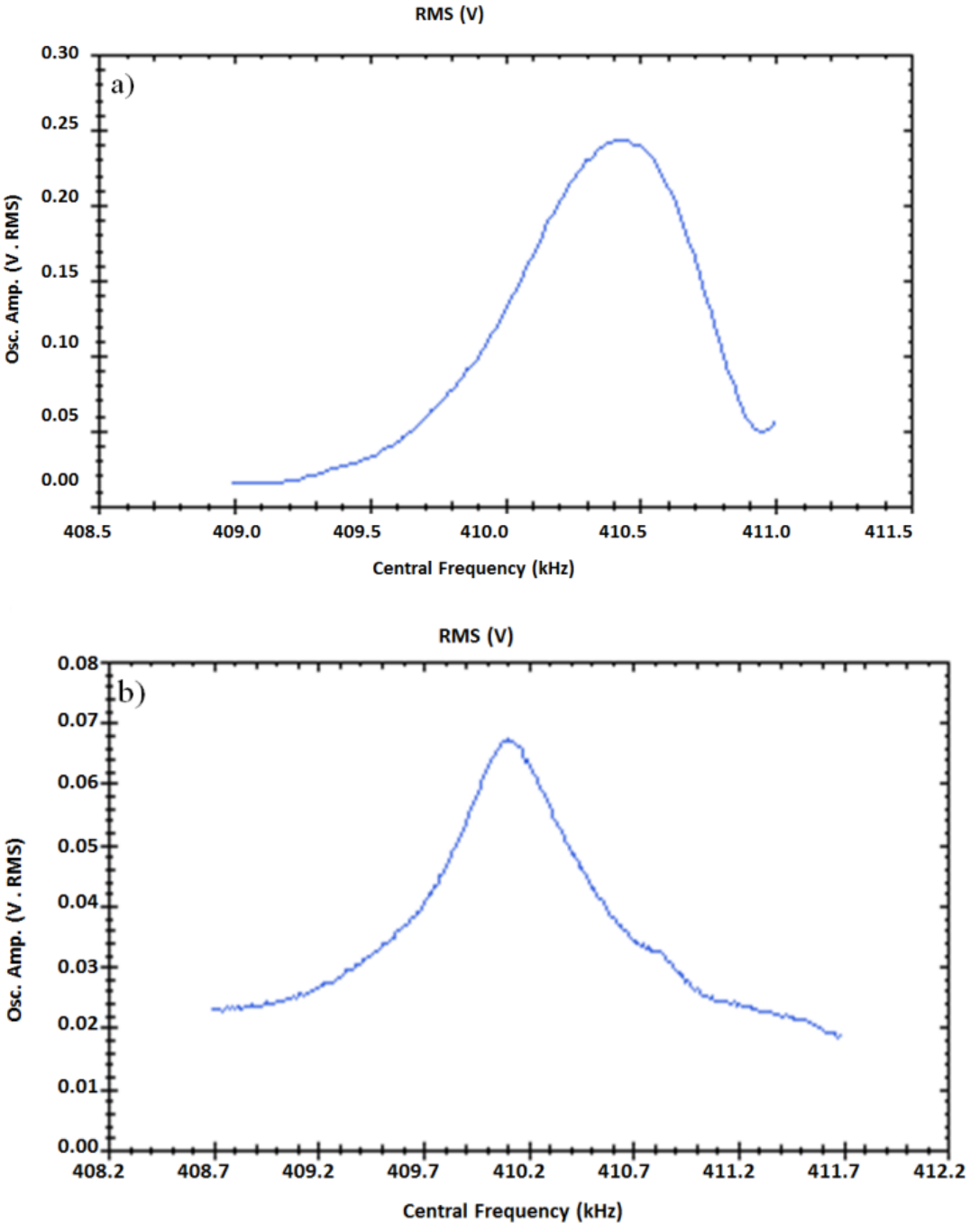

Figure 27: The frequency values of the cantilever in air a) before and b) after the immobilization of CPX-IPN.

For the liquid studies, first the immobilization of the CPX-IPN was recorded online (Figure 26). It took around 22 min for particles to be immobilized on the surface. The frequency shift obtained was around 480 Hz. However, it was noticed that there was huge amount of noise during this online recording. The noise itself had an effect of approximately 50 Hz in liquid system while performing binding studies. This high noise, arising from the device and the system, unfortunately would prevent the further frequency change analysis. Another reason why validation studies could not be performed in liquid was that desorption solution contained MeOH, and alcohol dissolved the epoxy of the cantilever holder mechanism. For this reason, the desorption step, where the molecules were desorbed from the cavities, could not be performed in online measurements. Nonetheless, a binding study was carried out in liquid just to have an idea about the adsorption behaviours of CPX on CPX-IPN cavities, that is; to determine the duration of binding to take place.

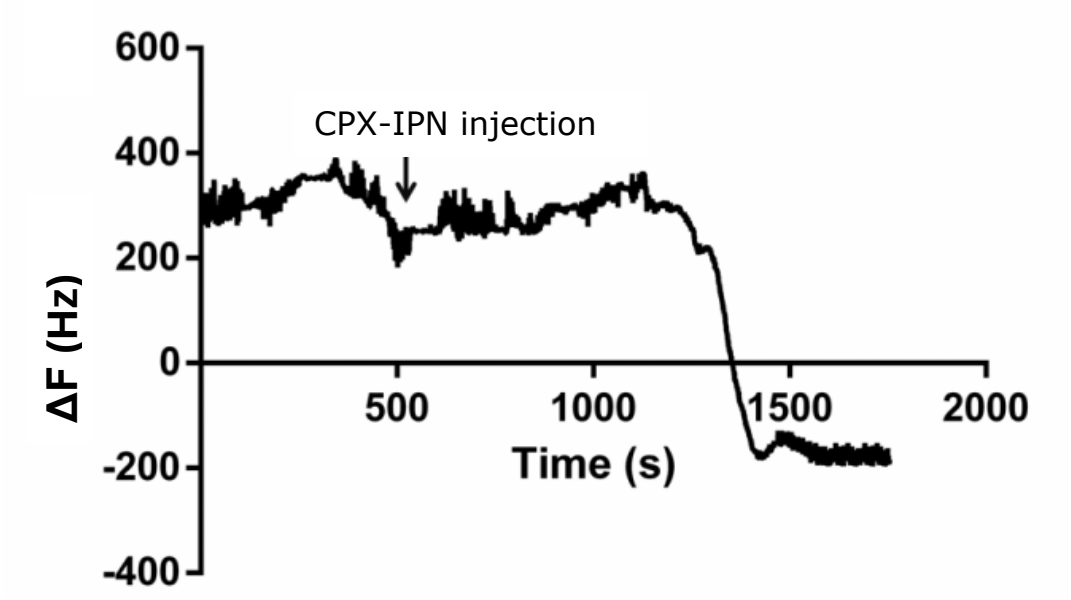

Figure 28: Real-time immobilization of CPX-IPN on the cantilever surface (in liquid).

Since the liquid system was problematic, the binding experiments were decided to be carried out in air. Another reason to have moved on carrying out the experiments in air was the Q. The Q value decreased dramatically in liquid due to the liquid damping. This issue hinders the possibility to detect small amount of molecules, which affects the sensitivity of the sensor system [87]. High Q lowers the minimum detectable resonance shift by increasing the frequency resolution. Even though the liquid studies was not successful, they provided background information regarding the time period required for binding to take place, which was determined as 5 min. The incubation time of the cantilever in CPX solution was therefore set to 5 min.

For the binding experiments in air, well-known dip-and-dry technique was employed. First the change in frequency after the immobilization of CPX-IPN was checked. The frequency was found to be decreased from 410.5 kHz to 410.1 kHz, resulting in a change of approximately 400 Hz (Figure 25b). Frequency responses for the concentrations of 1.5, 3.0, 15.1, 30.1 and 60.4 μM CPX were recorded one by one. For these

concentrations, frequency shifts of 48, 54, 62, 78 and 97 Hz were recorded, respectively. The calibration graph was drawn using frequency shifts (ΔF) and the corresponding concentration (C) (Figure 27a). The calibration curve presented high linearity and the sensor system developed showed 98% accuracy for the given concentration range. The total adsorbed mass on CPX-IPN for each concentration was calculated using the ΔF values and Eqn. 6. For the frequency shifts (ΔF) of 48, 54, 62, 78 and 97 Hz, adsorbed masses (Δm) of 18.4, 20.5, 24.1, 29.6 and 37.1 pg were calculated. The graph of ΔF versus Δm showed high linearity and the accuracy was calculated to the 99% (Figure 27b). Using the same graph, the sensitivity of the sensor was calculated as 2.2 Hz/pg. To calculate the LoD and LoQ values, cantilever left oscillating in air the frequency shifts at equilibrium were recorded. The LoD and LoQ values were found as 2.2 μM and 13.4 μM, respectively.

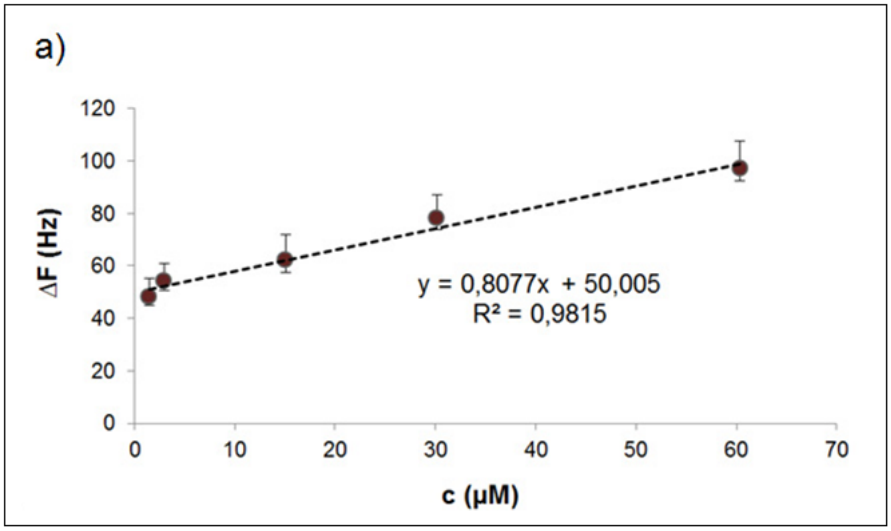

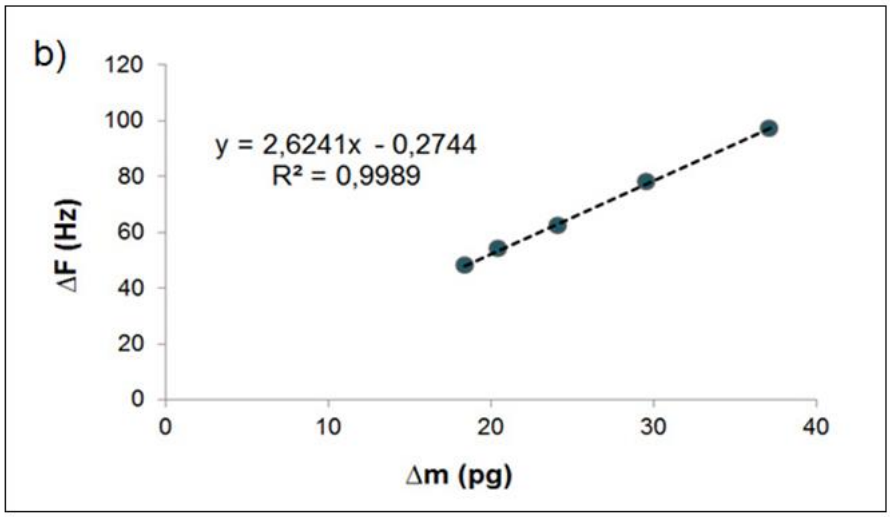

Figure 29: a) Calibration graph of the sensor system in air; frequency shifts (ΔF) vs. concentrations (c), b) Graph of frequency shifts (ΔF) vs. adsorbed masses (Δm).

The selectivity and specificity of the microcantilever sensor system was checked with another antibiotic, namely enrofloxacin (ENR) that is chemically and physically similar to CPX and NIP nanoparticles, respectively. These control studies were performed in air as well, using the same cantilever and same technique. Single concentration, 3.0 μM, was used during these experiments. The ΔF value was recorded as 54 Hz for 3.0 μM CPX, whereas for 3.0 μM ENR the shift as 8.1 Hz (Figure 28a). This showed that the affinity of ENR to CPX-IPN were 6.7 folds lower than that of CPX. On the basis of same result, that is the ΔF value of 54 Hz for 3.0 μM CPX, a shift of 11.8 Hz was obtained when 3.0 μM CPX molecules were adsorbed to NIP nanoparticles (Figure 28b). Therefore, the affinity of CPX to NIP nanoparticles was determined to be 4.6 folds lower compared to its affinity towards CPX-IPN.

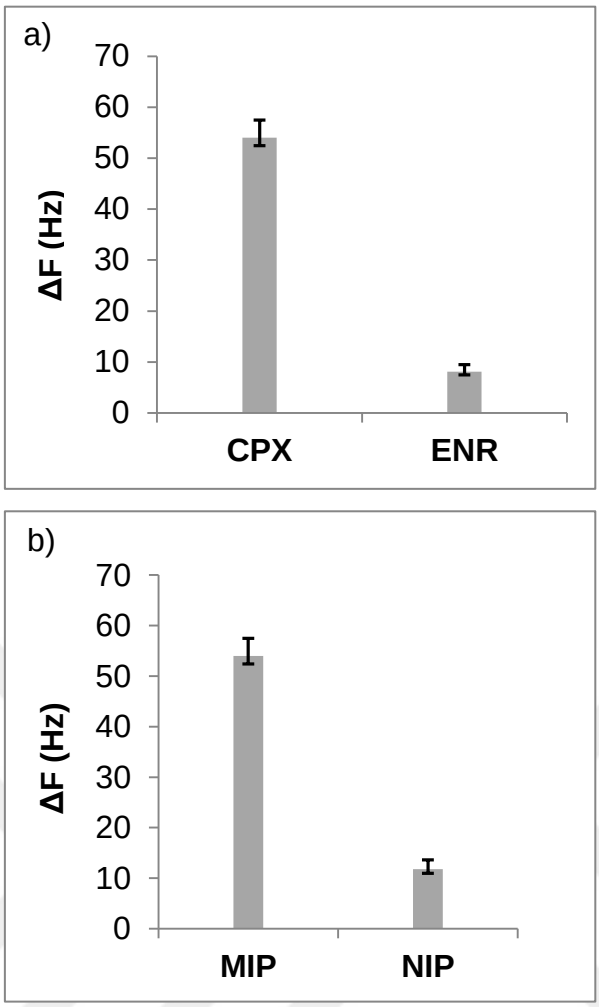

Figure 30: a) The ΔF resulting from binding of CPX and ENR molecules to CRY-IPN, b) The ΔF resulting from binding of CPX molecule to CPX-IPN and NIPs.

To investigate the change in frequency after each adsorption and desorption step, the reusability studies were performed for a chosen concentration. For this purpose, the same cantilever was incubated in the same concentration (3.0 μM) of CPX and then in desorption solution. This cycle was repeated 10 times. The ΔF responses for 3.0 μM CPX were found as 54, 53.4, 53.2 and 52.2 Hz in air. In fifth trial, the shift was only 23 Hz. This indicated that the sensor system prepared works properly up to 4 times. After the fourth binding experiment a reliable data could not be obtained. The relative standard deviation (RSD %) was calculated as 1.41% after having used the sensor

continuously for four times. If the fifth binding experiment was added to the calculation, this value would be 28.67%. Explanation of this phenomenon might be the damaged surface of the cantilever. That is, after a number of uses the alcohol in desorption solution starts harming the cantilever's surface. The aluminium coverage of the cantilever might be beginning to go through corrosion; therefore the physical properties of the cantilever are changed. This in return affects the resonance frequency features. Also, once the aluminium surface is harmed, the MIPs might naturally be removed from the surface as well.

4.1.2.2. Validation of ERY Specific Microcantilever Sensor

For this part of the study, in all binding experiments cantilever with the frequency of 150 kHz was used (this was mainly because cantilever D in some chips in the new batch were damaged and not working properly). Dynamic mode was employed during all measurements. As stated earlier, parameters such as mass, dimension and especially the resonance frequency affect the nature of the measurements. Therefore, before starting the binding trials, the measurement of the resonance frequency of the bare cantilever was performed to see whether it matches the value provided by the producing company. Also, the frequency after the immobilization of the nanoparticles was recorded as well. The cantilever's exact resonance frequency was determined as 164.4±0.01 kHz in air (figure 29a). The value was within the range (70-230 kHz), very close to the nominal value indeed, the measurements were performed with this cantilever. Also, Q is a crucial parameter in mass sensing applications, as explained in the Literature Review section, for it provides a measurement tool for the energy loss [93] [94] [95].The high Q values refer to low energy dissipations. The Q of the cantilever was determined as 269.51, which was quite a high value that would allow a good measurement environment.

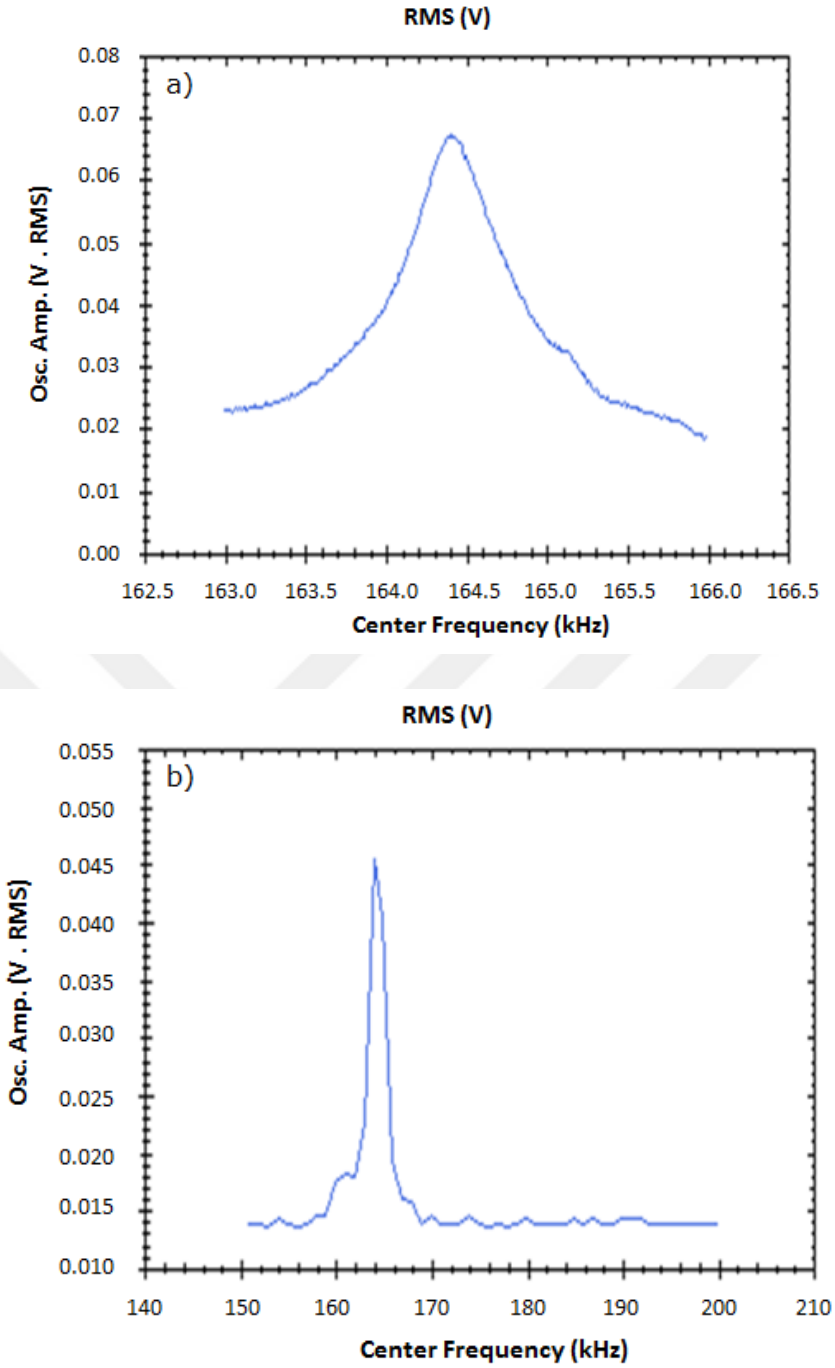

Figure 31: The frequency values of the cantilever in air a) before and b) after the immobilization of ERY-IPN.

It was found before that the prepared sensor system was not working properly in liquid environment. However, since a different cantilever was going to be used in this set of measurements, a trial for binding experiments in liquid was performed. Another reason for that was to

determine the adsorption and desorption periods of the molecules. The amount of time required for ERY to bind to the cavities was found to be very close to the value determined in the CPX specific sensor system (approximately 5 min).

First air measurement was performed after the MIP nanoparticles were immobilized on the cantilever surface via EDC/NHS activation, which resulted in a resonance frequency and Q values of 164.0±0.01 kHz and 81.5 kHz, respectively. Therefore, the ERY-IPN were triggered a frequency shift of approximately 400 Hz (Figure 29b). For the validation studies in air, the sensor system response for a concentration range of 0.68-27.18 µM was recorded after each adsorption and desorption step. The ΔF values for the concentrations of 0.68, 1.36, 6.79, 13.59 and 27.18 µM were found as 55.8, 72.6, 165.6, 357.4 and 485.4 Hz. The calibration curve (ΔF vs C) was drawn using the data obtained (Figure 30a). The curve showed high linearity, which indicated that the sensor system developed was working 96% accuracy for the given concentration range. The total mass of the molecules (ERY) adsorbed on the ERY-IPN was calculated using Eqn. 6. For the ΔF values of 55.8, 72.6, 165.6, 357.4 and 484.4 Hz, adsorbed masses (Δm) of 35.3, 46, 104.9, 226.8 and 308.4 pg were calculated. A graph of ΔF vs Δm was drawn, from which a coefficient of determination (R^2) of 1 was obtained (Figure 30b). This indicated that the sensor model defines all variability of the response data, which is Δm, was around their mean value. Using the data obtained (ΔF and Δm), the sensitivity of the sensor was calculated as 1.6 Hz/pg. For the determination of the LoD and LoQ, cantilever was oscillated in air, and its behaviour was recorded. The small changes in its frequency at equilibrium were measured. The LoD and LoQ values of the sensor system were found as 1 µM and 3 µM, respectively.

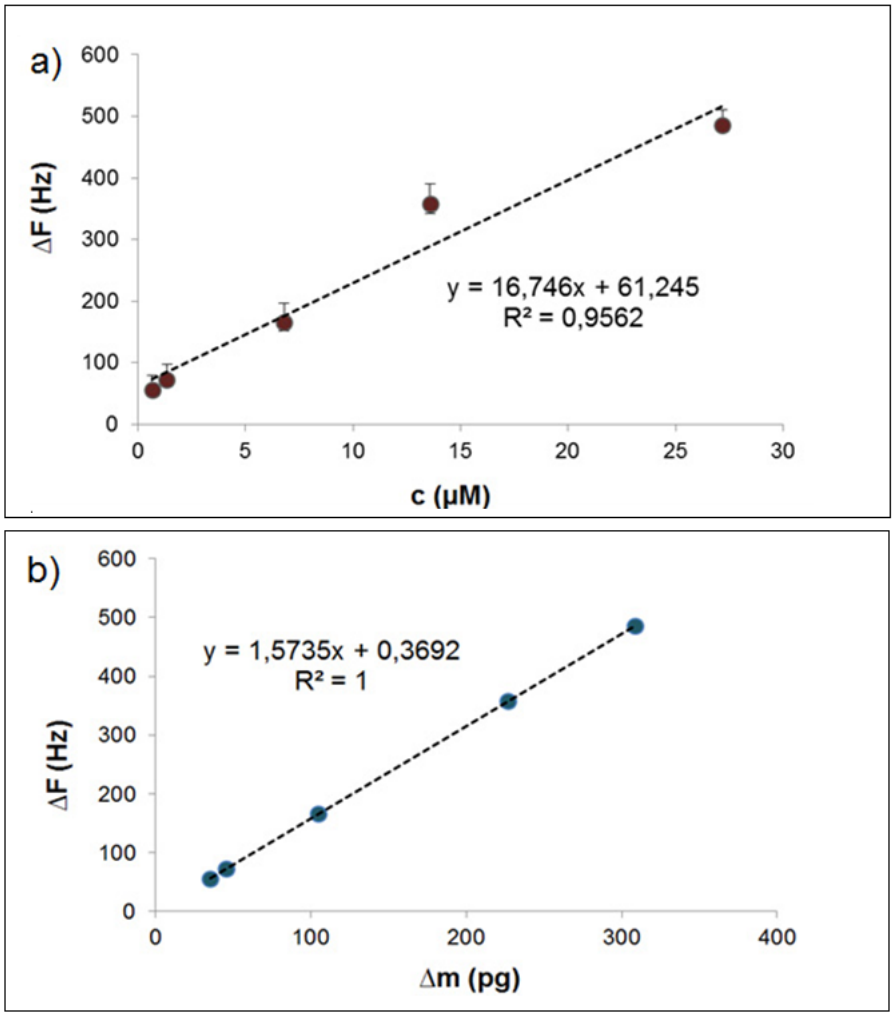

Figure 32: a) Calibration graph of the sensor system in air; frequency shifts (ΔF) vs. concentrations (c), b) Graph of frequency shifts (ΔF) vs. adsorbed masses (Δm).

A different antibiotic, Spiramycin (SPI), that is physically and chemically similar to ERY and NIPs were used in binding studies to reveal the selectivity and sensitivity. The binding affinities of SPI towards ERY-IPN and ERY towards NIPs were determined in air measurements, using the cantilever with same resonance frequency (150 kHz) and employing the same methods and procedures. During these experiments, a single

concentration (1.36 μM) was used. The ΔF response of ERY-IPN for 1.36 μM ERY and 1.36 μM SPI were determined as 72.6 Hz and 8.8 Hz, respectively (Figure 31a). The ΔF values recorded from the adsorption of 1.36 μM to ERY-IPN and NIPs were determined as 72.6 Hz and 23.8 Hz, respectively (Figure 31b). These results revealed that the affinity of SPI towards ERY-IPN was about 8 folds lower than that of ERY, and the affinity of ERY towards NIPs was about 3 folds lower than that of ERY-IPN.

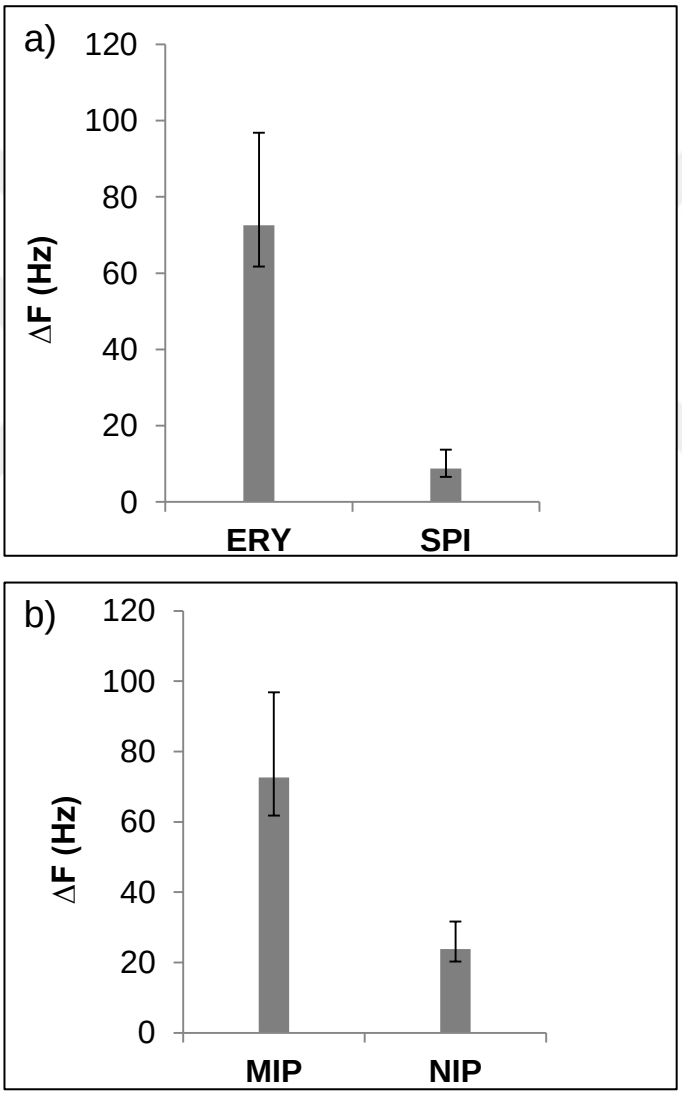

Figure 33: a) The ΔF resulting from binding of ERY and SPI molecules to ERY-IPN, b) The ΔF resulting from binding of ERY molecule to ERY-IPN and NIPs.

In order to investigate the reusability of the system, a cantilever was used over and over again by exposing it to a certain concentration of molecule. The frequency changes after each adsorption and desorption step were recorded. Using the same technique, the cantilever was exposed to 0.68 μM ERY to allow for adsorption and to desorption solution, a mixture of MeOH:HAc (9:1, v/v) afterwards. This set of adsorption-desorption experiments were repeated 5 times. ΔF values of 55.8, 56.7 and 54.9 Hz were recorded for the first 3 experiments. However, after using the same cantilever for 3 times, the RSD% was calculated as 1.89%. This means that the sensor system can be used up to 3 times.

4.2. Conclusion

In this thesis study, MIP based microcantilever sensor system capable of selective detection of antibiotics (CPX and ERY) in water resources was designed and developed. In this respect, MIPs were synthesized, characterized and covalently immobilized on a cantilever surface. A homogeneous and monolayer surface coverage was successfully accomplished via EDC/NHS activation method. An advantage of this method lies within the immobilization technique where a significant amount of energy required for the cleavage of covalent bonds. This type of bonding becomes crucial when dealing with repeated adsorption-desorption cycles in a designed system. In this developed sensor, the template molecules are adsorbed to the cavities of MIPs and leave those cavities with the help of desorption solution. The lasting of the immobilized MIP nanoparticles during these cycles depends on the mildness of desorption of the template molecules from the cavities [185]. To break-off such affinity interactions, like between a molecule and a cavity, require effective and harsh solutions, which was determined as a mixture of MeOH and HAc in this case. Not harming the surface coverage during this process is significant to preserve the

stability and reusability of the sensor system. By using a covalent attachment, these cycles were able to be performed troubleless.

During the immobilization, both sides of the cantilevers were exposed to MIP nanoparticles. Accordingly, both sides of cantilevers were coated. The SEM images showed that both MIPs were spherical in shape. The CPX-IPN and ERY-IPN had sizes of around 160 nm and 30 nm, respectively. The RMS roughness of the bare cantilever was determined as 2.3±0.1 nm. The value went up to 7.4±0.5 nm and 4.3±0.3 nm when CPX-IPN and ERY-IPN were immobilized on the surface, respectively. Essentially, both sensing modes (static deflection and dynamic) can be employed in mass sensing applications. However, if the static deflection mode was going to be used, recognition layer (MIP nanoparticles) should be applied only to the one side of the cantilever. Therefore, in this thesis, all measurements were performed using dynamic sensing mode. Once the issue regarding the surface coverage is solved, both bending and resonance frequency readouts can be performed simultaneously [81].

The LoD of the sensor were calculated as 2.2 μM and 1 μM for CPX and ERY systems, respectively. Sensitivities were determined as 2.2 Hz/pg and 1.6 Hz/pg for CPX and ERY sensors, respectively. The LoD values obtained in this thesis study can be lowered and better sensitivity can be accomplished simply by changing the immobilization technique of MIP nanoparticles on the surface of the cantilever. That is because, when the MIPs are covalently attached on the surface, their carboxyl groups are used. Those carboxyl groups are also responsible for capturing the analyte (CPX and ERY). Therefore, if those carboxyl groups, blocked during EDC/NHS activation, can be benefited from, lower detection limits can be attained.

The development of polymer based electromechanical systems and the combination of cantilevers with polymers are the new trend towards the

detection of molecules with mechanical systems [179] [180]. These systems enable tailor-made approaches for the detection of any compound of interest in any environment.

The developed sensors for the selective determination of CPX and ERY were found to be comparable with existing techniques in terms of performance characteristics and reusability. It is a low-cost setup due to the elimination of using a biological recognition layer and is a pioneer system by being simple, reliable and time-efficient in the microcantilever mass sensing applications.

The sensor designed in this thesis study eliminated the complicated and elaborated system preparations by employing a rather practical approach of direct immobilization of recognition element (MIP nanoparticles) on the cantilever surface. Both the sensor system and imprinting technology can be utilized for the detection of other PECs and vast numbers of molecules such as; hormones, drugs, pathogens, viruses and toxins in mass sensing applications.

BIBLIOGRAPHY

[1] J. Acar and B. Röstel, Antimicrobial resistance: an overview, *Revue Scientifique et Technique,* vol 26, pp. 797-810, **2001**.

[2] C. D. Miranda and R. Zemelman, Antimicrobial multiresistance in bacteria isolated from freshwater Chilean salmon farms., *Science of the Total Environment,* vol 293, pp. 207-218, **2002**.

[3] D. Li, Z. Y. Yan and W. Q. Cheng, Determination of ciprofloxacin with functionalized cadmium sulfide nanoparticles as a fluorescence probe., *Spectrochimica Acta Part A: Molecular and Biomolecular Spectroscopy,* vol 71, pp. 1204-1211, **2008**.

[4] J. Wang, M. Meng, Z. Song, J. Pan, Y. Yan and C. Li, Surface molecularly imprinted polymers based on yeast prepared by atom transfer radical emulsion polymerization for selective recognition of ciprofloxacin from aqueous medium., *Journal of Applied Polymer Science,* vol 131, pp. 1-10, **2014**.

[5] F. Qiao and H. Sun, Simultaneous extraction of enrofloxacin and ciprofloxacin from chicken tissue by molecularly imprinted matrix solid-phase dispersion, *Journal of Pharmaceutical and Biomedical Analysis,* vol 53, pp. 795-798, **2010**.

[6] B. Gao, X. P. He, Y. Jiang, J. T. Wei, H. Suo and C. Zhao, Computational simulation and preparation of fluorescent magnetic molecularly imprinted silica nanospheres for ciprofloxacin or norfloxacin sensing., *Journal of Separation Science,* vol 37, pp. 3753-3759, **2014**.

[7] A. A. J. Torriero, E. Salinas, J. Raba and J. J. Silber, Sensitive determination of ciprofloxacin and norfloxacin in biological fluids using an enzymatic rotating biosensor., *Biosensors and Bioelectronics,* vol 22, pp. 109-115, **2006b**.

[8] K. Griessmann, A. Kaunzinger, M. Schubert-Zsilavecz and M. Abdel-Tawab, A rapid HPLC-UV method for the quantification of erythromycin in dermatological preparations, *Die Pharmazie - An International Journal of Pharmaceutical Sciences,* vol 62, pp. 668-671, **2007**.

[9] R. Rattanapoltaveechai, W. Vongkom, W. Suntornsuk and L. Suntornsuk, Simple and rapid spectrophotometric method for the analysis of erythromycin in pharmaceutical dosage forms, *Journal of Food and Drug Analysis,* vol 15, **2007**.

[10] M. Ali, S. Sherazi and S. Mahesar, Quantification of erythromycin in pharmaceutical formulation by transmission Fourier transform infrared spectroscopy, *Arabian Journal of Chemistry,* vol 7, pp. 1104-1109, **2014**.

[11] W. Zheng, K. Chen, J. Zhu and L. Ji, A novel process for erythromycin separation from fermentation broth by resin adsorption–aqueous crystallization, *Separation and Purification Technology,* vol 116, pp. 398-404, **2013**.

[12] E. Caro, R. M. Marcé, P. A. Cormack, D. C. Sherrington and F. Borrull, Direct determination of ciprofloxacin by mass spectrometry after a two-step solid-phase extraction using a molecularly imprinted polymer, *Journal of Separation Science,* vol 29, no. 9, pp. 1230-1236, **2006**.

[13] E. C. L. Cazedey, R. Bonfilio, M. B. Araújo and H. R. N. Salgado, A First-Derivative Spectrophotometric Method for the Determination of Ciprofloxacin Hydrochloride in Ophthalmic Solution, *Physical Chemistry,* vol 2, no. 6, pp. 116-122, **2013**.

[14] D. Barrón, E. Jiménez-Lozano, J. Cano and J. Barbosa, Determination of residues of enrofloxacin and its metabolite ciprofloxacin in biological materials by capillary electrophoresis, *Journal of Chromatography B: Biomedical Sciences and Applications,* vol 759, pp. 73-79, **2001**.

[15] X. Zhou, D. Xing, D. Zhu, Y. Tang and L. Lia, Development and application of a capillary electrophoresis-electrochemiluminescent method for the analysis of enrofloxacin and its metabolite ciprofloxacin in milk., *Talanta,* vol 75, pp. 1300-1306, **2008**.

[16] J. L. Urraca, M. Castellari, C. A. Barrios and M. C. Moreno-Bondi, Multiresidue analysis of fluoroquinolone antimicrobials in chicken meat by molecularly imprinted solid-phase extraction and high performance liquid chromatography, *Journal of Chromatography A,* vol 1343, pp. 1-9, **2014**.

[17] U. H. Desai, A. H. Patwari, J. K. Maradiya, M. K. Sathawara, B. N. Suhagia and I. S. Rathod, RP-HPLC Method for Simultaneous Estimation of Ciprofloxacin and Dexamethasone in Eye / Ear Drops, *International Journal of Pharmaceutical Sciences and Drug Research,* vol 5, pp. 62-66, **2013**.

[18] R. E. Ionescua, N. Jaffrezic-Renaulta, L. Bouffier, C. Gondran, S. Cosnier, D. G. Pinacho, M. -P. Marco, F. J. Sánchez-Baeza, T. Healy and C. Martelet, Impedimetric immunosensor for the specific label free detection of ciprofloxacin antibiotic, *Biosensors and Bioelectronics,* vol 23, no. 4, p. 549–555, **2007**.

[19] A. A. J. Torriero, J. J. J. Ruiz-Díaz, E. Salinas, E. J. Marchevsky, M. I. Sanz and J. Raba, Enzymatic rotating biosensor for ciprofloxacin determination, *Talanta,* vol 69, pp. 691-699, **2006a**.

[20] A. A. J. Torriero, E. Salinas, J. Raba and J. J. Silber, Sensitive determination of ciprofloxacin and norfloxacin in biological fluids using an enzymatic rotating biosensor, *Biosensors and Bioelectronics,* vol 22, pp. 109-115, **2006b**.

[21] X. Sun, J. Wang, Y. Li, J. Yang, J. Jin, S. M. Shah and J. Chen, Novel dummy molecularly imprinted polymers for matrix solid-phase

dispersion extraction of eight fluoroquinolones from fish samples, *Journal of Chromatography A,* vol 1359, pp. 1-7, **2014**.

[22] H. Yan, K. H. Row and G. Yang, Water-compatible molecularly imprinted polymers for selective extraction of ciprofloxacin from human urine, *Talanta,* vol 75, pp. 227-232, 2008.

[23] J. B. Tepe and C. V. St. John, Determination of erythromycin by ultraviolet spectrophotometry, *Analytical Chemistry,* vol 27, pp. 744-746, **1955**.

[24] W. Lian, S. Liu, J. Yu, X. Xing, J. Li, M. Cui and J. Huang, Electrochemical sensor based on gold nanoparticles fabricated molecularly imprinted polymer film at chitosan–platinum nanoparticles/graphene–gold nanoparticles double nanocomposites modified electrode for detection of erythromycin, *Biosensors and Bioelectronics,* vol 38, pp. 163-169, **2012**.

[25] X. Hu, P. Wang, J. Yang, B. Zhang, J. Li, J. Luo and K. Wu, Enhanced electrochemical detection of erythromycin based on acetylene black nanoparticles, *Colloids and Surfaces B: Biointerfaces,* vol 81, pp. 27-31, **2010**.

[26] M. A. Ivić, S. Petrović, D. Mijin, F. Vanmoos, D. Orlović, D. Marjanović and V. Radović, The electrochemical behavior of erythromycin A on a gold electrode, *Electrochimica Acta,* vol 54, pp. 649-654, **2008**.

[27] Y. -C. Feng and C. -Q. Hu, Construction of universal quantitative models for determination of roxithromycin and erythromycin ethyl succinate in tablets from different manufacturers using near infrared reflectance spectroscopy, *Journal of Pharmaceutical and Biomedical Analysis ,* vol 41, pp. 373-384, **2006**.

[28] A. Lalloo and I. Kanfer, Determination of erythromycin and related substances by capillary electrophoresis, *Journal of Chromatography B: Biomedical Sciences and Applications,* vol 704, pp. 343-350, **1997**.

[29] P. T. T. Ha, A. Van Schepdael, E. Roets and J. Hoogmartens, Investigating the potential of erythromycin and derivatives as chiral selector in capillary electrophoresis, *Journal of Pharmaceutical and Biomedical Analysis,* vol 34, pp. 861-870, **2004**.

[30] R. Granja, A. M. Nio, R. Zucchetti, R. M. Nio, R. Patel and A. G. Salerno, Determination of erythromycin and tylosin residues in honey by LC/MS/MS, *Journal of AOAC International,* vol 92, pp. 975-980, **2009**.

[31] C. Benetti, R. Piro, G. Binato, R. Angeletti and G. Biancotto, Simultaneous determination of lincomycin and five macrolide antibiotic residues in honey by liquid chromatography coupled to electrospray ionization mass spectrometry (LC–MS/MS), *Food Additives & Contaminants,* vol 23, pp. 1099-1108, **2006**.

[32] J. Wang and D. Leung, Analyses of macrolide antibiotic residues in eggs, rawmilk, and honey using both ultra-performance liquid

chromatography/quadrupole time-of-flight mass spectrometry and high-performance liquid chromatography/tandem mass spectrometry, *Rapid Communications in Mass Spectrometry,* vol 21, pp. 3213-3222, **2007**.

[33] Y. -X. Li, K. Neufeld, J. Chastain, A. Curtis and P. Velagaleti, Sensitive determination of erythromycin in human plasma by LC–MS/MS, *Journal of Pharmaceutical and Biomedical Analysis,* vol 16, pp. 961-970, **1998**.

[34] K. Tsuji and M. P. Kane, Improved high-pressure liquid chromatographic method for the analysis of erythromycin in solid dosage forms, *Journal of Pharmaceutical Sciences,* vol 71, pp. 1160-1164, **1982**.

[35] B. Liawruangrath and S. Liawruangrath, High performance thin laye rchromatographic determination of erythromycin in pharmaceutical preparations, *Chromatographia,* vol 54, pp. 405-408, **2001**.

[36] J. Wardrop, D. Ficker, S. Franklin and R. J. Gorski, Determination of erythromycin and related substances in enteric-coated tablet formulations by reversed-phase liquid chromatography, *Journal of Pharmaceutical Sciences,* vol 89, pp. 1097-1105, **2000**.

[37] N. Güneş, R. Cibik, M. E. Güneş and L. Aydın, Erythromycin residue in honey from the Southern Marmar aregion of Turkey, *Food Additives & Contaminants,* vol 25, pp. 1313-1317, **2008**.

[38] S. T. Hassib, A. E. Farag and E. F. Elkady, Liquid chromatographic and spectrophotometric methods for the determination of erythromycin stearate and trimethoprim intablets, *Bulletin of Faculty of Pharmacy, Cairo University,* vol 49, pp. 81-89, **2011**.

[39] T. Cachet, M. Delrue, J. Paesen, R. Busson, E. Roets and J. Hoogmartens, Analysis of erythromycin estolate by liquid chromatography, *Journal of Pharmaceutical and Biomedical Analysis,* vol 10, pp. 851-860, **1992**.

[40] L. C. Clark Jr., Monitor and control of clood and tissue oxygen tensions, *Transactions American Society for Artificial Internal Organs,* vol 2, pp. 41-57, **1956**.

[41] L. C. Clark Jr. and C. Lyons, Electrode systems for continuous monitoring in cardiovascular surgery, *Annals of the New York Academy of Sciences,* vol 102, pp. 29-45, **1962**.

[42] C. R. Lowe and M. J. Goldfinch, Novel electrochemical sensors for clinical analysis, *Biochemical Society Transactions,* vol 11, pp. 449-451, **1983**.

[43] C. R. Lowe, An Introduction to the Concepts and Technology of Biosensors, *Biosensors,* vol 1, pp. 3-16, 1985.

[44] K. Cammann, Bio-Sensors Based on Ion-Selective Electrodes, *Analytische Chemie,* vol 287, pp. 1-9, **1977**.

[45] D. R. Thévenot, K. Toth, R. A. Durst and G. S. Wilson, Electrochemical Biosensors: Recommended Definitions and Classifications, *Pure and Applied Chemistry,* vol 71, no. 12, pp. 2333-2348, **1999**.

[46] C. R. Lowe, Overview of Biosensor and Bioarray Technologies, *Handbook of Biosensors and Biochips*, Wiley, **2007**, pp. 1-16.

[47] V. Perumal and U. Hashim, Advances in biosensors: Principle, architecture and applications, *Journal of Applied Biomedicine,* vol 12, pp. 1-15, **2014**.

[48] K. Suresh, G. Uma, B. S. Kumar, U. V. Kumar and M. Umapathy, Piezoelectric based resonant mass sensor using phase measurement, *Measurement,* vol 44, pp. 320-325, **2011**.

[49] G. Sauerbrey, Verwendung von Schwingquarzen zur Wägung dünner Schichten und zur Mikrowägung, *Zeitschrift fiir Physik,* vol 155, pp. 206-222, **1959**.

[50] V. M. Mecea, From Quartz Crystal Microbalance to Fundamental Principles of Mass Measurements, *Analytical Letters,* vol 38, p. 753–767, **2005**.

[51] K. K. Kanazawa and J. G. Gordon, Frequency of a Quartz Microbalance in Contact with Liquid, *Analytical Chemistry,* vol 57, pp. 1770-1771, **1985**.

[52] M. V. Voinova, M. Jonson and B. Kasemo, 'Missing mass' effect in biosensor's QCM applications, *Biosensors and Bioelectronics,* vol 17, no. 10, p. 835–841, **2002**.

[53] D. S. Ballantine Jr., S. J. Martin, A. J. Ricco, G. C. Frye, H. Wohltjen, R. M. White and E. T. Zellers, Acoustic Wave Sensors: Theory, Design, and Physico-Chemical Applications, San Diego, CA: Academic Press, **1997**.

[54] V. M. Mecea, Is quartz crystal microbalance really a mass sensor?, *Sensors and Actuators A: Physical,* vol 128, pp. 270-277, **2006**.

[55] H. Zeng, Y. Jiang, G. Xie and J. Yu, Polymer coated QCM sensor with modified electrode for the detection of DDVP, *Sensors and Actuators B: Chemical,* vol 122, pp. 1-6, **2007**.

[56] H. H. Lu, Y. K. Rao, T. Z. Wu and Y. M. Tzeng, Direct characterization and quantification of volatile organic compounds by piezoelectric module chips sensor, *Sensors and Actuators B: Chemical,* vol 137, pp. 741-746, **2009**.

[57] M. Duman, R. Saber and E. Pişkin, A new approach for immobilization of oligonucleotides onto piezoelectric quartz crystal for preparation of a nucleic acid sensor for following hybridization, *Biosensors and Bioelectronics,* vol 18, pp. 1355-1363, **2003**.

[58] Z. Shen, M. Huang, C. Xiao, Y. Zhang, X. Zeng and P. G. Wang, Non-labeled QCM Biosensor for Bacterial Detection using Carbohydrate

and Lectin Recognitions, *Analytical Chemistry,* vol 79, no. 6, pp. 2312-2319, **2007**.

[59] A. Osypova, D. Thakar, J. Dejeu, H. Bonnet, A. Van der Heyden, G. V. Dubacheva, R. P. Richter, E. Defrancq, N. Spinelli, L. Coche-Guérente and P. Labbé, Sensor Based on Aptamer Folding to Detect Low-Molecular Weight Analytes, *Analytical Chemistry,* vol 87, pp. 7566-7574, **2015**.

[60] R. J. Wilfinger, P. H. Bardell and D. S. Chhabra, The Resonistor: A Frequency Selective Device Utilizing the Mechanical Resonance of a Silicon Substrate, *IBM Journal of Research and Development,* vol 2, no. 1, pp. 113 - 118, **1968**.

[61] M. Hegner and Y. Arntz, Advanced Biosensing Using Micromechanical Cantilever Arrays, *Atomic Force Microscopy: Biomedical Methods and Applications*, Totowa, NJ, Humana Press, **2004**, pp. 39-49.

[62] K. S. Hwang, S. -M. Lee, S. K. Kim, J. H. Lee and T. S. Kim, Micro- and Nanocantilever Devices and Systems for Biomolecule Detection, *Annual Review of Analytical Chemistry,* vol 2, pp. 77-98, **2009**.

[63] F. L. Walls and J. J. Gagnepain, Environmental sensitivities of quartz oscillators, *IEEE Transactions on Ultrasonics, Ferroelectrics and Frequency Control,* vol 39, pp. 241-249, **1992**.

[64] T. Thundat, G. Y. Chen, R. J. Warmack, D. P. Allison and E. A. Wachter, Vapor Detection Using Resonating Microcantilevers, *Analytical Chemistry,* vol 67, pp. 519-521, **1995**.

[65] J. J. Caron, R. B. Haskell, P. Benoit and J. F. Vetelino, Surface acoustic wave mercury vapor sensor, *IEEE Transactions on Ultrasonics Ferroelectrics and Frequency Control,* vol 45, pp. 1393-1398, **1998**.

[66] J. Veris, Temperature compensation of silicon resonant pressure sensor, *Sensors and Actuators A: Physical,* vol 57, pp. 179-182, **1996**.

[67] R. G. Azevedo, W. Huang, O. M. O'Reilly and A. P. Pisano, Dual-mode temperature compensation for a comb-driven MEMS resonant strain gauge, *Sensors and Actuators A: Physical,* vol 144, pp. 374-380, **2008**.

[68] D. E. Pierce, Y. Kim and J. R. Vig, A temperature insensitive quartz microbalance, *IEEE Transactions on Ultrasonics Ferroelectrics and Frequency Control,* vol 45, pp. 1238-1245, **1998**.

[69] R. McKendry, J. Zhang, Y. Arntz, T. Strunz, M. Hegner, H. P. Lang, M. K. Baller, U. Certa, E. Meyer, H. -J. Güntherodt and C. Gerber, Multiple label-free biodetection and quantitative DNA-binding assays on a nanomechanical cantilever array, *Proceedings of the National Academy of Sciences,* vol 99, p. 9783–9788, **2002**.

[70] L. Zhai, T. Wang, K. Kang, Y. Zhao, P. Shrotriya and M. Nilsen-Hamilton, An RNA Aptamer-Based Microcantilever Sensor To Detect the Inflammatory Marker, Mouse Lipocalin-2, *Analytical Chemistry,* vol 84, no. 20, p. 8763–8770, **2012**.

[71] A. Kooser, K. Manygoats, M. P. Eastman and T. L. Porter, Investigation of the antigen antibody reaction between anti-bovine serum albumin (a-BSA) and bovine serum albumin (BSA) using piezoresistive microcantilever based sensors, *Biosensors and Bioelectronics,* vol 19, no. 5, pp. 503-508, **2003**.

[72] S. -H. Tark, A. Das, S. Sligar and V. P. Dravid, Nanomechanical detection of cholera toxin using microcantilevers functionalized with ganglioside nanodiscs, *Nanotechnology,* vol 21, no. 43, pp. 1-7, **2010**.

[73] G. A. Campbell and R. Mutharasan, PEMC sensor's mass change sensitivity is 20 pg/Hz under liquid immersion, *Biosensors and Bioelectronics,* vol 22, pp. 35-41, **2006**.

[74] R. Datar, S. Kim, S. Jeon, P. Hesketh, S. Manalis, A. Boisen and T. Thundat, Cantilever Sensors: Nanomechanical Tools for Diagnostics, *MRS Bulletin,* vol 34, pp. 449-454, **2009**.

[75] R. Berger, C. Gerber, H. P. Lang and J. K. Gimzewski, Micromechanics: A toolbox for femtoscale science: “Towards a laboratory on a tip", *Microelectronic Engineering,* vol 35, no. 1-4, pp. 373-379, **1997**.

[76] H. P. Lang, M. Hegner, E. Meyer and C. Gerber, Nanomechanics from atomic resolution to molecular recognition based on atomic force microscopy technology, *Nanotechnology,* vol 13, no. 5, p. R29, **2002**.

[77] J. Fritz, M. K. Baller, H. P. Lang, H. Rothuizen, P. Vettiger, E. Meyer, H. -J. Güntherodt, C. Gerber and J. K. Gimzewski, Translating Biomolecular Recognition into Nanomechanics, *Science,* vol 288, pp. 316-318, **2000**.

[78] R. Berger, E. Delamarche and H. P. Lang, Surface stress in the self-assembly of alkanethiols on gold, *Science,* vol 276, pp. 2021-2024, **1997**.

[79] H. P. Lang, M. Hegner and C. Gerber, Cantilever array sensors, *Materials Today, pp. 30-36, 2005.,* pp. 30-36, **2005**.

[80] T. Thundat, R. J. Warmack and G. Y. Chen, Thermal and ambient-induced deflections of scanning force microscope cantilevers, *Applied Physics Letters,* vol 64, no. 21, pp. 2894-2896, **1994**.

[81] F. M. Battiston, J. -P. Ramseyera, H. P. Lang, M. K. Ballera, C. Gerber, J. K. Gimzewski, E. Meyer and H. -J. Güntherodt, A chemical sensor based on a microfabricated cantilever array with simultaneous resonance-frequency and bending readout, *Sensors and Actuators B: Chemical,* vol 77, no. 1-2, p. 122–131, **2001**.

[82] E. A. Wachter and T. Thundat, Micromechanical sensors for chemical and physical measurements, *Review of Scientific Instruments,* vol 66, no. 6, pp. 3662-3667, **1995**.

[83] W. J. Weaver, S. P. Timoshenko and D. Young, Vibration Problems in Engineering, New York: Wiley, **1990**.

[84] D. Then, A. Vidic and C. Ziegler, A highly sensitive self-oscillating cantilever array for the quantitative and qualitative analysis of organic vapor mixtures, *Sensors and Actuators B: Chemical,* vol 117, no. 1, p. 1–9, **2006**.

[85] D. Then and C. Ziegler, Cantilever-Based Sensors, *Encyclopedia of Nanoscience and Nanotechnology Vol. 1*, American Scientific Publishers, **2004**, pp. 499-516

[86] G. Abadal, Z. J. Davis, B. Helbo, X. Borrisé, R. Ruiz, A. Boisen, F. Campabadal, J. Esteve, E. Figueras, F. Pérez-Murano and N. Barniol, Electromechanical model of a resonating nano-cantilever-based sensor for high-resolution and high-sensitivity mass detection, *Nanotechnology,* vol 12, no. 2, pp. 100-104, **2001**.

[87] P. A. Rasmussen, A. V. Grigorov and A. Boisen, Double sided surface stress cantilever sensor, *Journal of Micromechanics and Microengineering,* vol 15, p. 1088–1091, **2005**.

[88] P. Lu, H. P. Lee, C. Lu and S. J. O'Shea, Surface stress effects on the resonance properties of cantilever sensors, *Physical Review B,* vol 72, pp. 085405/1-5, **2005**.

[89] K. M. Goeders, J. S. Colton and L. A. Bottomley, Microcantilevers: Sensing Chemical Interactions via Mechanical Motion, *Chemical Reviews,* vol 108, no. 2, pp. 522-542, **2008**.

[90] M. Chaudhary and A. Gupta, Microcantilever-based Sensors, *Defence Science Journal,* vol 59, no. 6, pp. 634-641, **2009**.

[91] B. N. Johnson and R. Mutharasan, Biosensing using dynamic-mode cantilever sensors: A review, *Biosensors and Bioelectronics,* vol 32, pp. 1-18, **2012**.

[92] A. P. Davila, J. Jang, A. K. Gupta, T. Walter, A. Aronson and R. Bashir, Microresonator mass sensors for detection of Bacillus anthracis Sterne spores in air and water, *Biosensors and Bioelectronics,* vol 22, p. 3028–3035, **2007**.

[93] V. B. Braginsky, V. P. Mitrofanov and V. I. Panov, Systems with Small Dissipation, Chicago: University of Chicago Press, **1986**.

[94] J. Yang, T. Ono and M. Esashi, Energy Dissipation in Submicrometer Thick Single-Crystal Silicon Cantilevers, *Journal of Microelectromechanical Systems,* vol 11, no. 6, pp. 775-783, **2002**.

[95] R. Abdolvand, H. Johari, G. K. Ho, A. Erbil and F. Ayazi, Quality Factor in Trench-Refilled Polysilicon Beam Resonators, *Journal of Microelectromechanical Systems,* vol 15, no. 3, pp. 471-478, **2006**.

[96] W. Zhang and K. L. Turner, Noise Analysis in Parametric Resonance Based Mass Sensing, *ASME International Mechanical Engineering Congress and Exposition*, Anaheim, California, **2004**.

[97] K. Naeli, *Optimization of Piezoresistive Cantilevers for Static and Dynamic Sensing Applications,* Atlanta: Georgia Institute of Technology, **2009**.

[98] K. E. Petersen and C. R. Guarnieri, Young's modulus measurements of thin films using micromechanics, *Journal of Applied Physics,* vol 50, no. 11, pp. 6761-6766, **1979**.

[99] T. R. Albrecht, P. Grütter, D. Horne and D. Rugar, Frequency modulation detection using high-Q cantilevers for enhanced force microscope sensitivity, *Journal of Applied Physics,* vol 69, no. 2, pp. 668-673, **1991**.

[100] H. -J. Butt and M. Jaschke, Calculation of thermal noise in atomic force microscopy, *Nanotechnology,* vol 6, pp. 1-7, **1995**.

[101] E. Finot, A. Passian and T. Thundat, Measurement of mechanical properties of cantilever shaped materials, *Sensors,* vol 8, p. 3497–3541, **2008**.

[102] R. Sandberg, K. Mølhave, A. Boisen and W. Svendsen, Effect of gold coating on the Q-factor of a resonant cantilever, *Journal of Micromechanics and Microengineering,* vol 15, p. 2249–2253, **2005**.

[103] J. Tamayo, Study of the noise of micromechanical oscillators under quality factor enhancement via driving force control, *Journal of Applied Physics,* vol 97, pp. 044903/1-044903/10, **2005**.

[104] L. Fadel, I. Dufour, F. Lochon and O. Francais, Signal-to-noise ratio of resonant microcantilever type chemical sensors as a function of resonant frequency and quality factor, *Sensors and Actuators B: Chemical,* vol 102, p. 73–77, **2004**.

[105] K. Y. Yasumura, T. D. Stowe, E. M. Chow, T. Pfafman, T. W. Kenny, B. C. Stipe and D. Rugar, Quality Factors in Micron- and Submicron-Thick Cantilever, *Journal of Microelectromechanical Systems,* vol 9, no. 1, pp. 117-125, **2000**.

[106] Y. Lu, S. Peng, D. Luo and A. Lal, Low-concentration mechanical biosensor based on a photonic crystal nanowire array, *Nature Communications,* vol 578, no. 2, p. 1587, **2011**.

[107] K. L. Ekinci, Y. T. Yang and M. L. Roukes, Ultimate limits to inertial mass sensing based upon nanoelectromechanical systems, *Journal of Applied Physics,* vol 95, no. 5, pp. 2682-2689, **2004**.

[108] A. N. Cleland and M. L. Roukes, Noise processes in nanomechanical resonators, *Journal of Applied Physics,* vol 92, no. 5, pp. 2758-2769, **2002**.

[109] C. Lee, T. Itoh and T. Suga, Self-excited piezoelectric PZT microcantilevers for dynamic SFM -with inherent sensing and actuating capabilities, *Sensors and Actuators A: Physical,* vol 72, no. 2, pp. 179-188, **1999**.

[110] W. H. Han, S. M. Lindsay and T. W. Jing, A magnetically driven oscillating probe microscope for operation in liquids, *Applied Physics Letters,* vol 69, no. 26, pp. 4111-4113, **1996**.

[111] L. Voiculescu, M. E. Zaghloul and R. A. McGill, Electrostatically actuated resonant microcantilever beam in CMOS technology for the detection of chemical weapons, *IEEE Sensors Journal,* vol 5, no. 4, pp. 641-647, **2005**.

[112] J. R. Vig and Y. Kim, Noise in Microelectromechanical System Resonators, *IEEE Transactions on Ultrasonics, Ferroelectrics, and Frequency Control,* vol 46, no. 6, pp. 1558-1565, **1999**.

[113] T. B. Gabrielson, Mechanical-Thermal Noise in Micromachined Acoustic and Vibration sensors, *IEEE Transaction on Electron Devices,* vol 40, no. 5, pp. 903-909, **1993**.

[114] A. Gupta, D. Akin and R. Bashir, Single virus particle mass detection using microresonators with nanoscale thickness, *Applied Physics Letters,* vol 84, no. 11, pp. 1976-1978, **2004**.

[115] B. Ilic, D. Czaplewski, M. Zalalutdinov and H. G. Craighead, Single cell detection with micromechanical oscillators, *Journal of Vacuum Science & Technology B,* vol 19, no. 6, pp. 2825-2828, **2001**.

[116] B. Ilic, H. G. Craighead, S. Krylov, W. Senaratne and C. Ober, Attogram detection using nanoelectromechanical oscillators, *Journal of Applied Physics,* vol 95, no. 7, pp. 3694-3703, **2004**.

[117] S. Ghatnekar-Nilsson, E. Forsen, G. Abadal, J. Verd, F. Campabadal, F. Perez-Murano, J. Esteve, N. Barniol, A. Boisen and L. Montelius, Resonators with integrated CMOS circuitry for mass sensing applications, fabricated by electron beam lithography, *Nanotechnology,* vol 16, no. 1, p. 98–102, **2005**.

[118] H. F. Ji and T. Thundat, In situ detection of calcium ions with chemically modified microcantilevers, *Biosensors and Bioelectronics,* vol 17, p. 337–343, **2002**.

[119] H. F. Ji, E. Finot, R. Dabestani, T. Thundat, G. M. Brown and P. F. Britt, A novel self-assembled monolayer (SAM) coated microcantilever for low level caesium detection, *Chemical Communications,* no. 6, p. 457–458, **2000**.

[120] H. Xie, J. Vitard, S. Haliyo and S. Régnier, Enhanced sensitivity of mass detection using the first torsional mode of microcantilevers, *Measurement Science and Technology,* vol 19, no. 5, p. 055207, **2008**.

[121] T. P. Burg and S. R. Manalis, Suspended microchannel resonators for biomolecular detection, *Applied Physics Letters,* vol 83, no. 13, pp. 2698-2700, **2003**.

[122] S. S. Verbridge, J. M. Parpia, R. B. Reichenbach, L. M. Bellan and H. G. Craighead, High quality factor resonance at room temperature with

nanostrings under high tensile stress, *Journal of Applied Physics,* vol 99, no. 12, p. 013112, **2006**.

[123] S. Ghatnekar-Nilsson, J. Lindahl, A. Dahlin, T. Stjernholm, S. Jeppesen, F. Höök and L. Montelius, Phospholipid vesicle adsorption measured in situ with resonating cantilevers in a liquid cell, *Nanotechnology,* vol 16, pp. 1512-1516, **2006**.

[124] T. P. Burg, M. Godin, S. M. Knudsen, W. Shen, G. Carlson, J. S. Foster, K. Babcock and S. R. Manalis, Weighing of biomolecules, single cells and single nanoparticles in fluid, *Nature,* vol 446, pp. 1066-1069, **2007**.

[125] H. P. Lang, R. Berger, F. Battiston, J. P. Ramseyer, E. Meyer, C. Andreoli, J. Brugger, P. Vettiger, M. Despont, T. Mezzacasa, L. Scandella, H. J. Güntherodt, C. Gerber and J. K. Gimzewski, A chemical sensor based on a micromechanical cantilever array for the identification of gases and vapors, *Applied Physics A: Materials Science and Processing,* vol 66, pp. 61-64, **1998**.

[126] T. A. Betts, C. A. Tipple, M. J. Sepaniak and P. G. Datskos, Selectivity of chemical sensors based on micro-cantilevers coated with thin polymer films, *Analytica Chimica Acta,* vol 422, p. 89–99, **2000**.

[127] Y. Tang, J. Fang, X. Xu, H. F. Ji, G. M. Brown and T. Thundat, Detection of Femtomolar Concentrations of HF Using an SiO2 Microcantilever, *Analytical Chemistry,* vol 76, pp. 2478-2481, **2004**.

[128] J. Mertens, E. Finot, M. H. Nadal, V. Eyraud, O. Heintz and E. Bourillot, Detection of gas trace of hydrofluoric acid using microcantilever, *Sensors and Actuators B: Chemical,* vol 99, p. 58–65, **2004**.

[129] B. H. Kim, F. E. Prins, D. P. Kern, S. Raible and U. Weimar, Multicomponent analysis and prediction with a cantilever array based gas sensors, *Sensors and Actuators B: Chemical,* vol 78, no. 1-3, pp. 12-18, **2001**.

[130] M. Maute, S. Raible, F. E. Prins, D. P. Kern, H. Ulmer, U. Weimar and W. Göpel, Detection of volatile organic compounds (VOCs) with polymer-coated cantilevers, *Sensors and Actuators B: Chemical,* vol 58, no. 1-3, p. 505–511, **1999**.

[131] H. F. Ji, K. M. Hansen, Z. Hu and T. Thundat, Detection of pH variation using modi®ed microcantilever sensors, *Sensors and Actuators B: Chemical,* vol 72, pp. 233-238, **2001**.

[132] K. S. Hwang, J. H. Lee, J. Park, D. S. Yoon, J. H. Park and T. S. Kim, In-situ quantitative analysis of a prostate-specific antigen (PSA) using a nanomechanical PZT cantilever, *Lab on a Chip,* vol 4, no. 6, pp. 547-552, **2004**.

[133] B. L. Weeks, J. Camarero, A. Noy, A. E. Miller, L. Stanker and J. J. De Yoreo, A Microcantilever-Based Pathogen Detector, *Scanning,* vol 25, p. 297–299, **2003**.

[134] C. Grogan, R. Raiteri, G. M. O'Connor, T. J. Glynn, V. Cunningham, M. Kane, M. Charlton and D. Leech, Characterisation of an antibody coated microcantilever as a potential immuno-based biosensor, *Biosensors and Bioelectronics,* vol 17, p. 201–207, **2002**.

[135] M. Alvarez, A. Calle, J. Tamayo, L. M. Lechuga, A. Abad and A. Montoya, Development of nanomechanical biosensors for detection of the pesticide DDT, *Biosensors and Bioelectronics,* vol 18, pp. 649-653, **2003**.

[136] A. M. Moulin, S. J. O'Shea and M. E. Welland, Microcantilever-based biosensors, *Ultramicroscopy,* vol 82, no. 1-4, pp. 23-31, **2000**.

[137] A. Subramanian, P. I. Oden, S. J. Kennel, K. B. Jacobson, R. J. Warmack, T. Thundat and M. J. Doktycz, Glucose biosensing using an enzyme-coated microcantilever, *Applied Physics Letter,* vol 81, no. 2, pp. 385-387, **2002**.

[138] R. Marie, H. Jensenius, J. Thaysen, C. B. Christensen and A. Boisen, Adsorption kinetics and mechanical properties of thiol-modified DNA-oligos on gold investigated by microcantilever sensors, *Ultramicroscopy,* vol 91, p. 29–36, **2002**.

[139] E. Turiel and A. Martín-Esteban, Molecularly imprinted polymers for sample preparation: A review, *Analytica Chimica Acta,* vol 668, p. 87–99, **2010**.

[140] G. Wulff, Molecular Recognition in Polymers Prepared by Imprinting with Templates, *American Chemical Society Symposium Series,* vol 308, pp. 186-230, **1986**.

[141] K. Haupt and K. Mosbach, Plastic antibodies: developments and applications, *Trends in Biotechnology,* vol 16, pp. 468-475, **1998**.

[142] G. Wulff, Enzyme-like catalysis by molecularly imprinted polymers, *Chemical Reviews,* vol 102, pp. 1-27, **2002**.

[143] J. Haginaka, Monodispersed, molecularly imprinted polymers as affinity-based chromatography media, *Journal of Chromatography B,* vol 866, pp. 3-13, **2008**.

[144] L. I. Andersson, A. Miyabayashi, D. J. O'Shannessy and K. Mosbach, Enantiomeric resolution of amino acid derivatives on molecularly imprinted polymers as monitored by potentiometric measurements, *Journal of Chromatography,* vol 516, pp. 323-331, **1990**.

[145] L. I. Andersson, C. F. Mandenius and K. Mosbach, Studies on Guest Selective Molecular Recognition on an Octadecyl Silylateo Silicon Surface Using Ellipsometry, *Tetrahedron Letters,* vol 29, no. 42, pp. 5437-5440, **1988**.

[146] S. A. Piletsky, Y. P. Parhometz, N. V. Lavryk, T. L. Panasyuk and A. V. El'skaya, Sensors for low-weight organic molecules based on molecular imprinting technique, *Sensors and Actuators B: Chemical,* vol 19, no. 1-3, pp. 629-631, **1994**.

[147] W. Li and S. Li, Molecular imprinting: A versatile tool for separation, sensors and catalysis, *Advanced Polymer Science,* vol 206, p. 191–210, **2007**.

[148] E. Hedborg, F. Winquist, I. Lundström, L. I. Andersson and K. Mosbach, Some studies of molecularly imprinted polymer membranes in combination with field-effect devices, *Sensors and Actuators A: Physical,* Vol %1 / %237-38, pp. 796-799, **1993**.

[149] X. Kan, T. Liu, H. Li and B. Fand, Molecular imprinting polymer electrosensor based on gold nanoparticles for theophylline recognition and determination, *Microchimica Acta,* vol 171, pp. 423-429, **2010**.

[150] J. D. Huang, X. M. Zhang, S. Liu, Q. Lin, X. R. He and X. R. Xing, Electrochemical sensor for bisphenol A detection based on molecularly imprinted polymers and gold nanoparticles, *Journal of Applied Electrochemistry,* vol 41, pp. 1323-1328, **2011**.

[151] M. Riskin, R. Tel-Vered, T. Bourenko, E. Granot and I. Willner, Imprinting of molecular recognition sites through electropolymerization of functionalized Au nanoparticles: Development of an electrochemical TNT sensor based on π-Donor-acceptor interactions, *Journal of American Chemical Society,* vol 130, pp. 9726-9733, **2008**.

[152] S. Gam-Derouich, S. Mahouche-Chergui, S. Truong, D. B. Hassen-Chehimi and M. M. Chehimi, Design of molecularly imprinted polymer grafts with embedded gold nanoparticles through the interfacial chemistry of aryl diazonium salts, *Polymer,* vol 52, pp. 4463-4470, **2011**.

[153] X. Kan, Y. Zhao, Z. Geng, Z. Wang and J. J. Zhu, Composites of multiwalled carbon nanotubes and molecularly imprinted polymers for dopamine recognition, *Journal of Physical Chemistry C,* vol 112, pp. 4849-4854, **2008**.

[154] Y. Hu, Z. Zhang, H. Zhang, L. Luo and S. Yao, Selective and sensitive molecularly imprinted sol-gel film-based electrochemical sensor combining mercaptoacetic acid-modified PbS nanoparticles with Fe3O4@Au-multi-walled carbon nanotubes–chitosan, *Journal of Solid State Electrochemistry,* vol 16, pp. 857-867, **2012**.

[155] B. Sellergren, J. Wieschemeyer, K. S. Boos and D. Seidel, Imprinted Polymers for Selective Adsorption of Cholesterol from Gastrointestinal Fluids, *Chemistry of Materials,* vol 10, pp. 4037-4046, **1998**.

[156] H. Yan, F. Qiao and K. H. Row, Molecularly Imprinted-Matrix Solid-Phase Dispersion for Selective Extraction of Five Fluoroquinolones in Eggs and Tissue, *Analytical Chemistry,* vol 79, no. 21, p. 8242–8248, **2007**.

[157] B. Dirion, Z. Cobb, E. Schillinger, L. I. Andersson and B. Sellergren, Water-Compatible Molecularly Imprinted Polymers Obtained via High-Throughput Synthesis and Experimental Design, *Journal of American Chemical Society,* vol 125, pp. 15101-15109, **2003**.

[158] E. Benito-Peña, S. Martins, G. Orellana and M. C. Moreno-Bondi, Water-compatible molecularly imprinted polymer for the selective recognition of fluoroquinolone antibiotics in biological samples, *Analytical and Bioanalytical Chemistry,* vol 393, p. 235–245, **2009**.

[159] J. L. Urraca, A. J. Hall, M. C. Moreno-Bondi and B. Sellergren, A Stoichiometric Molecularly Imprinted Polymer for the Class-Selective Recognition of Antibiotics in Aqueous Media, *Angewandte Chemie,* vol 118, p. 5282 –5285, **2006**.

[160] J. L. Urraca, M. C. Moreno-Bondi, G. Orellana, B. Sellergren and A. J. Hall, Molecularly Imprinted Polymers as Antibody Mimics in Automated On-Line Fluorescent Competitive Assays, *Analytical Chemistry,* vol 79, pp. 4915-4923, **2007**.

[161] E. Sari, R. Üzek, M. Duman and A. Denizli, Fabrication of Surface Plasmon Resonance Nanosensor for the Selective Determination of Erythromycin via Molecular Imprinted Nanoparticles, *Talanta,* vol 150, pp. 607-614, **2015**.

[162] T. L. Panasyuk, V. M. Mirsky, S. A. Piletsky and O. S. Wolfbeis, Electropolymerized Molecularly Imprinted Polymers as Receptor Layers in Capacitive Chemical Sensors, *Analytical Chemistry,* vol 71, pp. 4609-4613, **1999**.

[163] B. Jakoby, G. M. Ismail, M. P. Byfield and M. J. Vellekoop, A novel molecularly imprinted thin film applied to a Love wave gas sensor, *Sensors and Actuators A: Physical,* vol 76, no. 1–3, p. 93–97, **1999**.

[164] F. L. Dickert, P. Forth and P. Lieberzeit, Molecular imprinting in chemical sensing – Detection of aromatic and halogenated hydrocarbons as well as polar solvent vapors, *Fresenius' Journal of Analytical Chemistry,* vol 360, p. 759–762, **1998**.

[165] F. L. Dickert and M. Tortschanoff, Molecularly Imprinted Sensor Layers for the Detection of Polycyclic Aromatic Hydrocarbons in Water, *Analytical Chemistry,* vol 71, no. 20, p. 4559–4563, **1999**.

[166] F. L. Dickert and S. Thierer, Molecularly imprinted polymers for optochemical sensors, *Advanced Materials,* vol 8, no. 12, pp. 987-990, **1996**.

[167] K. Haupt, K. Noworyta and W. Kutner, Imprinted polymer-based enantioselective acoustic sensor using a quartz crystal microbalance, *Analytical Communications,* vol 36, no. 11-12, pp. 391-393, **1999**.

[168] C. Malitesta, I. Losito and P. G. Zambonin, Molecularly Imprinted Electrosynthesized Polymers: New Materials for Biomimetic Sensors, *Analytical Chemistry,* vol 71, no. 7, p. 1366–1370, **1999**.

[169] H. -S. Ji, S. McNiven, K. Ikebukuro and I. Karube, Selective piezoelectric odor sensors using molecularly imprinted polymers, *Analytica Chimica Acta,* vol 390, no. 1-3, p. 93–100, **1999**.

[170] C. Liang, H. Peng, X. Bao, L. Nie and S. Yao, Study of a molecular imprinting polymer coated BAW bio-mimic sensor and its application to the determination of caffeine in human serum and urine, *Analyst,* vol 124, no. 12, pp. 1781-1785, **1999**.

[171] S. A. Piletsky, S. Subrahmanyam and A. P. F. Turner, Application of molecularly imprinted polymers in sensor for the environment and biotechnology, *Sensor Review,* vol 21, no. 4, pp. 292-296, **2001**.

[172] S. C. Huang, G. B. Lee, F. C. Chien, S. J. Chen, W. J. Chen and M. C. Yang, A microfluidic system with integrated molecular imprinting polymer films for surface plasmon, *Journal of Micromechanics and Microengineering,* vol 16, p. 1251–1257, **2006**.

[173] K. Haupt and K. Mosbach, Molecularly Imprinted Polymers and Their Use in Biomimetic Sensors, *Chemical Reviews,* vol 100, p. 2495−2504, **2000**.

[174] A. Kugimiya and T. Takeuchi, Molecularly Imprinted Polymer-Coated Quartz Crystal Microbalance for Detection of Biological Hormone, *Electroanalysis,* vol 11, no. 15, p. 1158–1160, **1999**.

[175] A. Johansson, G. Blagoi and A. Boisen, Polymeric cantilever-based biosensors with integrated readout, *Applied Physics Letters,* vol 89, p. 173505, **2006**.

[176] M. Hopcroft, T. Kramer, G. Kim, K. Takashima, Y. Higo, D. Moore and J. Brugger, Micromechanical testing of SU-8 cantilevers, *Fatigue & Fracture of Engineering Materials & Structures,* vol 28, no. 8, p. 735–742, **2005**.

[177] S. Keller, D. Haefliger and A. Boisen, Fabrication of thin SU-8 cantilevers: initial bending, release and time stability, *Journal of Micromechanics and Microengineering,* vol 20, p. 045024, **2010**.

[178] V. Seena, A. Nigam, P. Pant, S. Mukherji and V. R. Rao, Organic CantiFET: A Nanomechanical Polymer Cantilever Sensor With Integrated OFET, *Journal of Microelectromechanical Systems,* vol 21, no. 2, pp. 294-301, **2012**.

[179] C. Ayela, F. Vandevelde, D. Lagrange, K. Haupt and L. Nicu, Combining Resonant Piezoelectric Micromembranes with Molecularly Imprinted Polymers, *Angewandte Chemie,* vol 119, p. 9431–9434, **2007**.

[180] C. Ayela, G. Dubourg, C. Pellet and K. Haupt, All-Organic Microelectromechanical Systems Integrating Specifi c Molecular

Recognition – A New Generation of Chemical Sensors, *Advanced Materials,* vol 26, p. 5876–5879, **2014**.

[181] S. Song, A. Wu, X. Shi, R. Li, Z. Lin and D. Zhang, Development and application of molecularly imprinted polymers as solid-phase sorbents for erythromycin extraction, *Anal Bioanal Chem,* no. 390, p. 2141–2150, **2008**.

[182] G. Jungang, L. Zhanli, L. Pengyan and J. Ning, Preparation of MAA/TRIM molecularly imprinted polymers and binding selectivity for ciprofloxacin, *MDPI,* vol 9, no. 2, **2007**.

[183] M. Okan, E. Sari and M. Duman, Molecularly imprinted polymer based micromechanical cantilever sensor system for the selective determination of ciprofloxacin, *Biosensors and Bioelectronics,* vol 88, pp. 258-264, **2017**.

[184] H. J. Gruber, Amino-functionalization of AFM tips, 28 3 **2013**. Available: https://www.jku.at/biophysics/content/e257042/e257047/02_AFM_tip_aminofunctionalization_2013_03_28_eng.pdf.

[185] M. J. E. Fischer, Amine Coupling Through EDC/NHS: A Practical Approach, *Surface Plasmon Resonance, Methods in Molecular Biology*, Springer, **2010**, pp. 55-73.

CURRICULUM VITAE

Identifying Information

Name Surname: Meltem Okan
Birthplace: Çankaya, Ankara
Marital Status: Bachelor
E-mail: okanmelt@gmail.com
Address: Ağaçseven Sokak, Elit Blok No:6 Mutlukent Mahallesi, Ümitköy, ANKARA, TURKEY 06810

Education

High School: Aydın Anadolu College
Undergraduate Degree: Bilkent University, Department of Chemistry
Graduate Degree: -
Postgraduate Degree: -

Foreign Language Level

English; Advanced
German; Intermediate

Work History

-

Areas of Experience

Computational Chemistry;
By using B3LYP level of theory in 6-31g* basis set, the aim is to obtain a visible spectrum of Permanganate in UV-Vis spectroscopy range. Computations are done by the Gaussian program and the density functional theory method. Optimized HOMO-LUMO transitions and ionization energies are calculated in B3LYP/ 6-31g (d) basis set. The purpose is to see a peak at visible range in spectrum which is normally invisible.
Supervisor: Ulrike Salzner

Computer Science;
Laboratory Assistant, Bilkent University, Institute of Engineering, (2013-2014)
Teaching Assistant for CS121 “Introduction to Computing for Social Sciences”

Other Areas of Experience;
Atomic Force Microscopy, Tip Chemistry, Quartz Crystal Microbalance, Lateral Flow Assays, Molecularly Imprinted Polymers

Projects Arose From Thesis Study

-

Publications Arose From Thesis Study

Articles:

1. M. Okan, E. Sari and M. Duman, "Molecularly imprinted polymer based micromechanical cantilever sensor system for the selective determination of ciprofloxacin", *Biosensors and Bioelectronics*, vol. 88, p. 258-264, 2017.

2. M. Okan, E. Sari and M. Duman, "Molecularly Imprinted Polymer Based Microcantilever Sensor for the Selective Determination of Erythromycin in Water Resources", Analyst. (Submitted)

Book Chapters:

1. M. Okan and M. Duman, "Development of Molecularly Imprinted Polymer-based Microcantilever Sensor System", *Advanced Molecularly Imprinting Materials*, 637–680, 2016, Scrivener Publishing LLC

Poster and Oral Presentations Arose from Thesis Study

1. "Molecularly imprinted polymer based micromechanical cantilever sensor system for the selective determination of ciprofloxacin", 26th Anniversary World Congress on Biosensors, Gothenburg, Sweden 2016. (Poster Presentation.)
2. "Molecularly Imprinted Polymer Based Microcantilever Sensor for the Selective Determination of Erythromycin in Water Resources", 3rd International Congress on Biosensors, Ankara, Turkey, 2016. (Oral Presentation.)

Other Conferences and Workshops Attended;

1. Chemistry Symposium – International Year of Chemistry, 2011
2. Gazi University International Nanotechnology Conference, 2014
3. BIOMATEN, Nanobiomaterials and Nanomedicine Applications Workshop, 2014
4. HÜNİTEK, Advanced Technologies on Health Sciences, 2014
5. Hands-on Winter School, Johannes Kepler University of Linz, 2015
6. XVII. Annual Linz Winter Workshop, Linz, Austria, 2015

HACETTEPE UNIVERSITY
GRADUATE SCHOOL OF SCIENCE AND ENGINEERING
THESIS/DISSERTATION ORIGINALITY REPORT

HACETTEPE UNIVERSITY
GRADUATE SCHOOL OF SCIENCE AND ENGINEERING
TO THE DEPARTMENT OF NANOTECHNOLOGY AND NANOMEDICINE

Date: 16/12/2016

Thesis Title / Topic: A NOVEL MICROCANTILEVER SENSOR SYSTEM FOR THE SELECTIVE DETERMINATION OF ANTIBIOTICS

According to the originality report obtained by myself/my thesis advisor by using the *Turnitin* plagiarism detection software and by applying the filtering options stated below on 30/11/2016 for the total of 93 pages including the a) Title Page, b) Introduction, c) Main Chapters, d) Conclusion and e) Bibliography sections of my thesis entitled as above, the similarity index of my thesis is 10%.

Filtering options applied:

1. Bibliography/Works Cited excluded
2. Quotes excluded
3. Match size up to 5 words excluded

I declare that I have carefully read Hacettepe University Graduate School of Sciene and Engineering Guidelines for Obtaining and Using Thesis Originality Reports; that according to the maximum similarity index values specified in the Guidelines, my thesis does not include any form of plagiarism; that in any future detection of possible infringement of the regulations I accept all legal responsibility; and that all the information I have provided is correct to the best of my knowledge.

I respectfully submit this for approval. 16.12.2016

Name Surname: Meltem Okan

Student No: N14128751

Department: Nanotechnology and Nanomedicine Division

Program: Nanotechnology and Nanomedicine

Status: ■ Masters ☐ Ph.D. ☐ Integrated Ph.D.

ADVISOR APPROVAL

APPROVED.

Assoc. Prof. Dr. Memed Duman